Karlsruher Institut für Technologie

Masterthesis

Analysis of Qubit-Oscillator Dynamics in the Dispersive Regime

Maximilian Werling

05. April 2024

Advisor and first reviewer: Prof.Dr. Alexander Shnirman

Second reviewer: Prof. Dr. Ioan Pop

Fakultät für Physik

Karlsruher Institut für Technologie

Eidesstattliche Erklärung

Ich, Maximilian Werling, versichere wahrheitsgemäß, die Masterarbeit

Analysis of Qubit-Oscillator Dynamics in the Dispersive Regime

selbstständig verfasst, alle benutzten Hilfsmittel vollständig und genau angegeben und alles kenntlich gemacht zu haben, was aus Arbeiten anderer unverändert oder mit Abänderungen entnommen wurde sowie die Satzung des KIT zur Sicherung guter wissenschaftlicher Praxis in der jeweils gültigen Fassung beachtet zu haben.

Ort, Datum Unterschrift

Acknowledgements

Ich widme diese Arbeit meinem guten Freund Latif. Er war immer da um offen von Herzen zu geben, zuzuhören, zu reden und zu trommeln während der vielen schönen Stunden die wir gemeinsam im Park verbracht haben. Wir haben uns ungefähr zum Beginn meines Studiums kennengelernt. Während ich diese Arbeit geschrieben habe, wurde er verhaftet und aus Deutschland abgeschoben. Angeblich hat er kein "Bleibeinteresse" hier - Er wurde natürlich nicht danach gefragt. Jeder der ihn kennt weiß, dass seine Heimat hier ist, dass er hier hin gehört. Es ist einfach krank, dass die Stadt Karlsruhe, die Stadt der Grundrechte, das nicht so sieht. Ich hoffe, dass es ihm gut ergehen wird, wo auch immer es ihn hintreibt...

Meinen Dank richte ich aus an Prof. Shnirman, der mir nicht nur viel Freiraum gelassen hat eigene Ideen einzubringen und Impulse zu verfolgen, sondern sich auch viel Zeit genommen hat, um auf meine Fragen einzugehen und diese zusammen mit mir zu klären. Außerdem danke ich Tobi, Ida, Fed, Ozan und Lars die so nett waren ein bisschen auf Fehlersuche mit mir zu gehen. Zuletzt möchte ich gerne meinen Eltern danken, die mich während des ganzen Studium quasi bedingungslos unterstützt haben, und auch sonst immer für mich da sind.

Danke

Contents

1. Introduction

1.1. Motivation and background

This theses aims to provide a better understanding of the theory behind dispersively coupled qubits-oscillator systems within the basic framework of Circuit Quantum Electrodynamics (CQED)[1]. The focus is placed on explaining results presented in a series of papers by Blais et al. (2006 [2], 2008 [3] and 2010 [4]), and generalizing them to an arbitrary number of qubits. The main object of interest is the master equation governing the dynamics of the coupled system, and its solutions.

In their 2006 paper *"Qubit-photon interactions in a cavity: Measurement-induced dephasing and number splitting"* [2] an analytical solution to the master equation describing a superconducting qubit dispersively coupled to a driven transmission line resonator is introduced. By neglecting qubit relaxation, the time evolved density matrix of the coupled system is found to be given by an entangled superposition of coherent resonator states: Depending on the qubit's state ($|e\rangle$ and $|g\rangle$ for excited- and ground- state respectively), the oscillator is driven towards distinct coherent states $|\alpha^s_{e/g}\rangle$. This discovery provides a qualitative and quantitative understanding of the measurement induced dephasing of the qubit by the resonator, which is essential for performing qubit readout in the proposed design.

Following the seminal 2007 paper *"Charge insensitive qubit design derived from the Cooper pair box"* [5], which introduced the transmon as a promising architecture for quantum computing, the 2008 paper, *"Quantum trajectory approach to circuit QED: Quantum jumps and the Zeno effect"* [3] extends the 2006 results by presenting an *effective* master equation for the qubit, including qubit relaxation as well as measurement induced dephasing. The derivation employs a polaron transformation to trace out the resonator degrees of freedom from the full master equation. The resulting effective equation is exact, but the calculation is relatively technical and opaque regarding physical intuition due to its technical complexity.

In the 2010 paper *"Tunable joint measurements in the dispersive regime of cavity QED "* [4] the framework is expanded to include two qubits coupled to a single resonator. The time dependant density matrix is derived in a manner analogous to [2], proposing dynamics suitable for performing parity measurements and generating entangled states. Furthermore, following [3], an effective qubit equation is derived, which, while not exact, remains highly accurate when the resonator's relaxation rate, κ, is significantly greater than the qubit relaxation rate, γ_1. The derivation is not given, and it remains unclarified as to why the effective equation is not exact anymore.

Since these publications, the parity measurements proposed in [4], have been implemented in a recent experiment [6] to execute a three-bit quantum error correction protocol. Moreover, the theoretical framework has been expanded to incorporate parity measurements in 4-qubit systems, coupled to a nonlinear oscillator with a two-mode drive, as demonstrated in [7]. The readout of transmon qubits and enhancements to the standard dispersive setup continue to be vigorously researched (see for example [8], [9]). Dispersive measurement techniques have also been adopted in emerging areas such as circuit quantum acoustodynamics [10].

It is therefore of didactic interest to present and compile detailed explanations of the pioneering work by Blais et al. This work aims to provide students entering the field of quantum processing and readout with resources to help build physical intuition and understanding of the dynamics of the dispersive coupling, as well as to learn the basic

techniques employed in deriving them.

In the following section the structure of the present thesis is outlined.

1.2. Overview and structure

The primary aim of this thesis is to provide a comprehensive and detailed derivation of the master equations and their solutions as presented in the referenced papers by Blais et al. Furthermore, the framework is generalised to an arbitrary number of qubits. Numerical solutions are analyzed to understand the effects of qubit relaxation, before providing an analytical treatment that offers physical insight into the effect of qubit relaxation on the dispersive dynamics. Additionally, a derivation of the one-qubit effective equation presented in [3] is given, which is arguably less technical and much simpler. Moreover, a clear explanation of why only the reduced single qubit equation is exact is provided. Finally, an approximate solution to the master equation including qubit relaxation is obtained, yielding accurate results for $\kappa \gg \gamma_1$.

Chapters 2 and 3 focus on deriving the main Hamiltonian of this work, which describes the dispersive coupling of N qubits to a driven harmonic oscillator. After reviewing the uncoupled driven oscillator and N qubit registers, a brief derivation of the transmon qubit is presented. Next, the Rotating Wave Approximation (RWA) is applied to derive the driven Jaynes Cummings Hamiltonian. Finally we move to the dispersive frame by carrying out a Schrieffer-Wolff transformation.

In Chapters 4 and 5, the focus shifts to open system dynamics. The Lindblad master equation is reviewed, including a discussion on how to vectorize the Lindbladian and decompose given density matrices into the resulting eigenvectors - which is a key technique for solving the Lindblad equation numerically. Subsequently, microscopic derivations of the master equations for the systems under consideration are provided. The discussion begins with the treatment of the uncoupled system, followed by the derivation for the full coupled system.

Chapter 6 details the derivation of the N qubit solution of the master equation in the absence of qubit relaxation. Here, the calculation indicated in [2] is made explicit and extended to an arbitrary number of bits. The chapter concludes with an analysis of the resulting solution, explaining its physical interpretation aswell as its applications.

Chapter 7 focuses on the numerical analysis of the full master equation, taking into account qubit relaxation and drive effects. Specifically, the breakdown of the dispersive approximation for increased driving amplitudes is studied, aswell as the effects of γ_1 on the dynamics and formation of coherent states in the oscillator.

Finally, Chapter 8 presents the derivation of the reduced effective register equation. Starting with a perturbative analysis to clarify the effects of relaxation on the full density matrix, the chapter provides physical insight into the dissipative dynamics. We find analytical justification for the derivation of the effective register equation for $N > 1$, and solve it for the diagonal elements representing the decaying register weights. The thesis concludes by comparing the obtained analytic results with the numerical results obtained before.

2. Basic ingredients

The objective of this thesis is to understand the dynamics of a damped and driven oscillator coupled to N qubits in the dispersive regime. To build some intuition, establish notation and introduce techniques that will be used later on, we start first by reviewing the basic ingredients that go into the coupled system: the isolated, periodically driven oscillator, and a register consisting of N isolated qubits.

2.1. Periodically driven oscillator

Using the creation and annihilation operators $a^\dagger$ and a, the Hamiltonian of a periodically driven oscillator with energy ω_r is written as

$$H = \omega_r a^\dagger a + 2\epsilon \cos(\omega_d t)\left(a^\dagger + a\right). \tag{2.1}$$

Here, 2ϵ is the amplitude and ω_d the frequency of the driving force, which is assumed to be independent of $x \sim (a^\dagger + a)$

We are interested in the time evolution generated by H, especially the evolution of the vacuum state $|0\rangle$, defined by $a|0\rangle = 0$, in the near-resonant driving regime $\omega_d \approx \omega_r$. As will be shown, having a small detuning between the oscillator and the drive leads to a significant displacement of the oscillator vacuum state. It turns out that this basic phenomenon translates to the coupled qubit-oscillator system as well, where it can be used to perform qubit readout via the oscillator, by choosing the driving frequency appropriately (see Sec. 6.5).

In the $\omega_d \approx \omega_r$ regime, H can be simplified by removing its time dependence using the *Rotating Wave approximation* (RWA) [11]. To perform this approximation we will first introduce the concept of eigenoperators, which will not only be useful to carry out the RWA but is also needed to derive the jump operators for the master equations of the damped resonator- and qubit-systems in Secs. 5.2-5.4.

2.1.1. Eigenoperators

According to [12], eigenoperators of a (time-independent) Hamiltonian H_0 are operators $A(\omega)$ that evolve under H_0 as follows:

$$e^{\mathrm{i}H_0 t} A(\omega) e^{-\mathrm{i}H_0 t} = e^{-\mathrm{i}\omega t} A(\omega). \tag{2.2}$$

Similar to the *eigenstates* of H_0, they only acquire a phase-factor $e^{-\mathrm{i}\omega t}$ under time evolution. Differentiating Eq. 2.2 with respect to t yields the equivalent definition

$$[H_0,\, A(\omega)] = -\omega A(\omega). \tag{2.3}$$

An arbitrary operator A can always be split into a sum of eigenoperators of H_0 [12]: By decomposing A using the projectors $\Pi(\epsilon)$ on the (possibly degenerate) subspaces of eigenvectors with energy eigenvalues ϵ

$$A(\omega) \equiv \sum_{\epsilon' - \epsilon = \omega} \Pi(\epsilon')\, A\, \Pi(\epsilon). \tag{2.4}$$

it is easy to check that $A(\omega)$ satisfies Eq.2.2, since $\exp(-\mathrm{i}H_0 t)\Pi(\epsilon) = \exp(-\mathrm{i}\,\epsilon\, t)\Pi(\epsilon)$ and $\epsilon' - \epsilon = \omega$ for all terms in the sum. Furthermore, the completeness of the projectors $\sum_\epsilon \Pi(\epsilon) = \mathbb{1}$ ensures that $\sum_\omega A(\omega) = A$.

In the case of the harmonic oscillator where $H_0 = \omega_r a^\dagger a$ we can identify a and $a^\dagger$ as eigenoperators of H_0, since $[H_0,\, a] = \omega_r \left[a^\dagger a, a\right] = -\omega_r a$ and similarly $\left[H_0,\, a^\dagger\right] = \omega_r a^\dagger$. Their time evolution is given by

$$\begin{aligned} e^{\mathrm{i}\omega_r a^\dagger a\, t}\, a\, e^{-\mathrm{i}\omega_r a^\dagger a\, t} &= e^{-\mathrm{i}\omega_r t}\, a \\ e^{\mathrm{i}\omega_r a^\dagger a\, t}\, a^\dagger\, e^{-\mathrm{i}\omega_r a^\dagger a\, t} &= e^{\mathrm{i}\omega_r t}\, a^\dagger. \end{aligned} \tag{2.5}$$

Hence the following eigenoperators $A(\omega)$ can be identified for the Oscillator:

$$A(\omega_r) = a, \quad A(-\omega_r) = a^\dagger. \tag{2.6}$$

2.1.2. Rotating Wave Approximation

Now, to carry out the RWA, a transformation into a rotating frame defined by $|\psi_{\mathrm{RWA}}\rangle \equiv U(t)\,|\psi\rangle = \exp\!\big(\mathrm{i}\omega_d a^\dagger a t\big)\,|\psi\rangle$ is performed, inducing a counter rotation to the one generated by $H_0 = \omega_r a^\dagger a$. The Hamiltonian H_{RWA} in the rotating frame is obtained by calculating the time derivative of $|\psi_{\mathrm{RWA}}\rangle$:

$$\mathrm{i}\partial_t\,|\psi_{\mathrm{RWA}}\rangle = \mathrm{i}\dot{U}(t)U^\dagger(t)\,|\psi_{\mathrm{RWA}}\rangle + U(t)HU^\dagger(t)U(t)\,|\psi_{\mathrm{RWA}}\rangle\,, \tag{2.7}$$

which implies that

$$H_{\mathrm{RWA}} = \mathrm{i}\dot{U}(t)U^\dagger(t) + U(t)HU^\dagger(t). \tag{2.8}$$

The second term is calculated using the time-evolution of a and $a^\dagger$ 2.5. Rewriting $\cos(\omega_d t) = 1/2\,\left(\exp(\mathrm{i}\omega_d t) + \exp(-\mathrm{i}\omega_d t)\right)$ yields

$$U(t)HU^\dagger(t) = \omega_r a^\dagger a + \epsilon\left(e^{\mathrm{i}\omega_d t} + e^{-\mathrm{i}\omega_d t}\right)\left(a^\dagger e^{\mathrm{i}\omega_d t} + a e^{-\mathrm{i}\omega_d t}\right) \tag{2.9}$$

$$= \omega_r a^\dagger a + \epsilon\left(a^\dagger + a + a^\dagger e^{2\mathrm{i}\omega_d t} + a e^{-2\mathrm{i}\omega_d t}\right). \tag{2.10}$$

The RWA is performed by neglecting the time-dependent oscillating terms. This is justified for time spans large compared to $1/\omega_d$, since their contribution will average out quickly due to the oscillations [11]. Together with $\mathrm{i}\dot{U} = -\omega_d U$ and defining the detuning $\delta\omega_r \equiv \omega_r - \omega_d$ we obtain the Hamiltonian in the rotating frame:

$$H_{\mathrm{RWA}} = \delta\omega_r a^\dagger a + \epsilon\left(a^\dagger + a\right). \tag{2.11}$$

Recalling that $x \sim (a^\dagger + a)$, it is straight forward to see that this Hamiltonian now describes an oscillator with a constant force with amplitude $(-\epsilon)$

2.1.3. Evolution of the ground-state: classical analogy

Next, we want to determine the time evolution of the vacuum state $|0\rangle$ under the Hamiltonian 2.11. To build some intuition, we recall the classical oscillator first.

Classically, the ground state of a free oscillator with eigenfrequency $\delta\omega_r$ can be modelled by a mass on a spring resting at $x = 0$ with $p = 0$. If a constant force is suddenly applied (say a homogeneous gravitational field could be turned), the mass will fall down and start to oscillate forever with frequency $\delta\omega_r$ and a constant amplitude $\sim \epsilon/\delta\omega_r$. The trajectory of this harmonic motion in *phase space* is given by a perfect circle (after appropriately scaling p with respect to x) with radius $\sim \epsilon/\omega$ (see Fig. 2.1).

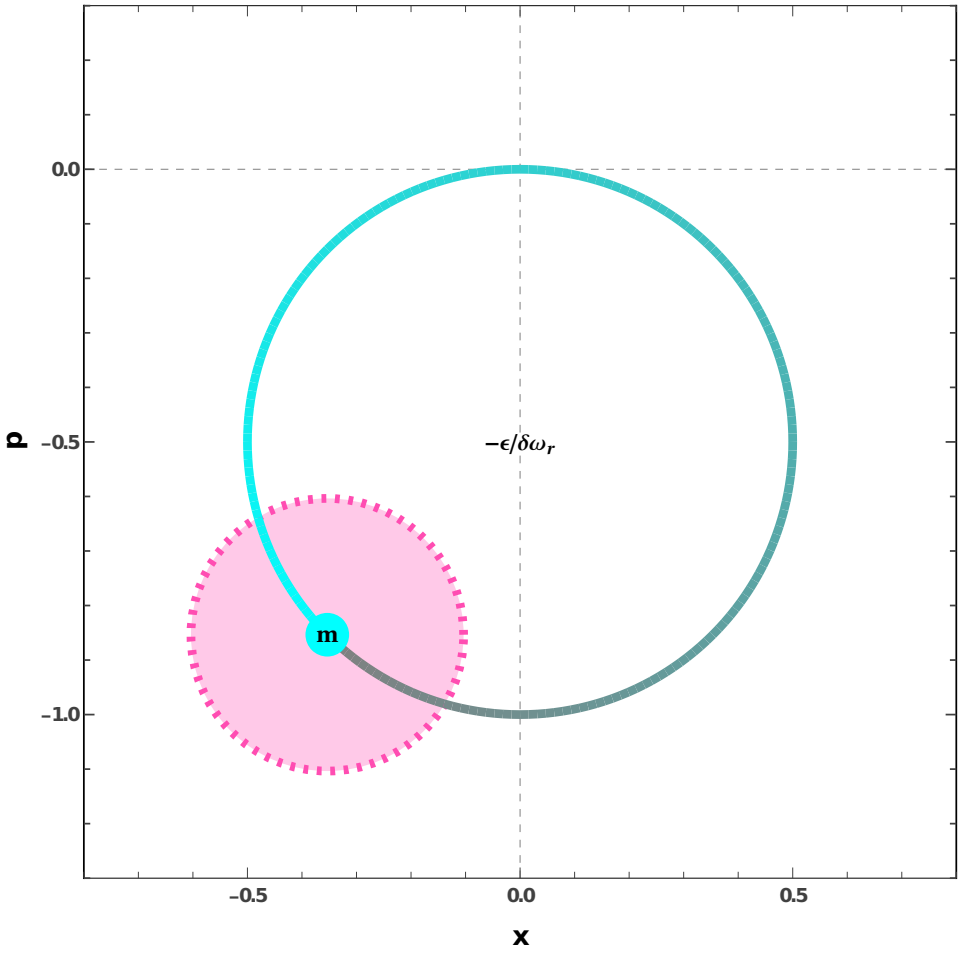

Figure 2.1.: Phase space trajectory of an oscillator suddenly "falling" down from its ground state for $\epsilon/\delta\omega_r = -0.5$. The cyan point labelled m represents the oscillating mass. The large circle represents the classical trajectory (anti-clockwise). The pink-opaque disk indicates the uncertainty of the corresponding coherent state, following the classical trajectory.

2.1.4. Coherent states and optical phase space

The time evolution of the vacuum state of the quantum mechanical oscillator can be understood in a similar way by introducing *coherent states*, also called *Glauber states* [13] [14]. A coherent state $|\alpha\rangle$ is defined by

$$|\alpha\rangle = e^{-\frac{|\alpha|^2}{2}} \sum_n \frac{\alpha^n}{\sqrt{n!}} |n\rangle , \tag{2.12}$$

satisfying the eigenvalue equation of the annihilation operator

$$a |\alpha\rangle = \alpha |\alpha\rangle , \tag{2.13}$$

where α is a complex number. By introducing the dimensionless position and momentum operators of the optical phase space [14]

$$x \equiv \frac{1}{2} \left(a^\dagger + a \right), \tag{2.14}$$

$$p \equiv \frac{1}{2\mathrm{i}} \left(a^\dagger - a \right), \tag{2.15}$$

also called *Quadratures* in the context of Cavity/Circuit QED, the annihilation operator can be expressed as $a = x + \mathrm{i}\, p$. This admits a simple phase space representation in the complex plane: Note that α is composed of the expectation values of x and p with respect to $|\alpha\rangle$:

$$\langle\alpha|a|\alpha\rangle = \alpha = \langle x\rangle + \mathrm{i}\langle p\rangle, \tag{2.16}$$

i.e. $\mathrm{Im}\,\alpha = \langle p\rangle$ and $\mathrm{Re}\,\alpha = \langle x\rangle$. Furthermore the coherent states $|\alpha\rangle$ are minimum uncertainty states with standard deviations $\Delta x = \Delta p = 1/2$ [15]. Therefore, by identifying the real and imaginary axis with the quadratures x and ip, a state $|\alpha\rangle$ can be represented in the complex plane by an "uncertainty disk" with radius 1/4 centered around α (see Fig. 2.1).

2.1.5. Quantum mechanical time evolution of the ground state

Now, to find the time-evolution of the vacuum state under H_{RWA} 2.11, it is helpful to first identify $|0\rangle$ as the coherent state with $\alpha = 0$, which follows trivially from $a|0\rangle = 0$. Next, we introduce the shifted ladder operator $A \equiv a + \epsilon/\delta\omega_r$ to complete the square in H_{RWA}:

$$H_{\mathrm{RWA}} = \delta\omega_r \left(a^\dagger a + \frac{\epsilon}{\delta\omega_r} \left(a^\dagger + a \right) \right) \tag{2.17}$$

$$= \delta\omega_r A^\dagger A - \frac{\epsilon^2}{\delta\omega_r^2}. \tag{2.18}$$

Noting that A obeys the same algebra as the usual annihilation operator $\left[A, A^\dagger\right] = \mathbb{1}$, we can deduce that according to 2.5, A is the eigenoperator of H_{RWA} with frequency $\delta\omega_r$, and thus evolves under H_{RWA} as follows:

$$e^{\mathrm{i}\delta\omega_r A^\dagger A t}\, A\, e^{-\mathrm{i}\delta\omega_r A^\dagger A t} = e^{-\mathrm{i}\delta\omega_r t} A. \tag{2.19}$$

Now applying a to the time evolved ground-state $|0(t)\rangle \equiv \exp(-\mathrm{i}H_{\mathrm{RWA}}t)\,|0\rangle$, we find that $|0\rangle$ remains a coherent state $|\alpha(t)\rangle$ for all t:

$$\begin{aligned} a\,|0(t)\rangle &= ae^{-\mathrm{i}H_{\mathrm{RWA}}t}\,|0\rangle \\ &= e^{-\mathrm{i}H_{\mathrm{RWA}}t}e^{\mathrm{i}\delta\omega_r A^\dagger At}\left(A-\frac{\epsilon}{\delta\omega_r}\right)e^{-\mathrm{i}\delta\omega_r A^\dagger At}\,|0\rangle \\ &= e^{-\mathrm{i}H_{\mathrm{RWA}}t}\left(e^{-\mathrm{i}\delta\omega_r t}A-\frac{\epsilon}{\delta\omega_r}\right)|0\rangle \\ &= e^{-\mathrm{i}H_{\mathrm{RWA}}t}\left(e^{-\mathrm{i}\delta\omega_r t}\left[a+\frac{\epsilon}{\delta\omega_r}\right]-\frac{\epsilon}{\delta\omega_r}\right)|0\rangle \\ &= \frac{\epsilon}{\delta\omega_r}\left(e^{-\mathrm{i}\delta\omega_r t}-1\right)|0(t)\rangle\,, \end{aligned} \tag{2.20}$$

where $a\,|0\rangle = 0$ was used in the last step. This proves that $|0(t)\rangle = |\alpha(t)\rangle$ with $\alpha(t) = \epsilon/\delta\omega_r\,(\exp(-\mathrm{i}\delta\omega_r t) - 1)$. Therefore, the x and p expectation values of the evolving ground-state are given by

$$\langle x\rangle = \frac{\epsilon}{\delta\omega_r}\left(\cos\left(\delta\omega_r t\right)-1\right) \quad \text{and} \quad \langle p\rangle = -\frac{\epsilon}{\delta\omega_r}\sin\left(\delta\omega_r t\right), \tag{2.21}$$

which describes the same trajectory as in the classical case (see Fig. 2.1).

From these results it is clear that the amplitude of the displacement is potentially unbounded, for $\lim_{\delta\omega_r\to 0}$ the magnitudes of both $\langle x\rangle$ and $\langle p\rangle$ grow linear in t without upper bound. This situation changes once we treat the oscillator as an open quantum system, effectively introducing damping. Intuitively we might expect that with damping included, the oscillator state will settle over time in a displaced coherent state, depending on the driving amplitude, its frequency and the damping factor κ.

In conclusion, using coherent states $|\alpha(t)\rangle$, the time evolution of the vacuum state under the influence of a constant force can be represented by the phase space trajectory of the classical oscillator, but with added uncertainty of $1/2$ in the x and p variable, which can be represented by a disk of radius $1/2$.

2.1.6. Phase space representations of oscillator states

Generally quantum mechanical states of an oscillator can be mapped to several different (quasi-) probability distributions on phase space like the *Wigner function* $W(x,p)$, which gives the quasi-probability to find the system with position x and momentum p [16] , or the *Husimi Q function* $Q(\alpha)$ [17] which gives the probability to find the system in a coherent state α [1]. The latter has the benefit of being an actual semi-positive probability distribution, with the drawback that it is more "smeared out" compared to the Wigner function, due to the built-in uncertainty of the coherent states.

While the Wigner function of a general quantum state represented by the density matrix ρ is relatively complicated, in the case of ρ representing a pure coherent state $|\beta\rangle$ it simplifies to: [1]

$$W_{|\beta\rangle}(x,p) = \frac{2}{\pi}e^{-2|\alpha(x,p)-\beta|^2} \quad \text{with} \quad \alpha = x+\mathrm{i}p. \tag{2.22}$$

A coherent state can therefore be represented by a Gaussian centered around α with variance $1/2$ in phase space. In contrast, the formula for the Husimi Q function is simple even for a general state matrix ρ: [1]

$$Q_\rho(\alpha) = \frac{1}{\pi}\,\langle\alpha|\rho|\alpha\rangle\,, \tag{2.23}$$

which, for $\rho = |\beta\rangle\langle\beta|$, reduces to

$$Q_{|\beta\rangle}(\alpha) = \frac{1}{\pi}e^{-\left(|\alpha|^2+|\beta|^2-2\,\mathrm{Re}\,(\alpha^*\beta)\right)}, \tag{2.24}$$

by using the scalar product between two coherent states [14]

$$\langle\beta|\alpha\rangle = e^{-\frac{1}{2}\left(|\alpha|^2+|\beta|^2-2\beta^*\alpha\right)}. \tag{2.25}$$

In chapter 7 we compare the oscillator state ρ obtained by numerical solution of the Lindblad equation with a coherent state $|\alpha\rangle\langle\alpha|$, in order to find potential differences. To this end, the Q representation is used, because of its simpler definition for (unknown) arbitrary states.

2.2. N-Qubit system

After treating the basics of a single driven harmonic oscillator, we continue with the quantum mechanical description of a N qubit system, referred to as the *register*. In the next chapter 3 we will then start to analyze a system of N qubits coupled to a driven oscillator.

2.2.1. Register states

The register Hilbert space $\mathcal{H}_N$ is given by the tensor product of N single qubit spaces $\mathcal{H}_1$:

$$\mathcal{H}_N = \underbrace{\mathcal{H}_1 \otimes \mathcal{H}_1 \otimes \cdots \otimes \mathcal{H}_1}_{\text{N times}}. \tag{2.26}$$

The corresponding register-basis consists of tensor products of the single-bit basis states $\{|e\rangle, |g\rangle\}$ which satisfy $\sigma_z |e\rangle = |e\rangle$ and $\sigma_z |g\rangle = -|g\rangle$.

Introducing the notation $|e\rangle \equiv |0\rangle$ and $|g\rangle \equiv |1\rangle$, the register-basis states can be indexed by binary numbers as follows:

$$\begin{aligned} |0\rangle &\equiv |\ldots 0,0,0\rangle \\ |1\rangle &\equiv |\ldots 0,0,1\rangle \\ |2\rangle &\equiv |\ldots 0,1,0\rangle \\ &\vdots \\ |2^N-1\rangle &\equiv |1,1,\ldots,1,1,1\rangle, \end{aligned} \tag{2.27}$$

where all bits are excited in $|0\rangle$ and only the first qubit is in its ground-state in $|1\rangle$, for example. An arbitrary state of the register can then be written as

$$|\psi\rangle = \sum_{x=0}^{2^N-1} c_x |x\rangle, \tag{2.28}$$

where x is a natural number whose binary representation indicates the register state according to Eq. 2.27.

2.2.2. Operators and Hamiltonian

Every qubit q in the register has its own set of operators $\{\mathbb{1}_N, \sigma_x^q, \sigma_y^q, \sigma_z^q\}$ where $\mathbb{1}_N$ is the 2^N dimensional square unit-matrix and the Pauli operators σ_i^q are given by:

$$\sigma_i^q = \underbrace{\mathbb{1}_1 \otimes \cdots \otimes \mathbb{1}_1}_{\text{N-q times}} \otimes \sigma_i \otimes \underbrace{\mathbb{1}_1 \otimes \cdots \otimes \mathbb{1}_1}_{\text{q-1 times}}. \tag{2.29}$$

In analytical calculations this tensor product structure involving the $\mathbb{1}_1$ unit matrices can simply be taken into account by the fact that the commutator between two Pauli matrices of different qubits vanish. However, when doing numerical calculations using *Mathematica* for example, it is necessary to obey this precise structure when implementing the matrix representations of the σ_z^q in the computer algebra program to obtain consistent results. Within the scope of this thesis, this will become relevant in chapter 7, when the dissipative coupled N-qubit system is solved and analyzed numerically.

Hamiltonian

Under the assumption of non-interacting qubits the Hamiltonian of the register, is just

$$H_N = \sum_{q=1}^{N} \frac{\omega_q}{2}\,\sigma_z^q \equiv \frac{\omega_q}{2}\,\sigma_z^q, \tag{2.30}$$

with the frequency of the qth bit ω_q. We also adopt the sum convention where terms with an upper ^{q} and a lower $_q$ imply the sum over all qubits, unless it is otherwise stated or obvious from the context.

This Hamiltonian serves as an approximation because, in an actual register, qubits inevitably interact with one another. Regarding qubit readout, intrinsic interactions of the qubits lead to a loss of stored information. In the context of this work, we are therefore interested in minimizing those interactions. In section 3.7 we explore the qubit-qubit interactions that emerge within the dispersive regime of multiple qubits coupled to a single resonator, and examine a strategy for how these interactions can be mitigated and disregarded.

Eigenoperators

We conclude this section with a short treatment of the eigenoperators of the register with respect to the Hamiltonian 2.30. Similarly to the eigenoperators of the oscillator, the eigenoperators of the register are the qubit ladder operators $\sigma_\pm^q$ defined by $\sigma_\pm \equiv 1/2\,(\sigma_x \pm \mathrm{i}\sigma_y)$. Their frequencies can be found according to 2.3:

$$\left[H_N, \sigma_\pm^p\right] = \frac{\omega_q}{2}\left[\sigma_z^q\,,\,\sigma_\pm^p\right] = \pm\omega_p\sigma_\pm^p, \tag{2.31}$$

implying that σ_+^q has the eigenfrequency $-\omega_q$ and σ_-^q has the frequency ω_q. Following Eq. 2.2 we find the time evolution under H_N:

$$e^{\mathrm{i}\frac{\omega_q}{2}\sigma_z^q t}\,\sigma_\pm^p\,e^{-\mathrm{i}\frac{\omega_q}{2}\sigma_z^q t} = e^{\pm\mathrm{i}\omega_p t}\,\sigma_\pm^p. \tag{2.32}$$

3. Setting up the Hamiltonian

This chapter is devoted to deriving the main Hamiltonian of interest in this thesis, describing the coupling between a driven resonator and a qubit register in the so-called *dispersive regime*. We start by providing a brief derivation of how to obtain a qubit Hamiltonian from a real physical system, exemplified by the *transmon artificial atom*, one of the most prominent candidates for realizing qubit registers using superconducting circuits. Coupling the transmon to a microwave-resonator transmission line then yields a Hamiltonian that formally describes the coupling of a qubit to an oscillator. To obtain the dispersive Hamiltonian, describing the system in the large detuning regime (when the detuning between the qubit frequencies and the oscillator frequency is large compared to the coupling strength g between qubits and the resonator), a Rotating Wave Approximation (RWA) is performed to cancel the fast-oscillating terms and remove the time dependency of the periodic oscillator drive, followed by a Schrieffer-Wolff Transformation, which approximately diagonalizes the Hamiltonian in the qubit z and oscillator Fock-basis.

We note that most of the work presented in this thesis does not depend on the physical system used to produce the resulting qubit Hamiltonian since, after deriving the qubit Hamiltonian, it will mostly be regarded as having no internal structure unique to the transmon.

3.1. Deriving the transmon-qubit Hamiltonian

The goal of this section is to provide a brief overview of the transmon and its implementation as a qubit coupled to a resonator. A more detailed and rigorous treatment is given in [1], which we will briefly summarize.

The transmon is a certain type of superconducting electrical circuit consisting of a *Josephson Junction* J connected in parallel to a capacitor C_s (see Fig. 3.1). The Josephson

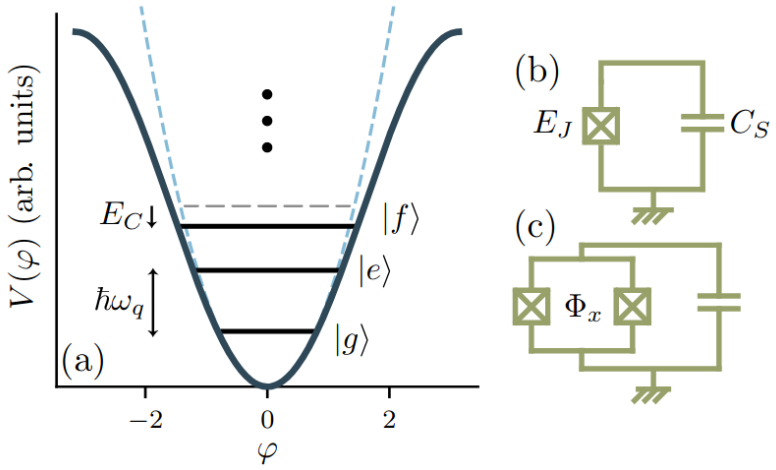

Figure 3.1.: **(a)** transmon Potential (solid line) in comparison to the harmonic oscillator potential of the linear LC-circuit (dashed). The energy levels of the transmon exhibit an anharmonicity due to the non-linearity of the potential. **(b)**: transmon Circuit. The crossed box represents the Josephson Junction. **(c)**: Flux-tunable transmon, obtained by exchanging the Josephson Junction by a *SQUID*. (Figure taken from [1])

Junction can be considered as a non-linear inductance, where "non-linear" refers to the fact that the Josephson inductance $L_J(\Phi)$ exhibits a non-linear dependency on the magnetic flux $\Phi(t)$ across the junction, as opposed to the inductance of a regular LC-circuit:

$$L_J(\Phi) = \frac{\Phi_0}{2\pi I_c} \frac{1}{\cos(2\pi\Phi/\Phi_0)}, \tag{3.1}$$

with the flux quantum $\Phi_0 = h/2e$ and the critical Josephson current I_c, which marks the maximum allowed current through the junction before superconductivity breaks down. Physically, the Josephson Junction is realized by two superconducting elements separated by a thin isolating-gap. As it turns out, below the critical current I_c, electron Cooper pairs tunnel through the gap, resulting in the current $I = I_c \sin(\varphi)$, where φ is the difference in the quantum mechanical phase of the two superconducting elements.

Regarding the realization of a qubit, this system is interesting because of the resulting Hamiltonian. Due to the non-linearity of the inductance, the combined Hamiltonian of the capacitance and the Josephson Junction resembles a particle in a cosine potential (similar to the pendulum in the gravitational field [18]):

$$H = 4E_C(\hat{n} - n_g)^2 - E_J \cos(\hat{\varphi}). \tag{3.2}$$

Here E_C is the charging energy and E_J the energy of the junction $E_J = \Phi_0 I_c/2\pi$. $\hat{\varphi}$ and $\hat{n}$ are canonically conjugate operators satisfying $[\hat{n}, \hat{\varphi}] = \mathrm{i}$. $\hat{n}$ is the charge-counting operator, counting the number of tunneled Cooper-pairs, while $\hat{\varphi} = (2\pi/\Phi_0)\hat{\Phi}$ is the phase operator. n_g is a charge offset that potentially occurs due to noise sources in the environment.

The idea of the transmon is to operate this circuit in the regime $E_J \gg E_C$, which comes with several benefits:

First, as explained in [18], this regime corresponds to a pendulum in a gravitational field where the gravitational energy dominates the total energy of the system. The resulting amplitude of the oscillation will therefore be small, and one is justified to truncate the cosine to the first nonlinear contribution to the potential.

Secondly, numerical analysis shows that in this regime, the lower energy levels of the transmon become essentially independent of the environmental charge noise represented by n_g, thus making it robust against environmentally induced dephasing due to charge fluctuations. We will come back to noise induced dephasing in Section 5.1. The resulting truncated Hamiltonian can be written using the annihilation and creation operators b and $b^\dagger$:

$$H \approx \hbar\omega_q b^\dagger b - \frac{E_C}{2} b^\dagger b^\dagger b b \tag{3.3}$$

$$\hbar\omega_q = \sqrt{8E_C E_J} - E_C, \tag{3.4}$$

where ω_q is the frequency of the transmon. The second term of the Hamiltonian can be understood as a non-linear correction to the usual harmonic oscillator potential. The resulting energy eigenstates of the system $|j\rangle$ exhibit an anharmonicity (see Fig. 3.1). This anharmonicity is crucial in operating the system in the qubit regime: Since, in the case of transmons, the energy difference ω_2 between the second and third level is typically $\sim 100\,\mathrm{MHz}$ smaller than ω_1 between the first and the second, it is possible to drive the transmon at ω_1 without accidentally exciting transitions to higher energy levels. Under suitable circumstances the system can therefore be treated as a qubit, and the transmon operators can effectively be truncated to the first two energy levels yielding

$$H \approx \hbar\frac{\omega_q}{2}\sigma_z. \tag{3.5}$$

It is furthermore possible to replace the single Josephson junction in the circuit by a SQUID loop, consisting of two junctions in parallel (see Fig. 3.1). This does not alter the

structure of the Hamiltonian, but it renders the Josephson energy E_J effectively dependent on the flux Φ, resulting in the flux-dependent transmon frequency

$$\hbar\omega_q(\Phi) = \sqrt{8E_C|E_J(\Phi)|} - E_C. \tag{3.6}$$

This allows to dynamically tune the frequency of the transmon by controlling the flux Φ, but in turn also makes the transmon more susceptible to flux-noise induced dephasing.

3.1.1. Coupling to a resonator

To enable further control and readout of the transmon qubit, it is coupled to a microwave-resonator transmission line [5][1]. From the point of view of circuits, the coupling is physically achieved by connecting a LC-circuit to the transmon via a gate capacitance C_g, which acts as a dynamical charge-offset to the transmon. The resulting Hamiltonian can be approximated by the sum of the system's individual Hamiltonians and an interaction Hamiltonian given by

$$2\,\frac{C_g}{C_s + C_J}\, eV^0\hat{n}(a^\dagger + a). \tag{3.7}$$

Here $a^\dagger$ and a are the resonator ladder operators and V^0 is the root-mean-square voltage at the gate. Using the eigenstates $|j\rangle$ of the transmon, this interaction operator can be rewritten as

$$H_I = \sum_{i,j} g_{ij}\,|i\rangle\langle j|\,(a^\dagger + a), \tag{3.8}$$

and, by truncating again to the first to energy levels, is equivalent (up to a unitary transformation of the matrix g_{ij}) to

$$H_I \approx g\,\sigma_x\,(a^\dagger + a). \tag{3.9}$$

The coupling constant g actually increases in the transmon regime: $g \sim (E_J/8E_C)^{1/4}$. This is highly desirable, since the strong coupling makes it possible to have qubit -readout and -control times shorter than the typical timescale of resonator- and qubit- relaxation $1/\kappa$ and $1/\gamma_1$. This is the so-called *strong coupling regime,* defined by $g \gg \kappa, \gamma_1$.

The full Hamiltonian of the coupled system in the qubit regime is then given by

$$H = \frac{\omega_q}{2}\,\sigma_z + \omega_r a^\dagger a + g\sigma_x\left(a^\dagger + a\right). \tag{3.10}$$

where ω_r is the resonator frequency.

This concludes the derivation of the qubit-resonator Hamiltonian, as exemplified by the transmon. We will assume this coupling as a building block from here on, to generalize it to multiple qubits coupled to a driven resonator in the next section.

3.2. Multi-Qubit driven Hamiltonian

The generalization to N qubits coupled to a single resonator is straightforward:

$$H = \omega_r\,a^\dagger a + \sum_q^N \left(\frac{\omega_q}{2}\,\sigma_z^q + g_q\,\sigma_x^q\left(a^\dagger + a\right)\right), \tag{3.11}$$

where ω_q is now the frequency of the q-th bit and g_q the coupling strength of the q-th bit to the resonator.

Finally, we consider a periodic drive of a homogeneous (x independent) external force, with amplitude ϵ and driving frequency ω_d. Introducing the sum convention by making

the sum over q implicit in all terms with one q up- and one q down-stairs, the resulting Hamiltonian is given by

$$H = \omega_r a^\dagger a + \frac{\omega_q}{2}\,\sigma_z^q + g_q\,\sigma_x^q\left(a^\dagger + a\right) + 2\epsilon\,\cos\omega_d t\left(a^\dagger + a\right). \tag{3.12}$$

The qubits energies ω_q and g_q can be tuned independently and will be chosen in a particular way suitable for our purposes at the end of this chapter in Sec. 3.9. Before that, the Hamiltonian 3.12 is our starting point to perform two important approximations in order to obtain the dispersive Hamiltonian, which is the main Hamiltonian considered in this thesis. The first of these approximations is the Rotating Wave approximation already encountered in Sec. 2.1.2.

3.3. RWA - Driven Jaynes Cummings Hamiltonian

In contrast to Sec. 2.1.2, the goal of this RWA is to eliminate the quickly oscillating terms of the resonator drive, as well as those implicit in the qubit-resonator coupling term. Applying the same transformation as in the ref to a section would now introduce time-dependent phases to the resonator operators multiplying $g_q\sigma_x^q$. To avoid this, a modified unitary transformation is chosen which also rotates in the qubit subspace:

$$U_{\mathrm{RWA}}(t) = e^{\mathrm{i}\omega_d\left(a^\dagger a + \sum_q \sigma_z^q/2\right)t}. \tag{3.13}$$

To transform the coupling term we first decompose the σ_x^q into the eigenoperators of U_{RWA}:

$$\sigma_x^q\left(a^\dagger + a\right) = \left(\sigma_+^q + \sigma_-^q\right)\left(a^\dagger + a\right), \tag{3.14}$$

which transforms under the RWA as

$$\begin{aligned} & e^{\mathrm{i}\omega_d\sigma_z^q/2\,t}\left(\sigma_+^q + \sigma_-^q\right)e^{-\mathrm{i}\omega_d\sigma_z^q/2\,t} \otimes e^{\mathrm{i}\omega_d a^\dagger a t}\left(a^\dagger + a\right)e^{-\mathrm{i}\omega_d a^\dagger a t} \\ &= \left(e^{\mathrm{i}\omega_d t}\sigma_+^q + e^{-\mathrm{i}\omega_d t}\sigma_-^q\right)\left(e^{\mathrm{i}\omega_d t}a^\dagger + e^{-\mathrm{i}\omega_d t}a\right) \\ &\approx a\,\sigma_+^q + a^\dagger\sigma_-^q, \end{aligned} \tag{3.15}$$

where the properties of the eigenoperators are presented in Secs. 2.1 and 2.2 were used to derive the second line, and only the non-oscillating terms were kept in the last line. The coupling now can be interpreted as an exchange of quanta between the qubits and the resonator: at a rate g_q the resonator can excite the q-th qubit by emitting a photon ($a\,\sigma_+^q$ process) or conversely, absorb a photon emitted by a qubit ($a^\dagger\sigma_-^q$ process).

The full Hamiltonian in the rotating wave approximation then reads

$$\begin{aligned} H_{\mathrm{RWA}} &= \dot{U}_{\mathrm{RWA}}U_{\mathrm{RWA}} + U_{\mathrm{RWA}}HU_{\mathrm{RWA}}^\dagger \\ &= \delta\omega_r a^\dagger a + \frac{\delta\omega_q}{2}\,\sigma_z^q + g_q\left(a\sigma_+^q + a^\dagger\sigma_-^q\right) + \epsilon\left(a^\dagger + a\right), \end{aligned} \tag{3.16}$$

with the resonator detuning $\delta\omega_r = \omega_r - \omega_d$ and the qubit detuning $\delta\omega_q = \omega_q - \omega_d$ respectively. The structure of this Hamiltonian is equivalent to the *Jaynes Cummings Model* [19] which originally was used to describe the interaction of a single atom with a single mode of the electromagnetic field. From now on, the H_{RWA} will be written as H again.

3.4. Schrieffer-Wolff transformation

Next, a *Schrieffer-Wolff Transformation* [20] is used to obtain the dispersive approximation of the qubit-resonator system [1]. It is performed by applying a Unitary transformation $U = \exp(S)$, with an anti-hermitian generator S, in order to block-diagonalize the Hamiltonian approximately up to a given order. In this sense, it can be thought of as a

type of perturbation theory. A more detailed, but simplified explanation of the Schrieffer-Wolff transformation as a method of approximate block-diagonalization is given in [21], a more mathematically rigorous one in [22].

We want to first think algebraically about this method: Suppose the Hamiltonian H can be split into a solved, (block-)diagonalized part H_0 and an unsolved (off-diagonal) perturbation V, which is assumed to be small in some sense compared to H_0

$$H = H_0 + V. \tag{3.17}$$

Aiming to somehow remove V from this equation, replacing it with a correction that is already diagonalized, we apply a unitary transformation generated by S:

$$\psi' = e^S \psi \tag{3.18}$$

$$H' = e^S H e^{-S}. \tag{3.19}$$

Using the Taylor expansion of the matrix exponentials, H' can be written as

$$H' = H + [S, H] + \frac{1}{2}[S, [S, H]] + \dots. \tag{3.20}$$

We would like to have V cancelled by the commutator terms, such that only small corrections remain. The easiest way to achieve this is to choose S such that

$$[S, H_0] = -V. \tag{3.21}$$

Under this assumption the first two terms become

$$H + [S, H] = H_0 + [S, V], \tag{3.22}$$

while the second-order commutator becomes

$$\frac{1}{2}[S, [S, H]] = \frac{1}{2}[S, [S, H_0] - V] = -\frac{1}{2}[S, V] + \mathcal{O}\left(S^2\right). \tag{3.23}$$

Therefore we find for the transformed Hamiltonian

$$H' = H_0 + \frac{1}{2}[S, V] + \mathcal{O}\left(S^2\right). \tag{3.24}$$

This expression has the desired properties if

1. S is small in some sense, such that the higher orders of S can be neglected to obtain a valid approximation,
2. or the commutator $[S, V]$ is (block-)diagonal.

The first requirement can be checked when a suitable S is found. The generator will typically be proportional to some parameter λ, which in turn will be a function of the physical parameters occurring in H_0 and V. Analyzing λ then tells us under which conditions higher-order terms can be neglected.

Regarding the second requirement we can think about the properties of block-on and -off-diagonal matrices: If H_0 is block-diagonal, while V is of block-off-diagonal form, then Eq. (3.21) tells us that also S must be of block-off-diagonal form, since its commutator with H_0 must produce $-V$. Now according to [21], the commutator of two block-off-diagonal matrices is always block-diagonal, which would ensure that the second requirement is always fulfilled for our desired S. However, the claim is provided without proof or further source. Yet, at least in our present case, where V will be given by the coupling term $g_q\left(a\,\sigma_+^q + a^\dagger \sigma_-^q\right)$ it is easy to check that the logic holds up. Using the z-basis matrix representation of the qubit-ladder operators we can write with $V \equiv \sum_q V_q$

$$V_q = g_q \begin{pmatrix} 0 & a \\ a^\dagger & 0, \end{pmatrix} \tag{3.25}$$

where we can restrict V_q to the q-th qubit subspace, since the commutator $[S, V]$ annihilates all mixing terms between $q \neq p$ subspaces. 2×2 block-off diagonal matrices do indeed fulfill the property that their commutator is always block-diagonal. Hence, in this case we can use the following strategy to find a generator S:

3.4.1. Finding the generator S

From the previous analysis, it is clear that we are looking for a block-off-diagonal matrix S. Since it is also true, that a block-off-diagonal matrix can be obtained via commuting another block-off-diagonal matrix with a block-diagonal one, we could try and find S by first computing

$$\eta \equiv [H_0, V], \tag{3.26}$$

which is guaranteed to yield a block-off-diagonal, anti-hermitian matrix. η is then generalized by introducing constants multiplying its individual anti-hermitian building blocks. The correct constants yielding S will then be determined by enforcing $[\eta, H_0] = -V$. This heuristic approach for finding S is proposed in [23]. However, again, it is presented without general proof but only by application to 5 specific models for which it does work, one of which is the Jaynes-Cummings Hamiltonian. Still, this method is followed as a guideline for two different approaches in this work. In 3.7 we will do another Schrieffer-Wolff transformation to show under which circumstances the emerging flip-flop interactions between qubits can be neglected. There we will find a limitation of the η method of determining S, although it will still be helpful.

3.5. Dispersive approximation

We are now in a position to carry out the dispersive approximation by applying a Schrieffer-Wolff transformation to our system. We seek to find a generator S which block-diagonalizes the first three terms of the Hamiltonian 3.16. The remaining drive-term $H_d \equiv \epsilon \left(a^\dagger + a\right)$ will be transformed into the new basis afterwards.

First, the Hamiltonian 3.16 is divided into three terms

$$H = H_0 + H_d + V, \tag{3.27}$$

where

$$H_0 = \delta\omega_r a^\dagger a + \frac{\delta\omega_q}{2}\,\sigma_z^q, \tag{3.28}$$

$$H_d = \epsilon\left(a^\dagger + a\right), \tag{3.29}$$

$$V \;= g_q\left(a\sigma_+^q + a^\dagger\sigma_-^q\right). \tag{3.30}$$

We want to find S such that $[S, H_0] = -V$. Using Eq. 3.20 yields the dispersive Hamiltonian up to first order in S

$$H_1' = H_0 + H_d + \frac{1}{2}\,[S, V] + [S, H_d] + \mathcal{O}(S^2). \tag{3.31}$$

$H_d + [S, H_d]$ is the transformed Drive-Hamiltonian. Following 3.26 we calculate η:

$$\eta = [H_0, V] = g_p\left[\left(\delta\omega_r a^\dagger a + \frac{\delta\omega_q}{2}\,\sigma_z^q\right), \left(a\sigma_+^p + a^\dagger\sigma_-^p\right)\right]. \tag{3.32}$$

Using the commutator relations

$$\begin{aligned} \left[a,\, a^\dagger a\right] &= a, & \left[a^\dagger,\, a^\dagger a\right] &= -a^\dagger, \\ \left[\sigma_z^q,\, \sigma_\pm^p\right] &= \pm 2\sigma_\pm^q\delta_{q,p}, & \left[\sigma_+^q,\, \sigma_-^p\right] &= \sigma_z^q\delta_{q,p}, \end{aligned} \tag{3.33}$$

yields for η:

$$\begin{aligned} \eta &= -g_q\left\{\delta\omega_r\left(a\sigma_+^q - a^\dagger\sigma_-^q\right) + \delta\omega_q\left(\sigma_-^q a^\dagger - \sigma_+^q a\right)\right\} \\ &= g_q\left(\delta\omega_q - \delta\omega_r\right)\left(\sigma_+^q a - \sigma_-^q a^\dagger\right). \end{aligned} \tag{3.34}$$

Our *Ansatz* for S now consists of replacing the constant in front of the anti-hermitian operator $\left(\sigma_+^q a - \sigma_-^q a^\dagger\right)$ by an arbitrary constant λ_q:

$$S \equiv \lambda_q \left(\sigma_+^q a - \sigma_-^q a^\dagger\right). \tag{3.35}$$

The correct value of λ_q is determined by demanding that 3.21 holds:

$$\begin{aligned}
[S, H_0] &= \lambda_q \left[\left(\sigma_+^q a - \sigma_-^q a^\dagger\right),\ \left(\frac{\delta\omega_p}{2}\,\sigma_z^p + \delta\omega_r a^\dagger a\right)\right] \\
&= -\lambda_q \left(\delta\omega_q - \delta\omega_r\right)\left(a^\dagger \sigma_-^q + a\sigma_+^q\right) \\
&\stackrel{!}{=} -g_q \left(a^\dagger \sigma_-^q + a\sigma_+^q\right).
\end{aligned} \tag{3.36}$$

It follows that

$$\begin{aligned}
\lambda_q &= \frac{g_q}{\left(\delta\omega_q - \delta\omega_r\right)} = \frac{g_q}{\left(\omega_q - \omega_r\right)} \\
&\equiv g_q/\Delta_q,
\end{aligned} \tag{3.37}$$

where the detuning $\Delta_q = \omega_q - \omega_r$ between the q-th qubit and the resonator was defined.

The regime in which our approximation will be valid is now apparent: λ_q is small if the coupling constant g_q is small compared to the detuning between the respective qubit and the resonator. This so-called *dispersive regime* [1] is thus characterized by the condition

$$g_q \ll \left|\omega_r - \omega_q\right|. \tag{3.38}$$

For the dispersive approximation to hold, another condition must be satisfied, limiting the number of photons in the oscillator. This will be discussed at the end of the chapter in Sec. 3.8.

3.5.1. The dispersive Hamiltonian

The dispersive Hamiltonian is calculated by plugging S into 3.31:

$$\begin{aligned}
[S,\, V] &= \lambda_q g_p \left[\left(\sigma_+^q a - \sigma_-^q a^\dagger\right),\ \left(a^\dagger \sigma_-^p + a\sigma_+^p\right)\right] \\
&= \lambda_q g_p \left(\left[\sigma_+^q a,\, a^\dagger \sigma_-^p\right] - \left[\sigma_-^q a^\dagger,\, a\sigma_+^p\right]\right).
\end{aligned} \tag{3.39}$$

The commutators here are

$$\begin{aligned}
\left[\sigma_+^q a, a^\dagger \sigma_-^p\right] &= a\left[\sigma_+^q\,,\, a^\dagger \sigma_-^p\right] + \left[a\,,\, a^\dagger \sigma_-^p\right]\sigma_+^q \\
&= aa^\dagger\, \sigma_z^q\, \delta^{qp} + \sigma_-^p \sigma_+^q \\
&= \left(a^\dagger a + 1\right)\sigma_z^q\, \delta^{qp} + \sigma_-^p \sigma_+^q
\end{aligned} \tag{3.40}$$

and

$$\begin{aligned}
-\left[\sigma_-^q a^\dagger,\, a\sigma_+^p\right] &= -a^\dagger\left[\sigma_-^q\,,\, a\,\sigma_+^p\right] - \left[a^\dagger\,,\, a\,\sigma_+^p\right]\sigma_-^q \\
&= a^\dagger a\, \sigma_z^q\, \delta^{qp} + \sigma_+^p \sigma_-^q.
\end{aligned} \tag{3.41}$$

For $[S,\, V]$ this gives:

$$[S,\, V] = \lambda_q g_q \left(2\, a^\dagger a + 1\right)\sigma_z^q + \lambda_q g_p \left(\sigma_-^p \sigma_+^q + \sigma_+^p \sigma_-^q\right). \tag{3.42}$$

Introducing the *Dispersive coupling strength* χ_q

$$\chi_q \equiv \lambda_q\, g_q = \frac{g_q^2}{\Delta_q} \tag{3.43}$$

and using $\left(\sigma_-^q\sigma_+^q + \sigma_+^q\sigma_-^q\right) = \mathbb{1}$, the second term can be rewritten as

$$\lambda_q g_p \left(\sigma_-^p\sigma_+^q + \sigma_+^p\sigma_-^q\right) = \sum_{q>p} J_{qp}\left(\sigma_+^q\sigma_-^p + \sigma_+^p\sigma_-^q\right) + \sum_q \chi_q. \tag{3.44}$$

Here, we have introduced the *Flip-Flop-Interaction* coupling constant

$$J_{qp} \equiv \frac{g_q\, g_p}{2}\left(\frac{1}{\Delta_q} + \frac{1}{\Delta_p}\right). \tag{3.45}$$

The correction to the driving Hamiltonian is easily calculated as

$$[S\,,\, H_d] = \frac{\epsilon\, g_q}{\Delta_q}\left(\sigma_+^q + \sigma_-^q\right). \tag{3.46}$$

Neglecting the global phase-shift $\sum_q \chi_q$ and introducing the shorthand notation $\sum_{q>p} J_{qp} \equiv J_{q>p}$, we find the system Hamiltonian in the *dispersive approximation* as

$$\begin{aligned} H^D = &\frac{\delta\tilde{\omega}_q}{2}\,\sigma_z^q + (\delta\omega_r + \chi_q\sigma_z^q)\; a^\dagger a + \epsilon\left(a^\dagger + a\right) \\ &+ J_{q>p}\left(\sigma_+^q\sigma_-^p + \sigma_+^p\sigma_-^q\right) + \frac{\epsilon\, g_q}{\Delta_q}\left(\sigma_+^q + \sigma_-^q\right), \end{aligned} \tag{3.47}$$

with the Lamb-shifted qubit frequency $\delta\tilde{\omega}_q \equiv \delta\omega_q + \chi_q$. This dispersive Hamiltonian is interpreted as follows:

- $\chi_q\sigma_z^q$ represents a qubit-dependant shift of the resonator frequency, called the dispersive shift,
- the $J_{q>p}$ term represents a resonator-mediated qubit-qubit interaction: the qubits exchange quanta by emitting into the resonator and exciting other qubits in the register. This term induces a *flip-flop* type dynamic between the qubits, where they are flipping each other's spins - hence the name *flip-flop-interaction* [4],
- the last term represents an additional qubit-driving term resulting from the resonator drive in the original frame. This is a consequence of the entangling between qubits and resonator induced by the couplings g_q, which will be explained in the next subsection.

3.5.2. Transformation of the basis states

The actions of the operators $a^\dagger a$ and σ_z^q, occurring in Eq. 3.47, on the basis states $|n, x\rangle$ are defined by

$$\begin{aligned} a^\dagger a\,|n,x\rangle &= n\;|n,x\rangle\,, \\ \sigma_z^q\,|n,x\rangle &= s_z^q(x)\;|n,x\rangle\,. \end{aligned} \tag{3.48}$$

However, since we work in a transformed frame now, the kets in Equations 3.48 are actually transformed versions of some states $|\psi(n,x)\rangle$ in the original frame, namely according to Eq. 3.18

$$|n,x\rangle = e^S\,|\psi(n,x)\rangle\,. \tag{3.49}$$

To find which state $\psi(n,x)$ is transformed into $|n,x\rangle$ via e^S, we perform the inverse transformation on $|n,x\rangle$ and find

$$\begin{aligned} |\psi(n,x)\rangle &= e^{-S}\,|n,x\rangle \\ &= |n,x\rangle - S\,|n,x\rangle + \mathcal{O}(\lambda^2) \\ &= |n,x\rangle - \lambda_q\left(|n-1, x_{q+}\rangle - |n+1, x_{q-}\rangle\right), \end{aligned} \tag{3.50}$$

indicating that states with an equal number of *overall* excitations (counting qubit and resonator quanta) are mixed by λ. This explains the presence of the qubit drive term in the dispersive frame, since the so-called *dressed states* $|n, x\rangle$ are entangled states of the original *bare* qubit and resonator eigenstates and vice versa. As a result, the resonator drive also acquires a qubit component in the new basis. This subtlety is important if we later want to check the validity of the dispersive approximation, by comparing the time evolution generated by the dispersive Hamiltonian, with that generated by the full Jaynes-Cummings Hamiltonian. For example, if we evolve the state $|n, m\rangle$ under H^D, then, for a proper comparison, we need to evolve the combination of states given by the last line of 3.50 under H. Generally, the inverse transformation e^{-S} must be applied to any state evolving under H^D to obtain the equivalent evolution under H.

3.6. Schrieffer-Wolff transformation for driven Jaynes-Cummings model

In this section a Schrieffer-Wolff transformation is presented which approximately diagonalizes the full Jaynes-Cummings Hamiltonian 3.16 including the drive term. As such, it is a slight variation of the usual dispersive approximation carried out in the previous section. Again, the η method presented in [23] will be used to find the generator S.

We start by splitting H into

$$H = H_0 + V, \tag{3.51}$$

where V is the coupling between the qubits and the resonator, and $H_0 = \delta\omega_r a^\dagger a + \frac{\delta\omega_q}{2}\sigma_z^q + \epsilon\left(a^\dagger + a\right)$. To find the generator S, η is calculated using the previous result 3.34:

$$\begin{aligned}\eta &= [H_0,\, V] \\ &= g_q\left(\delta\omega_q - \delta\omega_r\right)\left(\sigma_+^q a - \sigma_-^q a^\dagger\right) + \epsilon\, g_q\left[\left(a^\dagger + a\right),\, \left(\sigma_+^q a + \sigma_-^q a^\dagger\right)\right] \\ &= g_q\left(\delta\omega_q - \delta\omega_r\right)\left(\sigma_+^q a - \sigma_-^q a^\dagger\right) + \epsilon\, g_q\left(\sigma_-^q - \sigma_+^q\right).\end{aligned} \tag{3.52}$$

This leads us to the following *Ansatz* for S:

$$S = \lambda_q\left(\sigma_+^q a - \sigma_-^q a^\dagger\right) + \mu_q\left(\sigma_+^q - \sigma_-^q\right). \tag{3.53}$$

Compared to the usual generator of the dispersive transformations, we have an additional anti-hermitian operator proportional to $\sigma_+^q - \sigma_-^q$.

Plugging this S into 3.21 to determine the constants yields

$$\begin{aligned}[S, H_0] &= \left[\left(\lambda_q\sigma_+^q a - \sigma_-^q a^\dagger\right) + \mu_q\left(\sigma_+^q - \sigma_-^q\right),\, \left(\frac{\delta\omega_p}{2}\sigma_z^p + \delta\omega_r a^\dagger a + \epsilon\left(a^\dagger + a\right)\right)\right] \\ &= -\lambda_q\left(\delta\omega_q - \delta\omega_r\right)\left(a^\dagger\sigma_-^q + a\sigma_+^q\right) + \left(\lambda_q\epsilon - \mu_q\,\delta\omega_q\right)\left(\sigma_+^q + \sigma_-^q\right) \\ &\overset{!}{=} -g_q\left(a^\dagger\sigma_-^q + a\sigma_+^q\right).\end{aligned} \tag{3.54}$$

The Equation can only be satisfied if

$$\lambda_q = \frac{g_q}{\Delta_q} \tag{3.55}$$

$$\mu_q = \frac{\epsilon}{\delta\omega_q}\lambda_q, \tag{3.56}$$

where λ_q is the same as in 3.37 of the previous section 3.5. Since the transformed Hamiltonian is given by

$$H' = H_0 + \frac{1}{2}[S, V] + \mathcal{O}(\lambda_q^2), \tag{3.57}$$

the only new extra term we need to calculate compared to section 3.5 is

$$\mu_q \left[\left(\sigma_+^q - \sigma_-^q\right) , V \right] = \frac{\epsilon\, g_q}{\delta\omega_q} \lambda_q \, \sigma_z^q \left(a^\dagger + a\right), \tag{3.58}$$

resulting in the transformed Hamiltonian

$$\begin{aligned} H' = &\frac{\delta\widetilde{\omega}_q}{2}\,\sigma_z^q + \left(\delta\omega_r + \chi_q\sigma_z^q\right)\, a^\dagger a + \epsilon\left(a^\dagger + a\right) + J_{q>p}\left(\sigma_+^q\sigma_-^p + \sigma_+^p\sigma_-^q\right) \\ &+ \frac{\epsilon\, g_q}{\delta\omega_q}\lambda_q\,\sigma_z^q\left(a^\dagger + a\right). \end{aligned} \tag{3.59}$$

H' coincides with the dispersive Hamiltonian 3.47 except for the last term, which is now a qubit-state dependent shift of the driving amplitude of the oscillator, instead of a qubit drive. It is worth noting, that while the drive correction in Eq. 3.47 is proportional to λ_q, the drive amplitude correction in this frame is proportional to λ_q^2 in the limit $\delta\omega_r \to 0$, i.e. for (nearly) resonant driving. This also means that dropping the drive corrections in the dispersive regime is better justified in this modified Schrieffer-Wolff transformation, because the correction term will be one order of magnitude smaller than in the usual case.

Also following section 3.5 the dressed states $|n, x\rangle$ correspond to the original-frame states $|\psi(n, x)\rangle$:

$$|\psi(n,x)\rangle = |n,x\rangle - \lambda_q\left(|n-1, x_{q+}\rangle - |n+1, x_{q-}\rangle\right) - \frac{\epsilon}{\delta\omega_q}\lambda_q\left(|n, x_{q+}\rangle - |n, x_{q-}\rangle\right). \tag{3.60}$$

3.7. Flip-Flop interaction

In this section, we want to treat the flip-flop interaction term $J_{q>p}\left(\sigma_+^q\sigma_-^p + \sigma_+^p\sigma_-^q\right)$ which appears when transforming to the dispersive frame and show, under which circumstances it is justifiably neglected. As already mentioned, it can be understood as a resonator mediated qubit-qubit interaction. The qubits exchange quanta of energy through the resonator, relaxing and exciting each other's energy states. Regarding energy conservation, it seems plausible that the strength of this interaction is highest between qubits of the same frequency. Therefore, the flip-flop interaction should be suppressed for increased detuning between the individual qubits.

To prove that this reasoning is actually sound, we can perform another Schrieffer-Wolff transformation, now treating the flip-flop term as the potential V, while the rest of the Hamiltonian is considered as H_0:

$$H = H_0 + V, \tag{3.61}$$

with

$$H_0 = \frac{\delta\widetilde{\omega}_q}{2}\,\sigma_z^q + \left(\delta\omega_r + \chi_q\sigma_z^q\right)\, a^\dagger a + \epsilon\left(a^\dagger + a\right) \tag{3.62}$$

$$V = J_{q>p}\left(\sigma_+^q\sigma_-^p + \sigma_+^p\sigma_-^q\right). \tag{3.63}$$

The drive-correction terms are neglected, since we will consider weak resonator drives only, where ϵ is much smaller than the couplings g_q.

η is again calculated according to 3.26:

$$\begin{aligned} \eta &= J_{q>p}\left[\left(\sigma_+^q\sigma_-^p + \sigma_+^p\sigma_-^q\right)\,, \left\{\frac{\widetilde{\omega}_k}{2}\,\sigma_z^k + \left(\delta\omega_r + \chi_k\sigma_z^k\right)\, a^\dagger a + \epsilon\left(a^\dagger + a\right)\right\}\right] \\ &= J_{q>p}\left[\left(\sigma_+^q\sigma_-^p + \sigma_+^p\sigma_-^q\right)\,, \left\{\frac{\widetilde{\omega}_k}{2}\,\sigma_z^k + \chi_k\sigma_z^k\, a^\dagger a\right\}\right]. \end{aligned} \tag{3.64}$$

To calculate this commutator, we can use the third identity of 3.33 and find

$$\left[\sigma_z^k\,, \left\{\sigma_+^q\sigma_-^p \pm \sigma_+^p\sigma_-^q\right\}\right] = 2\delta^{q,k}\left\{\sigma_+^q\sigma_-^p \mp \sigma_+^p\sigma_-^q\right\} - 2\delta^{p,k}\left\{\sigma_+^q\sigma_-^p \mp \sigma_+^p\sigma_-^q\right\} \tag{3.65}$$

implying that for some constant c_k

$$\sum_k c_k \left[\sigma_z^k\,,\,\left\{\sigma_+^q\sigma_-^p \pm \sigma_+^p\sigma_-^q\right\}\right] = (c_q - c_p)\left\{\sigma_+^q\sigma_-^p \mp \sigma_+^p\sigma_-^q\right\}, \tag{3.66}$$

which will be a useful identity. Applying this to Eq. 3.64 yields

$$\eta = J_{q>p}\left[(\delta\tilde{\omega}_p - \delta\tilde{\omega}_q) + 2\,(\chi_p - \chi_q)\,a^\dagger a\right]\left\{\sigma_+^q\sigma_-^p - \sigma_+^p\sigma_-^q\right\}. \tag{3.67}$$

This is a sum of two anti-hermitian operators suggesting the Ansatz

$$S = \left(c_{q>p} + d_{q>p}\,a^\dagger a\right)\left\{\sigma_+^q\sigma_-^p - \sigma_+^p\sigma_-^q\right\}, \tag{3.68}$$

with $c_{q>p}$ and $d_{q>p}$ being constants depending on q and p. The notation $q > p$ implies the sum $\sum_{q>p}$. To determine the constants we again demand $[S, H_0] = -V$. Using 3.65 we find

$$\begin{aligned}[S, H_0] = &\left(c_{q>p} + d_{q>p}\,a^\dagger a\right)\left[(\delta\tilde{\omega}_p - \delta\tilde{\omega}_q) + 2\,(\chi_p - \chi_q)\,a^\dagger a\right]\left\{\sigma_+^q\sigma_-^p + \sigma_+^p\sigma_-^q\right\}\\ &+\; d_{q>p}a^\dagger a\,\epsilon\left(a^\dagger - a\right)\left\{\sigma_+^q\sigma_-^p - \sigma_+^p\sigma_-^q\right\}\\ &\stackrel{!}{=} -J_{q>p}\left\{\sigma_+^q\sigma_-^p + \sigma_+^p\sigma_-^q\right\}.\end{aligned} \tag{3.69}$$

To establish equality, all resonator-operator terms on the left-hand side must vanish. This is only achievable if $d_{q>p} = 0$. Furthermore, the following constraint on the parameters of the system Hamiltonian needs to be imposed: $\chi_p - \chi_q = 0\ \forall q, p$. This demonstrates that the η method proposed in [23] is not guaranteed to successfully find a generator in all cases.

However, here, we are interested in the $\chi_q - \chi_p = 0$ case anyways, to replicate the setup suited for parity measurements as presented in Ref. [4] (parity measurements are discussed in Sec. 6.5, after solving the relaxation free master equation of the dispersive system).

Accepting this condition on χ_q we can continue our calculation with

$$c_{qp} = -\frac{J_{qp}}{(\omega_q - \omega_p)}, \tag{3.70}$$

with J_{qp} defined in 3.45, and find the transformed Hamiltonian

$$\begin{aligned}H' &= H_0 + \frac{1}{2}\,[S, V]\\ &= \frac{\delta\tilde{\omega}_q}{2}\,\sigma_z^q + (\delta\omega_r + \chi_q\sigma_z^q)\;a^\dagger a + \epsilon\left(a^\dagger + a\right)\\ &\quad + \frac{J_{q>p}\,J_{k>l}}{\omega_q - \omega_p}\left[\left(\sigma_+^q\sigma_-^p - \sigma_+^p\sigma_-^q\right)\,,\,\left(\sigma_+^k\sigma_-^l + \sigma_+^l\sigma_-^k\right)\right].\end{aligned} \tag{3.71}$$

However, it is also possible to find a transformation that holds for arbitrary χ_q. If at the beginning of the derivation, we choose to split

$$H = H_0 + H_\chi + V, \tag{3.72}$$

with

$$\begin{aligned}H_0 &= \frac{\delta\tilde{\omega}_q}{2}\,\sigma_z^q + \delta\omega_r\,a^\dagger a + \epsilon\left(a^\dagger + a\right)\\ H_\chi &= \chi_q\sigma_z^q\,a^\dagger a\end{aligned} \tag{3.73}$$

and V given by the flip-flop term again, we can derive that $[S, H_0] = -V$ holds for

$$S = \frac{J_{q>p}}{\omega_q - \omega_p}\left\{\sigma_+^q\sigma_-^p + \sigma_+^p\sigma_-^q\right\}, \tag{3.74}$$

just as before and find

$$\begin{aligned} H' &= H_0 + H_\chi + [S, H_\chi] + \frac{1}{2}[S, V] \\ &= \frac{\delta\tilde{\omega}_q}{2}\sigma_z^q + (\delta\omega_r + \chi_q\sigma_z^q)\; a^\dagger a + \epsilon\left(a^\dagger + a\right) \\ &+ \frac{J_{q>p}\, J_{k>l}}{\omega_q - \omega_p}\left[\left(\sigma_+^q\sigma_-^p - \sigma_+^p\sigma_-^q\right),\, \left(\sigma_+^k\sigma_-^l + \sigma_+^l\sigma_-^k\right)\right] \\ &+ \frac{J_{q>p}}{\omega_q - \omega_p}\, 2\left(\chi_q - \chi_p\right)\; a^\dagger\left\{\sigma_+^q\sigma_-^p + \sigma_+^p\sigma_-^q\right\}. \end{aligned} \tag{3.75}$$

The last term corresponds to the correction $[S, H_\chi]$.

Considering these results and that $J_{qp} \sim \chi$, we see that the flip-flop interaction is negligibly small compared to the dispersive shift for $|\omega_q - \omega_p| \gg \chi$, and $\chi_q - \chi_p \sim 0$, confirming the intuition that increasing qubit-qubit detuning should suppress the flip-flops. In section 3.9 we will go into more detail on how to choose the qubit frequencies and coupling strengths appropriately.

3.8. Comparison to exact diagonalization - critical photon number

Before we end this chapter by choosing suitable frequencies ω_q, $\omega_{r,d}$ and couplings g_q, we compare the dispersive Hamiltonian with the one obtained by exact diagonalization. This leads to another limitation by showing that the exact dispersive shift χ is dependent on the number of photons in the resonator n_{crit}. Therefore, the dispersive approximation above is only valid if the mean number of photons $\bar{n}$ is well below the critical photon number n_{crit} [24].

In [24] and [25] an exact diagonalization of the (non-driven) Jaynes-Cummings Hamiltonian H_{JC} is derived. For a single qubit the corresponding unitary operator D is generated by

$$\Lambda(N_q) = -\frac{\arctan\left(2\lambda\sqrt{N_q}\right)}{2\sqrt{N_q}}\left\{\sigma_+ a - \sigma_- a^\dagger\right\}, \tag{3.76}$$

with $\lambda = g/\Delta_q$ as before. Here $N_q = a^\dagger a + \Pi(e)$ is the number operator counting all excitations in the system, and $\Pi(e)$ projects onto the excited state of the qubit. Diagonalizing the Jaynes-Cummings Hamiltonian via $D = \exp\{-\Lambda(N_q)\}$ leads to

$$D^\dagger H_{JC} D = \delta\omega_r\, a^\dagger a + \frac{\omega_q}{2}\,\sigma_z - \frac{\Delta_q}{2}\left(1 - \sqrt{1 + 4\lambda^2 N_q}\right)\sigma_z. \tag{3.77}$$

An "exact" dispersive shift is obtained by treating the operator N_q semi-classically and deriving the resulting amplitude of the driven oscillator in dependence on the qubit state.[26] This leads to [27],[26]

$$\chi(n) = \frac{\chi_0}{\sqrt{1 + n/n_{crit}}}, \tag{3.78}$$

where n is the number of photons in the resonator, $\chi_0 = g^2/\Delta_q$ and n_{crit} is the critical photon number

$$n_{crit} = \left(\frac{\Delta_q}{2g}\right)^2. \tag{3.79}$$

For $n \ll n_{crit}$, this reduces to χ_0 and the dispersive approximation is restored. The first order correction is

$$\chi(n) \approx \chi_0\left(1 - \frac{n}{2n_{crit}}\right). \tag{3.80}$$

In the case of multiple qubits coupled to the resonator, N_q can be generalized in a straightforward way to $N_q = a^\dagger a + \sum_q \Pi_e^q$, where Π_e^q projects onto the excited state of the q-th bit. However, the diagonalized Hamiltonian will only approximately be of the same form as in Eq. 3.77 [25], implying that 3.79 is also only approximately correct in the multi-qubit case.

For the scope of this work, we choose our parameters such that $n \ll n_{crit}$ approximately holds, such that we are justified to neglect the dependency of χ in n. In chapter 7 numerical solutions of the dispersive dynamics are compared with those of the exact Hamiltonian to check when the approximation breaks down.

3.9. Choosing the qubit frequencies and coupling strengths appropriately

In the previous chapters, several approximations were introduced, each imposing certain constraints on the parameters:

- the dispersive regime 3.38 defined by $|\omega_q - \omega_r| \gg g_q$ with the additional constraint 3.79 limiting the permissible number of photons in the resonator,
- the non-interacting regime defined by $|J_{qp}| \ll |\omega_q - \omega_p|$ (Equation 3.75), where the flip-flop interaction is negligible compared to the dispersive shift, combined with
- $\chi_q = \chi_p$, which suppresses the flip-flop interaction further and is also a necessary condition if the resonator is to be used for parity measurements as presented in [4],
- the qubit approximation, which allows us to treat the transmon (or any other artificial or real atom) as a two-level system in the first place.

The goal of this section is to introduce a tuning scheme that is used for the analytical and numerical calculations in the subsequent chapters. Additionally, we explore how the aforementioned conditions can be met within the framework of the scheme. Furthermore, realistic physical values for the transmon parameters are considered to assess the plausibility of our scheme.

3.9.1. Frequencies and coupling

We start by fixing the frequencies of the qubits. The core of our scheme is the following choice of the q-th frequency, where we make sure that all qubits are detuned with respect to the resonator, and with respect to each other:

$$\omega_q = \omega_r - q \cdot \delta\omega_1 \qquad \delta\omega_1 > 0 \tag{3.81}$$

$$\longrightarrow \quad \Delta_q = -q \cdot \delta\omega_1. \tag{3.82}$$

Here, $\delta\omega_1$ is the detuning between the first bit and the resonator. The detuning of all other qubits is a positive-integer multiple of $\delta\omega_1$.

Next, we to fix $\chi_q \equiv \chi$ to be equal for all qubits. Since $\chi_q = g_q^2/\Delta_q$ this is achieved by choosing:

$$g_q = \sqrt{q} \cdot g \quad \longrightarrow \quad \chi = -\frac{g^2}{\delta\omega_1}, \tag{3.83}$$

with some constant g. For the flip-flop constant J_{qp} (Equation 3.45), we obtain

$$J_{qp} = -\frac{g^2}{2\,\delta\omega_1} \cdot \frac{(q+p)}{\sqrt{q \cdot p}} = \frac{\chi}{2} \cdot \frac{(q+p)}{\sqrt{q \cdot p}} \approx \frac{\chi}{2}, \tag{3.84}$$

where the approximation holds since the function $(q+p)/\sqrt{q \cdot p} \sim 1$ for p and q of Order $\mathcal{O}(10)$. Finally, the critical photon number n_{crit} (Equation 3.79) is determined to be

$$n_{crit} = \min\left\{\frac{q \cdot \delta\omega_1^2}{4 \cdot g^2}\right\} = \frac{\delta\omega_1^2}{4 \cdot g^2}. \tag{3.85}$$

Next, the conditions listed at the beginning of this section will be presented in the frame of this tuning scheme.

3.9.2. Checking the coupling parameter conditions

The first condition to be checked is the one defining the dispersive regime (3.38). For our choices presented above, the condition reads

$$g \ll \sqrt{q} \cdot \delta\omega_1 \quad \forall q \quad \Leftrightarrow \quad g \ll \delta\omega_1. \tag{3.86}$$

The condition on the flip-flop coupling constant becomes

$$\left|\frac{\chi}{2}\right| \ll |(q-p)|\delta\omega_1 \quad \Leftrightarrow \quad \frac{g^2}{2 \cdot \delta\omega_1^2} \ll |(q-p)|. \tag{3.87}$$

This condition is easily satisfied in the dispersive regime since Eq. 3.86 implies that $g/\delta\omega_1 \ll 1$ while $|(q-p)| \geq 1$ for $q \neq p$.

3.9.3. Checking the qubit approximation condition

In the derivation of the transmon Hamiltonian (Sec. 3.1), it is assumed that all excited states beyond the first can be safely disregarded. This assumption remains valid only if none of the other qubits are tuned so that their first excited state resonates with a second or higher excited state of another qubit. For our scheme, we choose that the first-excited states of all qubits-qubits with $q \neq 1$ lie below the second excited state of the first qubit. Since all qubits are tuned with a linearly decreasing frequency, this imposes an upper limit on the number of qubits that can be integrated into this tuning setup.

According to [18] typical transmon frequencies have a range of up to 10 GHz and anharmonicities of up to 300 MHz. Now, say there is a difference of ~ 10 GHz between the second and the first excited state of the first transmon. The first excited state of the 2nd transmon will be $\delta\omega_1/2\pi$ Hz lower than the first one of the first transmon. Neglecting the anharmonicity for the moment, the difference between their second excited states will be $\sim 2\,\delta\omega_1/2\pi$ Hz. In general, it is clear that the q-th transmon has a second excited state with a frequency $\sim 2q\,\delta\omega_1/2\pi$ Hz below the second excited frequency of the first transmon. With a total number of N qubits we obtain the following approximate condition to ensure that all second excited states still lie above the first excited state of the first qubit:

$$2N\,\frac{\delta\omega_1}{2\pi} \lesssim 10\,\text{GHz} \quad \Leftrightarrow \quad N \lesssim \frac{\pi}{\delta\omega_1}\,10\,\text{GHz}. \tag{3.88}$$

This of course is only a very rough estimate at which numbers of qubits N the resonator might become "too crowded".
Now, since we want to work in the dispersive regime, the qubits detuning $\delta\omega_1$ must be much larger than the coupling strength g. According to [28] typical transmon coupling strengths lie around 100 MHz. This means, that $\delta\omega_1$ should at least be chosen to be ~ 1 GHz, which would limit our framework to $N \lesssim 5$ according to 3.88.

3.9.4. Critical photon number

The comparison of exact diagonalization with the dispersive approximation reveals that the mean number of photons $\bar{n}$ in the resonator must be much lower than the critical

photon number given by 3.85 in our scheme. The mean photon number of the resonator can only be determined after solving the master equation in the dispersive regime, as will be conducted in chapter 6. Still, we discuss the necessary parameter conditions already here. Solving the master equation yields the following expression for the maximum number of photons (see Sec. 6.5 Eq. 6.72)

$$\bar{n} = \frac{\epsilon^2}{\kappa^2/4}, \tag{3.89}$$

where κ is the dissipation rate of the resonator to be introduced in Chapter 5. The drive strength and dissipation rate can essentially be chosen independently of the qubit frequency and coupling strength g. Therefore, it should pose no challenge to satisfy the resulting condition

$$4\,\frac{\epsilon^2}{\kappa^2} \ll \frac{\delta\omega_1^2}{4g^2} = \left|\frac{\delta\omega_1}{4\chi}\right|, \tag{3.90}$$

especially since $\delta\omega_1/g$ is large in the dispersive approximation. We revisit this condition later when we solve the master equation numerically in chapter 7, where we also check how the discrepancy between the full dynamics given by 3.16 and the dispersive dynamics increases with increasing ϵ.

3.10. Summary and final dispersive Hamiltonian

In this section, we summarize the results of this chapter and write down the final dispersive Hamiltonian that will be solved analytically in Chapters 6 and 8. In the previous sections, two Hamiltonians were obtained (Eqs. 3.47 and 3.59). We consider the system at small drive strengths ϵ, as well as large qubit detunings, such that the flip-flop coupling can be neglected. The drive correction terms as well as the qubit-qubit interaction are dropped, and we arrive at the final dispersive Hamiltonian, employing the tuning scheme of the previous section:

$$H = (\delta\omega_r + \chi_q\sigma_z^q)\,a^\dagger a + \frac{\delta\tilde{\omega}_q}{2}\,\sigma_z^q + \epsilon\left(a^\dagger + a\right), \quad \text{where} \tag{3.91}$$

$$\delta\omega_r = \omega_r - \omega_d, \tag{3.92}$$

$$\delta\tilde{\omega}_q = \omega_q - \omega_d + \chi_q, \tag{3.93}$$

$$\omega_q = \omega_r - q\cdot\delta\omega_1, \tag{3.94}$$

$$\chi_q = \chi. \tag{3.95}$$

Unless otherwise stated, this Hamiltonian will be studied from now on in this thesis.

4. The Lindblad master equation

The preceding chapters have focused on the dynamics and formalism of dispersively coupled qubits, operating under the assumption that the system is isolated from any potentially surrounding systems.

In this chapter, we transition from closed systems to the treatment of open Markovian dynamics within the framework provided by the Gorini-Kossakowski-Sudarshan-Lindblad (GKSL) master equation [29] [30], by giving a short review of the Lindbladian, its most important properties and the context in which it emerges. Then we present a scheme to vectorize the Lindbladian superoperator $\mathcal{L}$ and the density matrix ρ, which is an important tool for the numerical calculations presented in chapter 7, as well as some useful manipulations that simplify the analytic calculations when solving for the density matrix. Finally, we show how an eigenvector decomposition of the vectorized density matrix can be used to numerically calculate the time evolution of ρ under $\mathcal{L}$.

A microscopic derivation of the Lindblad equation for the physical systems considered in this thesis is given in the next chapter 5.

4.1. Review of the Lindblad equation and open system dynamics

We consider our system S to be embedded in an environment (or bath) B. The combined system-bath density matrix evolves according to the von Neumann equation [12]

$$\dot{\rho} = -\mathrm{i}\,[H, \rho]\,, \tag{4.1}$$

where H is the Hamiltonian for the total system $S \otimes B$. The dynamics of the system S alone are obtained from the von Neumann equation by tracing out the bath-degrees of freedom. Denoting $\rho_S \equiv \mathrm{Tr}_B\,(\rho)$ as the reduced density matrix of the system, where Tr_B is the partial trace over all bath-degrees of freedom, we find the formal reduced master equation

$$\dot{\rho}_S = -\mathrm{i}\,\mathrm{Tr}_B\,[H, \rho]\,. \tag{4.2}$$

It can be shown that, if we require the derivative of $\rho_S(t)$ to be independent of ρ_S at earlier times - that is, if we impose markovian dynamics - there exists a super operator $\mathcal{L}$ which satisfies [31]

$$\dot{\rho}_S = \mathcal{L}\rho_S. \tag{4.3}$$

This superoperator is called the *Lindbladian*. It generates the time evolution of the reduced density matrix via

$$\rho_S(t) = e^{\mathcal{L}t}\rho_S(0), \tag{4.4}$$

where the exponential $e^{\mathcal{L}t}$ is a quantum mechanical dynamical map. Dynamical maps are linear, trace preserving and (completely) positive, thus preserving the properties of a state-matrix:

$$e^{\mathcal{L}t}\,(\rho_1 + \rho_2) = e^{\mathcal{L}t}\rho_1 + e^{\mathcal{L}t}\rho_2 \tag{4.5}$$

$$\mathrm{Tr}\{\mathcal{L}\rho_S\} = 0 \quad \Leftrightarrow \quad \mathrm{Tr}\big\{e^{\mathcal{L}t}\rho_S(0)\big\} = \mathrm{Tr}\{\rho_S(0)\} = 1 \tag{4.6}$$

$$\rho_S \geq 0 \quad \Leftrightarrow \quad e^{\mathcal{L}t}\rho_S \geq 0, \tag{4.7}$$

where $\rho_S \geq 0$ means that ρ_S is positive semi-definite, i.e. has non-negative eigenvalues. It can be shown that these requirements are fulfilled if $\mathcal{L}$ is of Lindbladian form

$$\mathcal{L}\rho_S = -\mathrm{i}\,[H, \rho_S] + \sum_i \kappa_i \mathcal{D}[A_i]\rho_S. \tag{4.8}$$

The commutator describes unitary evolution while the dissipators $\mathcal{D}[A_i]$, defined by

$$\mathcal{D}[A]\rho_S = A\rho_S A^\dagger - \frac{1}{2}\left\{A^\dagger A, \rho_S\right\} \tag{4.9}$$

can be interpreted as irreversible channels through which ρ_S exchanges energy and information with the bath at a rate κ_i. The first term in $\mathcal{D}$ is called the jump-term (which can be easily understood when considering that a typical jump-operator for the dissipative oscillator is $a\rho a^\dagger$), describing quantum jumps, while the anti-commutator ensures that the dissipator is trace preserving.

4.2. Vectorizing the Lindblad equation

In its usual form, the Lindblad equation is given as an operator equation, where the linear *super operator* $\mathcal{L}$ acts on the operator ρ_S. However, it is also possible to vectorize this equation and transform $\mathcal{L}$ into a linear operator acting on a vectorized state-matrix $\vec{\rho}_S$. This is desirable if one wants to solve the Lindblad equation numerically, since computer algebra programs like Mathematica can handle large matrices more easily than operators acting on matrices, which simplifies the development of numerical-solution programs. Furthermore, by transitioning to a vector equation more closely resembling those typically found in quantum mechanics, it becomes more straightforward to apply techniques familiar to state-vector quantum mechanics. This adaptation can simplify analytical calculations as well.

4.2.1. Vectorizing the density matrix

The first step to vectorize the Lindblad equation is to recognize that the state matrix ρ_S can be mapped to a vector in a product Hilbert space. Say we have a basis in $\mathcal{H}$ denoted by vectors $\{|n\rangle\}$. A general density matrix is then written as

$$\rho = \sum_{n,m} c_n c_m^* \,|n\rangle\langle m|\,, \tag{4.10}$$

where formally $|n\rangle\langle m| = |n\rangle \otimes \langle m|$ is a basis element of the product Hilbert space $\mathcal{H} \otimes \mathcal{H}^\dagger$. Therefore, we can interpret Eq. 4.10 as a decomposition of ρ into linearly independent basis vectors $|n\rangle\langle m|$ with coefficients $c_n c_m^*$ on the vector-space $\mathcal{H} \otimes \mathcal{H}^\dagger$. The vectorization can be made explicit by transposing the bras to introduce the vectorized state-matrix $\vec{\rho}$:

$$\vec{\rho} \equiv \sum_{n,m} c_n c_m^* \,|n\rangle \otimes |m\rangle\,. \tag{4.11}$$

It is evident that $\vec{\rho}$ contains the same information as ρ, albeit structured differently. For example, rather than being presented in a $N \times N$ matrix, the coefficients $c_n c_m^*$ are organized into a N^2 dimensional vector instead.

4.2.2. Vectorizing the Lindbladian

Having introduced the vectorization $\rho \to \vec{\rho}$, we need to find the corresponding vectorization of the Lindbladian.

It suffices to consider terms of the form $A\,|n\rangle\langle m|\,B$ where A and B are operators on $\mathcal{H}$. B acts on the bra from the right, yielding $\langle m|\,B$. Transposing gives $B^T\,|m\rangle$. Therefore, we can make the following identification:

$$A\,|n\rangle\langle m|\,B \quad \Leftrightarrow \quad A\,|n\rangle \otimes B^T\,|m\rangle = \left(A \otimes B^T\right)|n\rangle \otimes |m\rangle\,, \tag{4.12}$$

which, due to linearity, can be extended to an arbitrary state to yield the vectorization rule

$$A \cdot \rho \cdot B \quad \Leftrightarrow \quad \left(A \otimes B^T\right)\vec{\rho}. \tag{4.13}$$

Using this rule the Lindblad equation can be easily vectorized. For the commutator, we find

$$[H, \rho] \quad \Leftrightarrow \quad \Big[H \otimes \mathbb{1} + \mathbb{1} \otimes H^T\Big]\vec{\rho}, \tag{4.14}$$

while the vectorized dissipator is given by

$$\mathcal{D}[A]\rho \quad \Leftrightarrow \quad (A \otimes A^*)\,\vec{\rho} - \frac{1}{2}\left\{A^\dagger A \otimes \mathbb{1} + \mathbb{1} \otimes A^T A^*\right\}\vec{\rho}, \tag{4.15}$$

where $A^* \equiv \left(A^\dagger\right)^T$. We can see that the vectorized commutator is an anti-hermitian operator responsible for generating unitary dynamics. This is not the case for the dissipator, which is consistent with the fact that it describes the non-unitary part of the evolution. In total, the vectorized Lindbladian reads

$$\mathcal{L} = -\mathrm{i}\Big[H \otimes \mathbb{1} + \mathbb{1} \otimes H^T\Big] + \sum_i \kappa_i \left\{A_i \otimes A_i^* - \frac{1}{2}\left(A_i^\dagger A_i \otimes \mathbb{1} + \mathbb{1} \otimes A_i^T A_i^*\right)\right\}. \tag{4.16}$$

It is worth noting that the dynamical map $e^{\mathcal{L}t}$ is now a matrix exponential. Hence, the usual rules for matrix-exponentiation, like the Baker-Campbell-Hausdorff formula [14] can be applied as well. This can be useful if $\mathcal{L}$ can be split into two commuting parts. For $\mathcal{L} = \mathcal{L}_1 + \mathcal{L}_2$ with $[\mathcal{L}_1, \mathcal{L}_2] = 0$ we can factorize the time evolution operator as

$$e^{\mathcal{L}t} = e^{\mathcal{L}_1 t} e^{\mathcal{L}_2 t}. \tag{4.17}$$

Therefore, if the time-evolution generated by $\mathcal{L}_1$ is already known, we can use this factorization to effectively remove $\mathcal{L}_1$ from the equation and focus on solving $\dot{\rho} = \mathcal{L}_2\rho$ to find $e^{\mathcal{L}_2 t}$, which can simplify calculations significantly.

4.3. Eigenvector decomposition of the vectorized density matrix

With $\mathcal{L}$ being represented by a matrix, the possibility arises to find a complete set of eigenvectors $\left\{\vec{v}_i\right\}$ of $\mathcal{L}$ that form a basis of the product Hilbert space in which $\vec{\rho}$ lives in. In general, no property of the Lindblad equation would guarantee the resulting Lindbladian matrix to be diagonalizable. In fact, points in parameter-space where $\mathcal{L}$ is not diagonalizable are referred to as *exceptional points* in the literature [32]. However, as the name suggests, for most problems these points are the exception, not the rule. In this thesis, we will assume that we operate only at non-exceptional points where the eigenvectors of $\mathcal{L}$ do form a complete basis. In that case, it is possible to write any initial density matrix as a linear sum of these eigenvectors:

$$\vec{\rho}(0) = \sum_i c_i(0)\vec{v}_i. \tag{4.18}$$

Each vector $\vec{v}_i$ corresponds to a (possibly degenerate) eigenvalue λ_i. Using this decomposition, the time evolution of ρ is trivially given by

$$\vec{\rho}(t) = e^{\mathcal{L}t}\vec{\rho}(0) = \sum_i c_i(0)e^{\lambda_i t}\vec{v}_i. \tag{4.19}$$

4.3.1. Stationary state

Most dissipative dynamics are characterized by a stationary state, which is approached by the system as $t \to \infty$. This state must therefore satisfy

$$\mathcal{L}\vec{\rho}_s = 0 \quad \Leftrightarrow \quad e^{\mathcal{L}t}\vec{\rho}_s = \vec{\rho}_s, \tag{4.20}$$

i.e. it corresponds to an eigenvector of $\mathcal{L}$ with eigenvalue 0. We can conclude that the real parts of all λ_i must be negative: Over time all modes except for the stationary mode $\vec{\rho}_s$ decay [33]. The corresponding matrix ρ_s must have a trace of 1: $\mathrm{Tr}\,\rho_s = 1$. Since the eigenvectors λ_i can carry an arbitrary imaginary part, additionally to their negative real part, it follows that all eigenmodes except for the stationary one must correspond to matrices with trace zero: $\mathrm{Tr}\,v_i = 0$ for $i \neq s$, since otherwise the condition $\mathrm{Tr}\,\rho(t) = 1$ can not be satisfied for all times t and for arbitrary initial states $\rho(0)$.

Therefore, we identify two important properties of the stationary state:

1. it corresponds to an eigenmode of $\mathcal{L}$ with eigenvalue 0,
2. of all eigenmodes $\vec{v}_i$, it is the only one corresponding to a matrix with a non-vanishing trace.

These two traits will be used in Chapter 7 to correctly identify the stationary mode among the numerically calculated eigenvectors of different $\mathcal{L}$.

4.3.2. Decomposing a given initial state into eigenmodes

To find the time evolution of a given initial state $\vec{\rho}(0)$, the vector must be decomposed into a sum of the eigenmodes $\vec{v}_i$. The task here is to correctly find the coefficients $c_i(0)$ multiplying the eigenmodes. Adopting for a moment the usual bra-ket notation from Quantum mechanics, we can perform the decomposition by using the spectral decomposition of the identity $\mathbb{1}$:

$$\mathbb{1}\,|\rho(0)\rangle = \sum_i |v_i\rangle \underbrace{\langle v_i|\rho(0)\rangle}_{c_i(0)}. \tag{4.21}$$

Since $\mathcal{L}$ is not a hermitian operator, the "bra" $\langle v_i|$ corresponding to the eigenmode $|v_i\rangle$, is not generally given by the hermitian conjugate of $|v_i\rangle$. However, it is clear that $\langle v_i|$ must be a *left-sided eigenvector* of $\mathcal{L}$. This can be seen by applying the spectral decomposition to the time evolved state $|\rho(t)\rangle$:

$$\begin{aligned} \mathbb{1}\,|\rho(t)\rangle = \sum_i |v_i\rangle\langle v_i|\, e^{\mathcal{L}t}\,|\rho(0)\rangle \overset{!}{=} \sum_i |v_i\rangle\, c_i(0) e^{\lambda_i t} \\ \Leftrightarrow \quad \langle v_i|\, e^{\mathcal{L}t} = \langle v_i|\, e^{\lambda_i t}. \end{aligned} \tag{4.22}$$

Going back to the vector notation and denoting $\vec{u}_i \equiv \langle v_i|$ as the left-sided eigenvector of $\mathcal{L}$ to the eigenvalue λ_i we find

$$c_i = \vec{u}_i \cdot \vec{\rho} \tag{4.23}$$

$$\vec{u}_i\mathcal{L} = \vec{u}_i\lambda_i. \tag{4.24}$$

It follows that, to find the decomposition of $\vec{\rho}$ it is necessary to find the left-sided eigenvectors of $\mathcal{L}$, as well as the right-sided eigenvectors $\vec{v}_i$. Of course, both can be found by solving the respective eigenvalue equations. However, given the right-sided vectors $\vec{v}_i$, it is also possible to construct the left-sided ones, without the need to solve the left-sided eigenequation. We start with the eigenvalue equation for $\vec{v}_i$:

$$\mathcal{L}\vec{v}_k = \lambda_k\vec{v}_k. \tag{4.25}$$

Rewriting this equation in component notation (using the Einstein sum convention) yields

$$\mathcal{L}_{ij} v_{jk} = v_{ij} \lambda_{jk}, \tag{4.26}$$

where v_{jk} is the j component of the k-th eigenvector, and we introduced the diagonal matrix $\hat{\lambda}$, defined by its components $\left(\hat{\lambda}\right)_{ij} = \delta_{ij}\lambda_j$. Furthermore, we can introduce the matrix $\hat{v}$ whose columns are given by the eigenvectors $\vec{v}_i$: $(\hat{v})_{jk} = v_{jk}$. Using this notation, the eigenvalue equation is cast into the form of a matrix equation:

$$\mathcal{L}\hat{v} = \hat{v}\hat{\lambda}. \tag{4.27}$$

Multiplying with $\hat{v}^{-1}$ from the left and the right yields the left-sided eigenvalue equation:

$$\hat{v}^{-1}\mathcal{L} = \hat{\lambda}\hat{v}^{-1} \tag{4.28}$$

$$\Leftrightarrow \quad (\hat{v}^{-1})_{ij}\mathcal{L}_{jk} = \lambda_{ij}(\hat{v}^{-1})_{jk}. \tag{4.29}$$

To see that this is the correct equation we define $\hat{u} \equiv \hat{v}^{-1}$ and label the i-th row of $\hat{u}$ as $\vec{u}_i$. This leads to

$$u_{ij}\mathcal{L}_{jk} = \lambda_{ij}u_{jk} \quad \Leftrightarrow \quad \vec{u}_i\mathcal{L} = \lambda_i\vec{u}_i. \tag{4.30}$$

In summary, to construct the left-sided eigenvectors from the right-sided ones, the following protocol can be identified:

1. Construct the matrix $\hat{v}$ by arranging the right-sided vectors $\vec{v}_i$ as its columns.
2. Compute $\hat{u} = \hat{v}^{-1}$.
3. Identify the i-th left-sided eigenvector as the i-th row of $\hat{u}$.

We will follow this protocol in Section 7.4 to numerically find the time evolution of various initial density matrices.

5. Microscopic derivation of the dispersive master equation

Having introduced the Lindblad formalism describing markovian open system dynamics, we now turn to microscopic derivations of the master equations describing the pure dephasing of qubits, as well as the dissipation of the uncoupled systems first, followed by a derivation of the master equation of the coupled qubit-oscillator system.

5.1. Pure dephasing of qubits

To calculate the pure dephasing of a qubit due to energy fluctuations, we first give a recapitulation of the density matrix and its use in statistical quantum physics.

The pure density matrix ρ of a Quantum system in state $|\psi\rangle$ is given by

$$\rho = |\psi\rangle \langle\psi| . \tag{5.1}$$

A classical statistical mixture of quantum states $\{|\psi_n\rangle\}$ is then just constructed via

$$\rho = \sum_n p_n \ |\psi_n\rangle \langle\psi_n| , \tag{5.2}$$

where the real numbers p_n are the classical probabilities to find the system in $|\psi_n\rangle$, or in the case of a continuous index n:

$$\rho = \int p(n) \ |\psi_n\rangle \langle\psi_n| \ \mathrm{d}n, \tag{5.3}$$

where $p(n)$ is now a probability density [34].

The following calculation shows how fluctuations in the energy levels of a qubit lead to similar statistical mixtures of the density matrix, which in turn then shows to have decaying off-diagonal elements. This process is called *Dephasing*

5.1.1. Energy fluctuations lead to random phase shifts

According to [5] the charge Q, flux Φ and critical current I_c (on which the Josephson Energy E_J depends) are typical noise sources for the transmon energy 3.6. Let's say these quantities λ_i, where the index i runs through Q, Φ and I_c, fluctuate independently. At any moment t we can write

$$\lambda_i(t) = \lambda_i^0 + \delta\lambda_i(t), \tag{5.4}$$

where λ_i^0 is the mean value of the quantity, and $\delta\lambda(t)$ its deviation at time t due to random fluctuations. For small fluctuations, the transmon Hamiltonian can then be expanded in a Taylor series as follows [5].

$$H_{tm} \approx \frac{E_{tm}}{2}\sigma_z + \sum_i \frac{\partial E_{tm}}{\partial \lambda_i}\delta\lambda_i \, \sigma_z. \tag{5.5}$$

Given an initial transmon state $|\psi(0)\rangle = a\,|e\rangle + b\,|g\rangle$, the time evolved state is

$$|\psi(t)\rangle = a\, e^{-\mathrm{i}\, E_{tm} t/\hbar - \mathrm{i}\theta(t)} \,|e\rangle + b\, e^{\mathrm{i}\, E_{tm} t/\hbar + \mathrm{i}\theta(t)} \,|g\rangle , \tag{5.6}$$

where

$$\theta(t) \equiv \frac{1}{\hbar} \sum_i \frac{\partial E_{tm}}{\partial \lambda_i} \int_0^t \delta\lambda_i(s)\, \mathrm{d}s \tag{5.7}$$

is the random phase accumulated between the ground and the excited state due to the energy fluctuations.

Our goal now is to obtain the probability density $P_t(\theta)$ of finding a phase shift θ at time t. Having found $P_t(\theta)$, we then construct the density matrix of the transmon according to equation (5.3).
The following calculation is a simplified qualitative derivation of the resulting dephasing times. A more rigorous and quantitative treatment can be found in [5] and [35].

5.1.2. White noise approximation

For our simplified treatment, we assume that the fluctuations $\delta\lambda_i$ are a source of *white noise*. White noise X is characterized by: [36]

- its expectation value $\mathrm{E}(X(t)) = 0$, and
- its auto correlation function $\mathrm{E}(X(t)X(0)) \propto \delta(t)$.

We assume the most simple form of white noise, where the proportionality factor of the auto-correlation function, which characterizes the amplitude of the noise, is constant in time

$$\mathrm{E}(\delta\lambda_i(t_1)\delta\lambda_i(t_2)) = A_i^2 \delta(t_1 - t_2), \tag{5.8}$$

and furthermore assume that all time instances are not only uncorrelated but also independent, which enables us to find the resulting probability density more easily.

With this setup, the variance $\sigma_\theta^2 \equiv \mathrm{Var}\,(\theta)$ and expectation value $\langle\theta\rangle$ of θ are calculated: Using [37] and [36]

$$\begin{aligned} \mathrm{Var}\,(X) &\equiv \mathrm{E}\left(X^2\right) - \left(\mathrm{E}\,(X)\right)^2 \\ \mathrm{Var}\,(a \cdot X) &= a^2 \cdot \mathrm{Var}(X) \\ \mathrm{E}\left(\int X\, \mathrm{d}t\right) &= \int \mathrm{E}(X)\, \mathrm{d}t \end{aligned} \tag{5.9}$$

gives

$$\begin{aligned} \langle\theta\rangle &= 0 \\ \sigma_\theta^2(t) &= \sum_i \frac{\gamma_i}{2} \cdot t, \end{aligned} \tag{5.10}$$

where we defined the dephasing rates $\gamma_i/2 \equiv \left(\frac{\partial E}{\partial \lambda_i}\right)^2 A_i^2/\hbar^2$.
As a last step, we argue that θ must follow the normal distribution $\mathcal{N}\left(0, \sigma_\theta^2(t)\right)$.
Essentially, the claim follows from the *Central Limit Theorem*. It guarantees that the distribution of any sum of a large number of independent, equally distributed random variables, approaches a normal distribution. Since we can write θ as a limit of such a sum of independent equally distributed variables $\delta\lambda(n\Delta t)$:

$$\theta(t) = \lim_{N\to\infty} \frac{1}{\hbar} \sum_i \frac{\partial E}{\partial \lambda_i} \sum_n^N \delta\lambda_i(n\Delta t)\Delta t, \quad \Delta t = t/N \tag{5.11}$$

it follows, that θ must be normally distributed itself [38]. Therefore, the probability density of having a phase shift θ at time t must be

$$P_t(\theta) = \frac{1}{\sqrt{\pi \sum_i \gamma_i t}} e^{-\frac{1}{\sum_i \gamma_i t}\theta^2}. \tag{5.12}$$

The variance of this normal distribution grows linearly in time, which actually defines a *Wiener Process* or *Brownian Motion* [39], indicating that θ undergoes a continuous random walk.

5.1.3. Dephasing of the density matrix

We are now in a position to calculate the density matrix of the system. Due to the random phase-shifts it must be represented by a statistical mixture at time t according to equation (5.3). First, the pure state density matrix $|\psi_\theta\rangle\langle\psi_\theta|$ of a state of the form (5.6) is

$$\rho_\theta = a^2 |e\rangle\langle e| + b^2 |g\rangle\langle g| + ab^* e^{-\mathrm{i}2E_{tm}t/\hbar - \mathrm{i}2\theta(t)} |e\rangle\langle g| + a^* b\, e^{\mathrm{i}2E_{tm}t/\hbar + \mathrm{i}2\theta(t)} |g\rangle\langle e| \quad (5.13)$$

The complete density matrix is computed using the Gaussian integral formula

$$\int_{-\infty}^{\infty} e^{-(ax^2+bx)}\, dx = \sqrt{\frac{\pi}{a}} \exp\left(\frac{b^2}{4a}\right). \quad (5.14)$$

With $a = 1/2\,\sigma_\theta(t)$ and $b = \pm 2\mathrm{i}$, the averaged density matrix is

$$\rho = \int P_t(\theta)\, \rho_\theta \,\mathrm{d}\theta \quad (5.15)$$

$$= a^2 |e\rangle\langle e| + b^2 |g\rangle\langle g| + e^{-\sum_i \gamma_i t} \left(ab^* e^{-\mathrm{i}2E_{tm}t/\hbar} |e\rangle\langle g| + a^* b\, e^{-\mathrm{i}2E_{tm}t/\hbar} |g\rangle\langle e|\right). \quad (5.16)$$

We see that the random phase-changes caused by shifts in the energy parameters λ_i lead to an exponential decay in the off-diagonal elements of the system's density matrix. This decrease happens at a rate $\sum_i \gamma_i$ in the white noise model, and is known as *Dephasing*. The off-diagonal elements, also known as *Coherences*, are crucial for creating interference effects. These effects are interpreted to show the presence of "Quantum Superposition". Because of this, dephasing can be thought to cause a kind of collapse of the quantum superposition. It effectively removes any visible interference between the ground and excited states, and reduces the state to a classical mixture of ground and excited state, a phenomenon referred to as "Decoherence" [40].

Master equation for pure dephasing

Next the master equation of the density matrix (5.15) is derived and brought into Lindblad form. The time derivative is given by the usual unitary evolution, plus a correction term that comes from the derivative of the exponential decay factor:

$$\dot{\rho} = -\mathrm{i}\,[H_{tm}, \rho] - \sum_i \gamma_i \mathcal{O}[\rho], \quad (5.17)$$

where $\mathcal{O}$ is a superoperator acting on ρ which needs to fulfill the condition that it annihilates the diagonal elements, and acts as the identity on the off-diagonal elements, to produce the correct time derivative of (5.15).

To achieve this, we write $\mathcal{O}[\rho] = -1/2\,\sigma_z \rho\, \sigma_z + 1/2\,\rho$. The first term always gives an extra minus sign for off-diagonal elements, since either the σ_z from the left or the right gives a minus, while the other one gives a plus. For diagonal elements, it always gives an extra plus, since either both σ_z give plus or both minus, thus annihilating the diagonal elements together with the second term.

Now observing that $\sigma_z \sigma_z^\dagger = \mathbb{1}$ and remembering that the Pauli matrices are hermitian, we can write $\mathcal{O}$ in Lindbladian form:

$$\mathcal{O}[\rho] = -\frac{1}{2}\sigma_z \rho\, \sigma_z^\dagger + \frac{1}{4}\left(\sigma_z^\dagger \sigma_z\, \rho + \rho\, \sigma_z^\dagger \sigma_z\right) \equiv -\frac{1}{2}\mathcal{D}[\sigma_z]\ \rho, \quad (5.18)$$

with the *dissipator superoperator* $\mathcal{D}[\sigma_z]$. Defining $\gamma_\phi \equiv \sum_i \gamma_i$, the master equation for a transmon qubit suffering pure dephasing in Lindbladian form is obtained:

$$\dot{\rho} = -\mathrm{i}\,[H_{tm}, \rho] + \frac{\gamma_\phi}{2}\mathcal{D}[\sigma_z]\ \rho. \quad (5.19)$$

The generalization to multiple qubits is straightforwardly performed by adding multiple dissipators acting on the individual qubits:

$$\dot{\rho} = -\mathrm{i}\,[H, \rho] + \sum_q \frac{\gamma_{\phi q}}{2} \mathcal{D}\,[\sigma_z^q]\ \rho. \tag{5.20}$$

5.1.4. Quantitative remarks

In [5] the dephasing rates of a transmon qubit are calculated under the more realistic assumption of pink noise fluctuations in the parameters $\lambda_i(t)$, characterized by a spectral density proportional to $1/f$. Under these assumptions, the dephasing rate turns out to be given by the square root of the one obtained in our discussion. They estimate the following coherence times T_i due to fluctuations in Q, Φ and I_c:

$$T_Q = 400\,000\,\mathrm{ns}, \tag{5.21}$$
$$T_\Phi = 3\,600\,000\,\mathrm{ns}, \tag{5.22}$$
$$T_{I_c} = 35\,000\,\mathrm{ns}, \tag{5.23}$$

which is orders of magnitude better compared to the previous superconducting qubit designs based on the ratio $E_J/E_C \approx 1$.

5.2. Master equation for N-qubit system

This section gives a quick microscopic derivation of the Lindblad equation for N qubits coupled to a zero temperature bath B. The microscopic derivation in the general case has been given in *Breuer & Petruccione* [12] for example. Here, we focus only on the parts of the derivation that are specific to our system in question: First setting up the Hamiltonian of the full Qubit-Bath system, the system operators of the interaction Hamiltonian H_I is then decomposed into the eigenoperators of the system Hamiltonian H_S, to find the resulting jump operators by performing the *Secular approximation.*[12]

Model for bath-qubit-interaction

The following derivation is a generalization of the single qubit case presented in [12], [41] and [42] for example, to a multi-qubit system. It is assumed that N non-interacting qubits with Hamiltonian $H_S = \sum_q \omega_q/2\,\sigma_z^q$ are coupled equally to a bath of bosonic oscillators with $H_B = \sum_k \omega_k a^\dagger a$, where k sums over all modes of the bath. The full Hamiltonian then reads

$$H = H_S + H_B + H_I, \tag{5.24}$$

with the interaction Hamiltonian

$$H_I = \left(\sum_q \sigma_x^q\right) \otimes \left(\sum_k \lambda_k \left(a_k^\dagger + a_k\right)\right). \tag{5.25}$$

For brevity we define $X \equiv \sum_k \lambda_k \left(a_k^\dagger + a_k\right)$ and $S \equiv \sum_q \sigma_x^q$ to write $H_I = S \otimes X$.

To further simplify the calculation, we assume the bath temperature to be $T = 0\,\mathrm{K}$, i.e. that the bosonic oscillators are all in the ground state. The density matrix of the system-bath is then given by

$$\rho = \rho_S \otimes \rho_B = \rho_S \otimes |\Omega\rangle\langle\Omega| \tag{5.26}$$

where $|\Omega\rangle = |0\rangle \otimes |0\rangle \otimes \cdots$ is the ground state of the bath.

Decomposition of S into eigenoperators of H_S

The derivation is performed by first transforming into the interaction picture via $U_0(t) \equiv e^{-\mathrm{i}(H_S+H_B)\,t}$, followed by the *Born-Markov* approximation, which is valid under the assumption that the bath correlation time is much shorter than the typical timescale of the system-evolution (given by the inverse of the system-frequencies). Next, the secular approximation is performed, whereby only non-oscillating terms are kept since oscillating terms are assumed to average out during the typical relaxation time of the system-density matrix due to its interaction with the bath. The oscillating terms are separated from the non-oscillating terms by first decomposing the system-interaction operator S into eigenoperators of H_S. As explained in section 2.1.1 the decomposition is formally found using the register projectors $\Pi(x) \equiv |x\rangle\langle x|$ leading to

$$\begin{aligned} S &= \sum_q \sigma_x^q \\ &= \sum_{q,x,y} |x\rangle\langle x|\, \sigma_x^q\, |y\rangle\langle y| \\ &= \sum_{q,x} |x_{q-}\rangle\langle x| + |x_{q+}\rangle\langle x| \\ &= \sum_q \left(\sigma_+^q + \sigma_-^q\right), \end{aligned} \tag{5.27}$$

where $|x_{q\pm}\rangle \equiv \sigma_\pm^q\, |x\rangle$. From section 2.2.2 we already know that the spin-ladder operators satisfy

$$\left[H_S, \sigma_\pm^q\right] = \frac{\omega_q}{2}\left[\sigma_z^q, \sigma_\pm^q\right] = \pm\,\omega_q \sigma_\pm, \tag{5.28}$$

leading to their time evolution

$$\sigma_\pm^q(t) = e^{\pm \mathrm{i}\omega_q t}\sigma_\pm^q \equiv e^{-\mathrm{i}\omega_q^\pm t}\sigma_\pm, \tag{5.29}$$

with eigenfrequencies

$$\begin{aligned} \sigma_+^q: &\quad \omega_q^+ = -\omega_q, \\ \sigma_-^q: &\quad \omega_q^- = +\omega_q. \end{aligned} \tag{5.30}$$

Thus, the time evolution of S is given by

$$S(t) = \sum_q \left(\sigma_-(t) + \sigma_+(t)\right) = \sum_{q,\nu} e^{-\mathrm{i}\omega_q^\nu t}\sigma_\nu^q, \tag{5.31}$$

with $\nu \in \{+,-\}$ labeling the eigenoperators to a given q.

Secular approximation

According to [12], the secular approximation is performed on the interaction picture equation

$$\frac{\mathrm{d}\rho_S(t)}{\mathrm{d}t} = \sum_{\nu,\nu'}\sum_{q,p} e^{-\mathrm{i}(\omega_p^\nu - \omega_q^{\nu'})}\Gamma_{qp}(\omega_p^\nu)\left(\sigma_\nu^p \rho_S(t)\sigma_{\nu'}^{q\dagger} - \sigma_{\nu'}^{q\dagger}\sigma_\nu^p\rho_S(t)\right) + \text{H.c.}, \tag{5.32}$$

where Γ is the Laplace transformed bath correlation function

$$\Gamma_{qp}(\omega) = \int_0^\infty \mathrm{Tr}_B\left[X^\dagger(t)X(t-s)e^{\mathrm{i}\omega s}\,\mathrm{d}s\right], \tag{5.33}$$

which is independent of q and p in this case, since every qubit is assumed to be coupled to the same bath X. $X(t)$ denotes the bath operator in the interaction picture.

Now the $\mathrm{Re}\,\Gamma(\omega)$ correspond to the relaxation rates $\gamma(\omega)$ for our jump operators. In [41] it is shown that for $\langle n\rangle = 0$ only positive frequencies in $\Gamma(\omega)$ will contribute, reflecting the fact that the bath can only *absorb* quanta of frequency ω and never *excite* the system by emitting a boson. This is fulfilled since we assume the bath to be in the vacuum state. Therefore, we can restrict the sum immediately to the terms where $\omega_p^\nu = \omega_p^-$ since ω_p^+ is negative according to Eq. (5.30).

Furthermore, since the considered qubits shall be detuned, with respect to each other according to Eq. (3.81), the only way the exponent can vanish is for $p = q$ and $\nu' = -$. All other terms oscillate with frequencies $(p \pm q)\delta\omega_1$. The jump operators are consequently just given by σ_-^q and we obtain the master equation (after transforming back to the Schrödinger picture and neglecting the Lamb-shift term proportional to $\mathrm{Im}\,\Gamma(\omega)$)

$$\begin{aligned}\dot{\rho}_S &= -\mathrm{i}\left[H_S, \rho_S\right] + \sum_q \gamma_q \left(\sigma_-^q \rho_S \sigma_-^q - \frac{1}{2}\left\{\sigma_+^q \sigma_-^q, \rho_S\right\}\right) \\ &= -\mathrm{i}\left[H_S, \rho_S\right] + \sum_q \gamma_q \mathcal{D}\left[\sigma_-^q\right]\rho_s,\end{aligned} \tag{5.34}$$

where the relaxation rates γ_q are given by

$$\gamma_q \equiv 2 \cdot \mathrm{Re}\,\Gamma(\omega_q). \tag{5.35}$$

5.3. Damped driven oscillator

In this section, we present a derivation of the Lindblad equation for the resonantly driven harmonic oscillator in the rotating frame, described by the Hamiltonian 2.11. Again, we adapt the general microscopic derivation that was given in [12]. Starting with the definition of the system-, bath-, and interaction Hamiltonians, we then calculate the interaction Hamiltonian in the interaction picture and decompose it into terms oscillating at different frequencies. Finally, we perform the secular approximation. Here, it is discovered that the Lindblad equation essentially simplifies to that of the free oscillator, except for a re-normalization of the drive amplitude, which is negligible for $\delta\omega_r \approx 0$

5.3.1. Model for bath-oscillator interaction

Following [12] we employ the standard dipole interaction between the oscillator and a bosonic bath. In the non-rotating frame, the corresponding interaction Hamiltonian is expressed as

$$\tilde{H}_I = \left(a + a^\dagger\right) \otimes \sum_k \lambda_k \left(b_k + b_k^\dagger\right) \equiv \left(a + a^\dagger\right) \otimes X, \tag{5.36}$$

where a denotes the annihilation operator of the oscillator, and b_k represents the annihilation operator of the k-th bath mode.

In the rotating frame, defined by the unitary transformation $U_{\mathrm{RWA}} = \exp\left(\mathrm{i}\omega_d a^\dagger a t\right)$, the interaction Hamiltonian transforms to

$$H_I = \left(e^{-\mathrm{i}\omega_d t}\, a + e^{\mathrm{i}\omega_d t}\, a^\dagger\right) \otimes X, \tag{5.37}$$

where we utilize the eigenoperator evolution of a, as outlined in equation 2.5. It's important to note that the calculation begins off-resonance with $\omega_r \neq \omega_d$, and only later do we consider the limit $\omega_d \to \omega_r$. Consequently, the total system-bath Hamiltonian in this frame is expressed as

$$H = H_S + H_B + H_I, \tag{5.38}$$

where $H_S = (\omega_r - \omega_d)\, a^\dagger a + \epsilon\left(a + a^\dagger\right)$ and H_B remains as defined in the previous section. Additionally, we continue to assume that the bath is in its ground state $|\Omega\rangle$:

$$\rho = \rho_S \otimes |\Omega\rangle\langle\Omega|\,. \tag{5.39}$$

5.3.2. Calculating H_I in the interaction-picture

To perform the secular approximation and find the jump operators, we first need to compute the time evolution of the interaction Hamiltonian H_I in the interaction-picture, defined by the unitary transformation $U = \exp(\mathrm{i}H_S t)$. We can use a similar trick as in section 2.1: Defining $\delta\omega_r \equiv \omega_r - \omega_d$ we rewrite H_S by introducing $A \equiv a + \epsilon/\delta\omega_r$:

$$H_S = \delta\omega_r A^\dagger A - \frac{\epsilon^2}{\delta\omega_r^2}. \tag{5.40}$$

Next we rewrite H_I using A:

$$H_I = \left\{ e^{-\mathrm{i}\omega_d t} A + e^{\mathrm{i}\omega_d t} A^\dagger - \frac{\epsilon}{\delta\omega_r}\left(e^{\mathrm{i}\omega_d t} + e^{-\mathrm{i}\omega_d t}\right) \right\} \otimes X. \tag{5.41}$$

To calculate the time evolution of A in the interaction picture, generated by 5.40, we first observe that $\left[A, A^\dagger\right] = \mathbb{1}$. Recalling Eq. 2.5, it follows that A is an eigenoperator of H_S oscillating with frequency $\delta\omega_r$. Since $\omega_d + \delta\omega_r = \omega_r$ this leads to the interaction-picture Hamiltonian

$$H_I^I(t) \equiv e^{\mathrm{i}H_S t} H_I e^{-\mathrm{i}H_S t} = \underbrace{\left\{ e^{-\mathrm{i}\omega_r t} A + e^{\mathrm{i}\omega_r t} A^\dagger - \frac{\epsilon}{\delta\omega_r}\left(e^{\mathrm{i}\omega_d t} + e^{-\mathrm{i}\omega_d t}\right) \right\}}_{\equiv S(t)} \otimes X(t), \tag{5.42}$$

where $X(t) = \exp(\mathrm{i}H_B t) X \exp(-\mathrm{i}H_B t)$.

$S(t)$ is already decomposed into operators oscillating at different frequencies. Writing $S(\omega)$ for the part of $S(t)$ that oscillates with frequency ω, we identify

$$\begin{aligned} S(\omega_r) &= A, & S(-\omega_r) &= A^\dagger \\ S(\omega_d) &= -\frac{\epsilon}{\delta\omega_r}\cdot\mathbb{1}, & S(-\omega_d) &= -\frac{\epsilon}{\delta\omega_r}\cdot\mathbb{1}, \end{aligned} \tag{5.43}$$

and rewrite $H_I^I(t)$ as

$$H_I^I(t) = \sum_\omega e^{-\mathrm{i}\omega t} S(\omega) \otimes X(t), \tag{5.44}$$

which completes the calculation of H_I in the interaction-picture.

5.3.3. Performing the secular approximation

Following [12], leads to the equation

$$\frac{\mathrm{d}}{\mathrm{d}t}\rho_S(t) = \sum_{\omega,\omega'} e^{\mathrm{i}(\omega'-\omega)t}\,\Gamma(\omega)\left(S(\omega)\rho_S(t)S^\dagger(\omega') - S^\dagger(\omega')S(\omega)\rho_S(t)\right) + \mathrm{h.c.}, \tag{5.45}$$

where $S^\dagger(\omega) = [A(\omega)]^\dagger$ and

$$\Gamma(\omega) = \int_0^\infty e^{\mathrm{i}\omega s}\,\mathrm{Tr}_B\left\{X^\dagger(s)X(0)\rho_B\right\}\mathrm{d}s, \tag{5.46}$$

for a stationary bath state ρ_B.

The secular approximation usually consists of only keeping terms where $\omega' = \omega$. However, since we want to consider (near) resonant driving of the oscillator $\delta\omega_r \approx 0$, we also keep those terms where $\omega' - \omega = \pm(\omega_r - \omega_d)$. Therefore, neglecting only fast-oscillating and negative frequency terms, we find the master equation in the interaction picture

$$\dot\rho_S = \kappa(\omega_r)\cdot\mathcal{D}\left[A\right]\rho_S + \frac{\epsilon}{\delta\omega_r}\frac{\kappa(\omega_d)}{2}\left(e^{\mathrm{i}\delta\omega_r t}\left[A^\dagger, \rho_S\right] - e^{-\mathrm{i}\delta\omega_r t}\left[A, \rho_S\right]\right), \tag{5.47}$$

with $\kappa(\omega) \equiv 2\,\mathrm{Re}\,(\Gamma(\omega))$ being the dissipation rate of the oscillator at frequency ω. Transforming back to the Schrödinger picture, the time-dependent phases cancel, and we find

$$\dot{\rho}_S = -\mathrm{i}\,[H_S, \rho_S] + \kappa(\omega_r)\mathcal{D}\,[A]\,\rho_S + \frac{\epsilon}{\delta\omega_r}\frac{\kappa(\omega_d)}{2}\left(\left[a^\dagger\,, \rho_S\right] - \left[a\,, \rho_S\right]\right), \tag{5.48}$$

where we have used $[A, \rho] = [a, \rho]$. Compared to the Lindblad equation of the free-oscillator [12][43]

$$\dot{\rho_S} = -\mathrm{i}\,[H_S, \rho_S] + \kappa\mathcal{D}\,[a]\,\rho_S, \tag{5.49}$$

we note that the jump operator of the driven oscillator is given by the shifted annihilation operator A. Furthermore, there is a term proportional to ϵ which can be interpreted as an additional driving term in the Hamiltonian (this will be made explicit in the next subsection).

We now show that for $\delta\omega_r \approx 0$ Eq. 5.48 approaches Eq. 5.49.

5.3.4. Lindblad equation for near-resonant driving

Expanding $\mathcal{D}\,[A] = \mathcal{D}\,[a + \epsilon/\delta\omega_r]$ yields

$$\mathcal{D}\,[A] = \mathcal{D}\,[a] - \frac{\epsilon}{2\cdot\delta\omega_r}\left(\left[a^\dagger\,, \rho_S\right] - \left[a\,, \rho_S\right]\right), \tag{5.50}$$

which upon insertion into 5.48 and defining $\delta\kappa = \kappa(\omega_d) - \kappa(\omega_r)$ gives

$$\dot{\rho}_S = -\mathrm{i}\,[H_S, \rho_S] + \kappa(\omega_r)\mathcal{D}\,[a]\,\rho_S + \epsilon\,\frac{\delta\kappa}{2\delta\omega_r}\left[a^\dagger - a\,, \rho_S\right]. \tag{5.51}$$

The operator $a^\dagger - a$ in the last commutator is anti-hermitian and can thus be added to the Hamiltonian:

$$H_S \longrightarrow H_S' = H_S + \mathrm{i}\epsilon\,\frac{\delta\kappa}{2\delta\omega_r}\left(a^\dagger - a\right) \tag{5.52}$$

$$\longrightarrow \dot{\rho}_S = -\mathrm{i}\left[H_S', \rho_S\right] + \kappa(\omega_r)\mathcal{D}\,[a]\,\rho_S. \tag{5.53}$$

This equation is structurally equivalent to the free-oscillator Lindbladian, with the only difference being the modified unitary evolution due to H_S'. Defining

$$\epsilon' = \epsilon + \mathrm{i}\epsilon\,\frac{\delta\kappa}{2\delta\omega_r}, \tag{5.54}$$

enables us to write H_S' as

$$H_S' = \delta\omega_r a^\dagger a + \epsilon' a^\dagger + \epsilon'^* a, \tag{5.55}$$

which is the Hamiltonian of an oscillator with external force ϵ'.

The final step is to show that $\delta\kappa/\delta\omega_r \ll 1$ for $\delta\omega_r \to 0$. This needs further assumptions about the Bath and the nature of the coupling between the system and the bath. Typically, in Circuit Quantum Electrodynamics, the interactions between the system and its environment are due to electromagnetic forces. It is, therefore, reasonable to assume that the coupling (and thus the bath-correlation function) is similar in structure to the one presented in the presentation of the optical master equation in [12]. Here the system is assumed to interact with the modes of the electromagnetic field. The sum over k entails the sum over all wave vectors $\vec{k}$ of the bath photons. The coupling constant λ_k is proportional to $\omega_k/\sqrt{V}$, where ω_k is the frequency of the mode and V is the volume of the bath. In this setup, it turns out that the dissipation rates $\kappa(\omega)$ are given by (in the limit $T = 0\,\mathrm{K}$)

$$\kappa(\omega) = \frac{\omega^3}{c^3}\cdot d^2, \tag{5.56}$$

where c is the speed of light and d^2 is a constant characterizing the dipole moment of the oscillator coupled to the electromagnetic field. Generally, the exponent of ω coincides with the number of dimensions considered. I.e. an oscillator coupled to a two-dimensional electromagnetic bath has a dissipation rate $\kappa(\omega) \sim \omega^2/c^2$. As a result, for a dissipation rate proportional to ω^n we have the following resonance limit:

$$\lim_{\omega_d \to \omega_r} \frac{\omega_d^n - \omega_r^n}{\omega_d - \omega_r} = n \cdot \omega_r^{n-1} \quad \Leftrightarrow \quad \lim_{\omega_d \to \omega_r} \frac{\kappa(\omega_d) - \kappa(\omega_r)}{\omega_d - \omega_r} = n \cdot \frac{\kappa(\omega_r)}{\omega_r}. \tag{5.57}$$

This is just the derivative of the dissipation rate with respect to ω. Given that the relaxation rate of the system is significantly smaller than the intrinsic system rates denoted by ω_r, the fraction $\kappa(\omega_r)/\omega_r$ can be assumed to be much less than one. Consequently, this modification of the drive amplitude can be safely neglected, thereby restoring the unperturbed Hamiltonian as a good approximation. However, a rigorous analysis necessitates a precise physical definition of all parameters involved.

5.3.5. Conclusion

We conclude that the master equation of a driven oscillator under the RWA can be derived microscopically. In the case of near resonant driving this leads to a master equation (5.52) equivalent to the free-oscillator Lindbladian, but with a unitary evolution generated by a driven oscillator with a driving amplitude that is shifted with respect to the unperturbed drive. Assuming that the dissipation rate $\kappa(\omega)$ is proportional to some ω^n (as is the case for a dipole coupled to an electromagnetic bath at temperature $T \approx 0\,\mathrm{K}$), this shift of the driving amplitude is small compared to the original amplitude and as $\delta\omega_r \to 0$ and the Lindbladian structure of the free-oscillator is restored as a good approximation:

$$\lim_{\delta\omega_r \to 0} \dot{\rho}_S = -\mathrm{i}\,[H_S, \rho_S] + \kappa(\omega_r)\mathcal{D}\,[a]\,\rho_S \tag{5.58}$$

5.4. Lindbladian for dispersive Hamiltonian

In this section the final master equation of the combined oscillator-register system, defined by the dispersive Hamiltonian 3.91.

In the derivation it is assumed that each element of the combined system is coupled to its own bath. Physically this assumption is justified, since in the laboratory frame, the qubits are detuned from the resonator as well as detuned with respect to each other, thus probing the spectral density of the environment at well-separated frequencies. This simplifies the calculation notably, since in the derivation of the jump-operators only operators corresponding to the same bath connect to each other, since the bath correlation function $\Gamma_{\alpha\beta}$ between two distinct baths α and β vanishes.

In the rotating frame, the resulting bath-system interaction Hamiltonian is therefore assumed to take the form

$$H_I = \sum_q \underbrace{\left(\sigma_-^q e^{-\mathrm{i}\omega_d t} + \mathrm{h.c.}\right)}_{S_q} \otimes X_q + \underbrace{\left(a e^{-\mathrm{i}\omega_d t} + \mathrm{h.c.}\right)}_{S_{Osc}} \otimes X_{Osc}, \tag{5.59}$$

where the bath operators X_i are of the form as given in Eq. 5.25.

Actually, for a complete derivation of the master equation, it would be necessary to consider additional terms in the interaction Hamiltonian, arising from the Schrieffer-Wolff transformation applied to H_I. These terms are treated in [1] and [24] especially, where it is shown that the resulting corrections to the jump operators are of the order λ^2. Therefore, they are neglected here. However, we will consider the full driven-system Hamiltonian when transforming S_i to the interaction picture, which to the author's knowledge has not been considered before, and leads to new corrections to the final master equation.

5.4.1. Oscillator jump operators

First, the jump operators due to the interaction of the oscillator with its bath are calculated. To transform S_{Osc} to the interaction frame, we consider the action of the dispersive system Hamiltonian H_s on a register projector $\Pi(x)$:

$$H_s\Pi(x) = \left[(\delta\omega_r + \chi(x))\, a^\dagger a + \epsilon(a^\dagger + a) + \frac{\tilde{\omega}_Q(x)}{2} \right] \Pi(x), \tag{5.60}$$

where $\tilde{\omega}_Q(x) \equiv \sum_q \delta\tilde{\omega}_q \langle x|\, \sigma_z^q\, |x\rangle$. By introducing the shifted annihilation operator $A(x) \equiv a + c_x$, with $c_x \equiv \epsilon/(\delta\omega_r + \chi(x))$, the Hamiltonian can be rewritten in a similar manner as in the previous section, and we find

$$H_s\Pi(x) = \left[\underbrace{(\delta\omega_r + \chi(x))}_{\equiv\delta\omega(x)} A^\dagger(x)A(x) - c_x^2 + \frac{\tilde{\omega}_Q(x)}{2} \right] \Pi(x). \tag{5.61}$$

The time-evolution operator $U_s(t)$ used to transform into the interaction frame can therefore be decomposed as

$$U_s(t) = \sum_x e^{-\mathrm{i}\left[(\delta\omega_r+\chi(x))A^\dagger(x)A(x) - c_x^2 + \frac{\tilde{\omega}_Q(x)}{2}\right]t} \Pi(x). \tag{5.62}$$

To calculate the transformed S_{Osc} we further use

$$\Pi(x)\, a\, \Pi(y) = [A(x) - c_x]\ \Pi(x), \tag{5.63}$$

which allows us to employ the eigenoperator evolution 2.13 of $A(x)$ under $\exp\big(-\mathrm{i}\delta\omega(x)A^\dagger(x)A(x)\, t\big)$. Recalling that $\delta\omega_r = \omega_r - \omega_d$, we find

$$\begin{aligned} S^I_{Osc}(t) &\equiv U_s(t) S_{Osc} U_s^\dagger(t) \\ &= \sum_x \left(A(x) e^{-\mathrm{i}(\omega_r + \chi(x))} - c_x e^{-\mathrm{i}\omega_d t} + \text{h.c.} \right) \Pi(x), \end{aligned} \tag{5.64}$$

for the oscillator-bath interaction operator in the interaction frame. This expression implies that the operators $S_{Osc}(\omega)$ oscillating with frequency ω can be identified as (with $\omega(x) \equiv \omega_r - \chi(x)$)

$$\begin{aligned} S_{Osc}(\omega(x)) = A(x)\Pi(x), \quad S_{Osc}(-\omega(x)) = A^\dagger(x)\Pi(x) \\ S_{Osc}(\omega_d) = -\sum_x c_x \Pi(x) = S_{Osc}(-\omega_d). \end{aligned} \tag{5.65}$$

Since we again are interested in near resonant driving, i.e. we consider ω_d to be close to $\omega(x)$, we want to keep all terms with positive frequency and allow $\omega(x)$ to be "combined" with ω_d in the following equation:

$$\begin{aligned} \frac{\mathrm{d}}{\mathrm{d}t}\rho_S(t) = \sum_{\omega,\omega'} e^{\mathrm{i}(\omega'-\omega)t} \Gamma(\omega) \left(S_{Osc}(\omega)\rho_S(t) S^\dagger_{Osc}(\omega') - S^\dagger_{Osc}(\omega') S_{Osc}(\omega)\rho_S(t) \right) \\ + \text{h.c.} \end{aligned} \tag{5.66}$$

Keeping the terms where $\omega = +\omega(x), +\omega_d$ connects to $+\omega(x)$ and $+\omega_d$, transforming back to the Schrödinger picture and using the shorthand notation A_x and Π_x yields the equation

$$\begin{aligned}
\dot{\rho} = &-\mathrm{i}\,[H_s,\,\rho] \\
&+ \sum_{x,y} \kappa(\omega(x)) \left\{ A_x \Pi_x\, \rho\, \Pi_y A_y^\dagger - \frac{1}{2} A_y^\dagger \Pi_y \Pi_x A_x\, \rho \,- \frac{1}{2}\, \rho\, \Pi_x A_x^\dagger \Pi_y A_y \right\} \\
&- \sum_{x,y} \frac{\kappa(\omega(x))}{2} \left\{ A_x \Pi_x\, \rho\, c_y - c_y \Pi_y \Pi_x A_x\, \rho \,+ c_y \Pi_y\, \rho\, \Pi_x A_x^\dagger - c_y\, \rho\, A_x^\dagger \Pi_x \Pi_y \right\} \\
&+ \sum_{x,y} \frac{\kappa(\omega_d)}{2} \left\{ -c_y \Pi_y\, \rho\, \Pi_x A_x^\dagger + A_x^\dagger \Pi_x \Pi_y c_y\, \rho \,- A_x \Pi_x\, \rho\, \Pi_y c_y + \,\rho\, \Pi_y \Pi_x A_x^\dagger c_y \right\} \\
&+ \sum_{xy} \kappa(\omega_d) c_x c_y \left\{ \Pi_x\, \rho\, \Pi_y - \frac{1}{2} \Pi_y \Pi_x\, \rho \,- \frac{1}{2}\, \rho\, \Pi_x \Pi_y \right\}.
\end{aligned} \tag{5.67}$$

Luckily most of these terms cancel and by using $A(x) = a + c_x$ the RHS reduces to

$$\begin{aligned}
\dot{\rho} = &-\mathrm{i}\,[H_s,\,\rho] + \sum_x \frac{\kappa(\omega(x))}{2} \left\{ a \Pi(x)\, \rho\, a^\dagger + a\, \rho\, \Pi(x)\, a^\dagger - a^\dagger a\, \Pi(x)\, \rho - \rho \Pi(x)\, a^\dagger a \right\} \\
&+ \sum_x c_x\, \frac{[\kappa(\omega(x)) - \kappa(\omega_d)]}{2} \left\{ \left[\Pi(x)\, \rho,\, a^\dagger \right] + [a,\, \rho\, \Pi(x)] \right\}.
\end{aligned} \tag{5.68}$$

The second sum is similar to the drive correction term obtained in the last section: in the limit $\chi \to 0$ we can perform the summation over x and use $\sum_x \Pi(x) = \mathbb{1}$ to restore the same correction as for the uncoupled driven oscillator. The first sum similarly is a modified version of the usual dissipation super operator $\mathcal{D}[a]$. The modification stems from the fact that for different register states $|x\rangle$, the environment is probed at different frequencies $\omega(x)$, leading to a register-state dependent dissipation and jump-rate $\kappa(\omega(x))$. More precisely: On the subspaces given by $\langle x|\, \rho\, |x\rangle$ the structure of the master equation reduces exactly to the one obtained for the driven oscillator alone. The different subspaces are separated from each other by their difference in κ.

In the limit where $\kappa(\omega(x)) \approx \kappa(\omega_d)$ and $\omega_d \approx \omega_r$ the usual Lindbladian of the harmonic oscillator is restored:

$$\dot{\rho} \approx -\mathrm{i}\,[H_s,\,\rho] + \kappa(\omega_r) \mathcal{D}[a]\, \rho. \tag{5.69}$$

This equation only contains the decay channel due to the oscillator. Now, we turn to the dissipation due to the qubit-register.

5.4.2. Register jump operators

The register-Hamiltonian representing the interaction with the bath is given by

$$\sum_q S_q = \sum_q \left(\sigma_-^q e^{-\mathrm{i}\omega_d t} + \sigma_+^q e^{-\mathrm{i}\omega_d t} \right). \tag{5.70}$$

To perform the transformation into the interaction picture, we start by decomposing $U_s(t)$ in the same way as in Eq. 5.62, leading to

$$\begin{aligned}
\sum_q S_q^I(t) = &\sum_{x,q} e^{-\mathrm{i}(\delta\tilde{\omega}_q + \omega_d)\, t} e^{-\mathrm{i}\delta\omega(x_{q-}) \left(A^\dagger(x_{q-}) A(x_{q-}) - c_{x_{q-}}^2 \right) t}\, |x_{q-}\rangle\langle x|\, e^{-\mathrm{i}\delta\omega(x) \left(A^\dagger(x) A(x) - c_x^2 \right) t} \\
&+ \text{ h.c.},
\end{aligned} \tag{5.71}$$

where the notation $|x_{q-}\rangle \equiv \sigma_-^q\, |x\rangle$ is introduced. The two exponential operators can not be combined into one since $\left[A^\dagger(x) A(x),\, A^\dagger(y) A(y) \right] \neq 0$ for $x \neq y$. The expression can be

resolved further using the Fock decomposition $\mathbb{1} = \int |n\rangle\langle n|\, \mathrm{d}n$ or the decomposition using coherent states $\mathbb{1} = 1/\pi \int |\alpha\rangle\langle\alpha|\, \mathrm{d}\alpha$. However, both methods lead to representations that seem problematic, since the resulting terms oscillate at a frequency depending on c_x. This would imply, that the spectral density of the bath is probed at $\sim \delta\omega(x) + c_x^2$, which poses a problem, since c_x diverges at resonance. This issue could not be resolved in the present thesis. However, it is straightforward to derive the master equation in the simplified cases where $\chi \to 0$ or $\epsilon \to 0$ respectively.

Master-equation for $\chi = 0$

In this limit, the register effectively decouples from the oscillator. We can expect that the resulting register jump-operator reduces to $\mathcal{D}[\sigma_-]$ as derived in Sec. 5.2. Regarding Eq. 5.71, it is easy to see that for $\chi \to 0$ we have $A(x) \to A$. Thus, the unresolved exponential operators cancel, the dependence of all terms on x vanishes the uncoupled case is restored:

$$\begin{aligned} \lim_{\chi\to 0} \sum_q S_q^I(t) &= \sum_{x,q} e^{-\mathrm{i}(\delta\tilde{\omega}_q - \omega_d)t}\, |x_{q-}\rangle\langle x| + \text{h.c.} \\ &= \sum_q \left(\sigma_-^q\, e^{-\mathrm{i}(\delta\tilde{\omega}_q - \omega_d)t} + \sigma_+^q\, e^{\mathrm{i}\delta\tilde{\omega}_q t} \right), \end{aligned} \tag{5.72}$$

which leads directly to the Lindbladian 5.34 as obtained in Sec. 5.2.

Master-Equation for $\epsilon \to 0$

This case is more interesting. For $\epsilon \to 0$ the shifted operators $A(x)$ reduce to a, but the dependency of $\delta\omega(x)$ on x is maintained:

$$\begin{aligned} \sum_q S_q^I(t) &= \sum_{x,q} e^{-\mathrm{i}(\delta\tilde{\omega}_q + \omega_d)t} e^{\mathrm{i}\,2\,\chi a^\dagger a t}\, |x_{q-}\rangle\langle x| + \text{h.c.} \\ &= \sum_{x,q,n} e^{-\mathrm{i}((\delta\tilde{\omega}_q + \omega_d)t - 2\,n\,\chi)t}\, |n\rangle\langle n| \otimes |x_{q-}\rangle\langle x| + \text{h.c.} \\ &= \sum_{q,n} e^{-\mathrm{i}((\delta\tilde{\omega}_q + \omega_d)t - 2\,n\,\chi)t}\, |n\rangle\langle n| \otimes \sigma_-^q + \text{h.c.}, \end{aligned} \tag{5.73}$$

where $\delta\omega(x_{q-}) - \delta\omega(x) = -2\chi$ was used in the first step, and the spectral resolution using Fock states in the second step. The following operators $S(\omega)$ oscillating at frequencies ω can be identified:

$$S((\delta\tilde{\omega}_q + \omega_d) - 2\,n\,\chi) = |n\rangle\langle n| \otimes \sigma_-^q, \quad S(-(\delta\tilde{\omega}_q + \omega_d) + 2\,n\,\chi) = |n\rangle\langle n| \otimes \sigma_+^q. \tag{5.74}$$

In the dispersive approximation χ is much smaller than the Lamb-shifted bare qubit frequency $(\delta\tilde{\omega}_q + \omega_d) = \omega_q + 2\chi$. However, interestingly, for large enough oscillator occupation numbers n, the qubit dissipators start to probe the bath at negative frequencies, implying that at $T = 0$ qubit relaxation would be suppressed. Correspondingly, the qubit-excitation operator starts to probe at positive frequencies. This suggests that for a register coupled to a highly excited oscillator, energy is not dissipated from the register to the bath, but the other way around. A possible physical explanation is, that the register absorbs photons from the oscillator. It is important to note, however, that in the case where the dispersive Hamiltonian is obtained via a Schrieffer-Wolff transformation from the Jaynes-Cummings Hamiltonian, the dispersive approximation breaks down for large n. The Hamiltonian H_s used to derive the results above will therefore not be a valid description of the system anymore.

For this reason, only $S((\delta\tilde{\omega}_q + \omega_d) - 2\,n\,\chi)$ is considered as having a positive frequency and contributing to the time evolution of ρ. In the Schrödinger picture we obtain the

following induced time evolution: (writing $|n\rangle\langle n| \equiv \Pi_n$)

$$\begin{aligned}\dot{\rho} &= -\mathrm{i}\,[H_s,\,\rho] + \sum_{q,n,m} \frac{\gamma((\delta\tilde{\omega}_q + \omega_d) - 2\chi\, n)}{2} \left\{\sigma_-^q \Pi_n \rho \Pi_m \sigma_-^q - \sigma_+^q \sigma_-^q \Pi_m \Pi_n\, \rho\right\} + \text{h.c.} \\ &= -\mathrm{i}\,[H_s,\,\rho] \\ &+ \sum_{q,n} \frac{\gamma((\delta\tilde{\omega}_q + \omega_d) - 2\chi\, n)}{2} \left\{\sigma_-^q \Pi_n \rho \sigma_+^q + \sigma_-^q\, \rho \Pi_n \sigma_+^q - \sigma_+^q \sigma_-^q\, \Pi_n\, \rho - \rho\, \Pi_n \sigma_+^q \sigma_-^q\right\}.\end{aligned} \tag{5.75}$$

Similarly to the oscillator dissipation for the dispersive system, this equation reduces to the usual Lindbladian on the subspaces defined by $\langle n|\,\rho\,|n\rangle$, being again separated by a difference in their relaxation rate γ.

In the limit of small χ where the rates of all subspaces can be considered as equal, the equation simplifies to

$$\dot{\rho} = -\mathrm{i}\,[H_s,\,\rho] + \sum_q \gamma(\omega_q)\mathcal{D}[\sigma_-^q]\rho. \tag{5.76}$$

This concludes the derivation of the Lindbladian for the coupled system. In the next section, the results are summarized

5.5. Final full master equation

Combining the approximate Lindbladians 5.69 and 5.76, valid in the regimes $\chi \ll \omega_q$, $\omega_d \approx \omega_r + \chi$, assuming that the corresponding dissipation rates are also approximately equal, together with the pure-dephasing Lindbladian 5.20, the final master equation for the dispersively coupled qubits and oscillator is given by

$$\dot{\rho} \approx -\mathrm{i}\,[H,\,\rho] + \kappa\mathcal{D}[a]\rho + \frac{\gamma_{\phi q}}{2}\mathcal{D}[\sigma_z^q]\rho + \gamma_{1q}\mathcal{D}[\sigma_-^q]\rho, \tag{5.77}$$

where the sum over q is implied and $\kappa \approx \kappa(\omega_r)$ as well as $\gamma_{1q} \approx \gamma(\omega_q)$. This equation is the main object of study for the remainder of the thesis. However, a more accurate master equation can be obtained by combining Eqs. 5.68 and 5.75, which takes into account, that the qubit and oscillator dissipation rates are subspace dependent, due to the dispersive coupling. This could be an interesting starting point for future numerical calculations and further analysis.

6. Solution of the master equation for $\gamma_1 = 0$

In this chapter, we start the analysis of the master equation for N dispersively coupled qubits, which is the main object of interest in this thesis. Following the results of the previous chapters, the Lindblad equation for the coupled qubits-resonator system reads

$$\dot{\rho} = -\mathrm{i}\,[H, \rho] + \kappa\mathcal{D}[a]\rho + \gamma_{1q}\mathcal{D}[\sigma_-^q]\rho + \frac{\gamma_{\phi q}}{2}\mathcal{D}[\sigma_z^q]\rho, \tag{6.1}$$

with the sum $\sum_{q=1}^{2^N-1}$ being implied and terms of order λ^2 and other small correction terms have been neglected (see Sec. 5.4). The Hamiltonian is given by Eq. 3.91:

$$H = \left(\delta\omega_r + \chi_q\sigma_z^q\right) a^\dagger a + \delta\tilde{\omega}_q\frac{\sigma_z^q}{2} + \epsilon\left(a^\dagger + a\right). \tag{6.2}$$

6.1. Procedure and motivation: Neglecting qubit relaxation

First, we solve for ρ neglecting the qubit relaxation term $\mathcal{D}[\sigma_-]\rho$. This is because σ_- introduces coupling terms between different qubit states, resulting in a set of coupled differential equations that are impossible to solve analytically. The case $\gamma_1 \neq 0$ is treated in Chapter 8 via a perturbation theory on the $\gamma_1 = 0$ solutions obtained in this chapter.

To see that the inclusion of the qubit-dissipator leads to a set of coupled differential equations, ρ is decomposed in the register z-eigenbasis $|x\rangle$: (see section 2.2)

$$\rho = \sum_{x,y}\rho_{xy}\otimes|x\rangle\langle y|\,. \tag{6.3}$$

Here, ρ_{xy} is an operator on the resonator Hilbert space only. Applying the qubit-dissipator superoperator to this decomposition leads to

$$\mathcal{D}[\sigma_-^q]\rho = \sum_{xy}\rho_{xy}\otimes\left\{\left|x_{q_-}\right\rangle\!\left\langle y_{q_-}\right| - \frac{1}{4}\Big[\left(\mathbb{1}+\sigma_z^q\right)|x\rangle\langle y| + |x\rangle\langle y|\left(\mathbb{1}+\sigma_z^q\right)\Big]\right\}, \tag{6.4}$$

where we introduced the notation $|x_{q_\pm}\rangle \equiv \sigma_\pm^q|x\rangle$ and used $\sigma_+\sigma_- = 1/2(\mathbb{1}+\sigma_z)$. Clearly only the first term, given by $\sigma_-\rho\sigma_+$, couples different register states to each other. All other qubit operators in 6.1 are proportional to σ_z or $\mathbb{1}$. Neglecting the relaxation jump-term thus leads to a differential equation that is decoupled in the $|x\rangle$ basis, as will be shown explicitly in the next section. The master equation that is solved first is given by

$$\dot{\rho} = -\mathrm{i}\,[H, \rho] + \kappa\mathcal{D}[a]\rho + \frac{\gamma_{\phi q}}{2}\mathcal{D}[\sigma_z^q]\rho. \tag{6.5}$$

In our approach, we follow the solution that is roughly outlined in [2] and expand on it explicitly. But first, a trick to simplify the equation is employed.

6.2. Separating the resonator operators from the rest

We start the calculation by splitting the Lindbladian into two parts, $\mathcal{L}_Q$ and $\mathcal{L}_r$. $\mathcal{L}_Q$ contains all the terms that act on the qubit Hilbert space only, and $\mathcal{L}_r$ contains those terms acting on the resonator density matrix:

$$\mathcal{L}\rho = \underbrace{-\mathrm{i}\frac{\delta\tilde{\omega}_q}{2}\,[\sigma_z^q, \rho] + \frac{\gamma_{\phi q}}{2}\mathcal{D}\left[\sigma_z^q\right]\rho}_{\mathcal{L}_Q\rho} \underbrace{-\,\mathrm{i}\left[\left(\delta\omega_r + \chi_q\sigma_z^q\right)a^\dagger a + \epsilon\left(a^\dagger + a\right), \rho\right] + \kappa\mathcal{D}[a]\rho}_{\mathcal{L}_r\rho}. \tag{6.6}$$

Since $\mathcal{L}_Q$ only contains operators proportional to σ_z^q, it is represented by a diagonal matrix in the $|x\rangle\otimes|y\rangle$ basis upon vectorization. Now, because the only qubit operator in $\mathcal{L}_r$ is also given by σ_z, it is straightforward to check that $[\mathcal{L}_Q, \mathcal{L}_r] = 0$ holds for the Lindbladians. As discussed in section 4.2, it therefore suffices to solve the reduced equation

$$\dot{\rho} = \mathcal{L}_r \rho, \tag{6.7}$$

to find $\rho(t) = \exp(\mathcal{L}_r t)\rho(0)$. The full solution of Eq. 6.5 is then given by

$$\rho(t) = e^{\mathcal{L}_Q t} e^{\mathcal{L}_r t} \rho(0). \tag{6.8}$$

To determine $\exp(\mathcal{L}_Q t)$ we first apply $\mathcal{L}_Q$ to $|x\rangle\langle y|$:

$$\mathcal{L}_Q |x\rangle\langle y| = -\mathrm{i}\frac{\delta\tilde{\omega}_q}{2}\left(\sigma_z^q |x\rangle\langle y| - |x\rangle\langle y| \sigma_z^q\right) + \frac{\gamma_{\phi q}}{2}\left(\sigma_z^q |x\rangle\langle y| \sigma_z^q - \mathbb{1}^q |x\rangle\langle y|\right), \tag{6.9}$$

because $\sigma_z^q\sigma_z^q = \mathbb{1}^q$. Introducing the notation $\sigma_z^q |x\rangle = Z^q(x)|x\rangle$ to denote the z-spin of the qth bit in the register state $|x\rangle$, we can write

$$\mathcal{L}_Q |x\rangle\langle y| = \underbrace{\left(-\mathrm{i}\frac{\delta\tilde{\omega}_q}{2}\left[Z^q(x) - Z^q(y)\right] - \frac{\gamma_{\phi q}}{2}\left[1^q - Z^q(x)Z^q(y)\right]\right)}_{\equiv\mathcal{L}_Q(x,y)} |x\rangle\langle y|. \tag{6.10}$$

The q on 1^q serves to keep the summation convention intact. The action on an arbitrary density matrix can then be written using the projection operators $\Pi(x) \equiv |x\rangle\langle x|$:

$$\mathcal{L}_Q\rho = \sum_{x,y} \mathcal{L}_Q(x,y)\,\Pi(x)\,\rho\,\Pi(y) \quad \Leftrightarrow \quad \mathcal{L}_Q\vec{\rho} = \sum_{x,y} \mathcal{L}_Q(x,y)\,\Pi(x)\otimes\Pi(y)\,\vec{\rho}. \tag{6.11}$$

The vectorized equation is trivially exponentiated to find

$$e^{\mathcal{L}_Q t}\vec{\rho}(0) = \sum_{x,y} e^{\mathcal{L}_Q(x,y)t}\,\Pi(x)\otimes\Pi(y)\,\vec{\rho}(0) \tag{6.12}$$

$$\Leftrightarrow \quad e^{\mathcal{L}_Q t}\rho(0) = \sum_{x,y} e^{\mathcal{L}_Q(x,y)t}\,\Pi(x)\,\rho(0)\,\Pi(y). \tag{6.13}$$

From the definition of $\mathcal{L}_Q(x,y)$, it is clear that it generates no time evolution for all diagonal elements $|x\rangle\langle x|$. The off-diagonal elements acquire, additionally to the exponential decay which is the effect of the pure dephasing derived in section 5.1, a phase proportional to the energy difference of the respective states. Having found the qubit-time evolution we can now move on to solve Eq.6.7.

6.3. The differential-equation for ρ_{xy} and positive P-representation

Using the decomposition 6.3, we find a differential equation for ρ_{xy}, by projecting the equation 6.7 with $\langle x|$ from the left and $|y\rangle$ from the right:

$$\begin{aligned}\dot{\rho}_{xy} &= \langle x|\,\dot{\rho}\,|y\rangle = \langle x|\,\mathcal{L}_r\rho\,|y\rangle \\ &= -\mathrm{i}\delta\omega_r\left[a^\dagger a, \rho_{xy}\right] - \mathrm{i}\chi(x)a^\dagger a\rho_{xy} + \mathrm{i}\chi(y)\rho_{xy}a^\dagger a \\ &\quad - \mathrm{i}\epsilon\left[\left(a^\dagger + a\right), \rho_{xy}\right] + \kappa\mathcal{D}[a]\rho_{xy}.\end{aligned} \tag{6.14}$$

Here it was used that the resonator operators commute with $|x\rangle$ and $\langle y|$ and we have introduced the expectation value of the dispersive shift with respect to the register state $|x\rangle$:

$$\chi(x) \equiv \sum_q \langle x|\,\chi\sigma_z^q\,|x\rangle = \chi\left(N_e(x) - N_g(x)\right), \tag{6.15}$$

with $N_e(x)$ and $N_g(x)$ the number of qubits in $|x\rangle$ in the excited- and ground-state respectively.

We can see that without the qubit's dissipator-jump term, the master equation reduces to a set of uncoupled differential equations for the operators ρ_{xy}. To solve these equations, we can choose a decomposition of ρ_{xy} into basis states of the oscillator Hilbert space. From our previous analysis of the driven oscillator in section 2.1, we might expect that the coherent states $|\alpha\rangle$ are a suitable choice. Since $\{|\alpha\rangle\}$ is an *over complete basis* of the oscillator Hilbert space [14], there are several possible coherent-state decompositions of oscillator operators (see [43], [44] for example). Here we follow [2] and choose the *positive P-representation*, defined by [45]

$$\rho_{xy} = \int \mathrm{d}^2\alpha \int \mathrm{d}^2\beta \frac{|\alpha\rangle\langle\beta^*|}{\langle\beta^*|\alpha\rangle} P_{xy}(\alpha,\beta), \tag{6.16}$$

where $\int \mathrm{d}^2\alpha = \int \mathrm{d}(\mathrm{Re}(\alpha)) \int \mathrm{d}(\mathrm{Im}(\alpha))$ is the integral over the whole complex plane. This representation always exists for physical density matrices and $P(\alpha,\beta)$ can be interpreted as a proper positive-valued probability density (which is only the case for the diagonal elements ρ_{xx} in this case). Introducing the short-hand notation $\boldsymbol{\alpha} = (\alpha,\beta)$ and

$$\Lambda(\boldsymbol{\alpha}) \equiv \frac{|\alpha\rangle\langle\beta^*|}{\langle\beta^*|\alpha\rangle} \quad , \quad \int \mathrm{d}^4\boldsymbol{\alpha} \equiv \int \mathrm{d}^2\alpha \int \mathrm{d}^2\beta, \tag{6.17}$$

leads to the simplified notation

$$\rho_{xy} = \int \mathrm{d}^4\boldsymbol{\alpha}\, \Lambda(\boldsymbol{\alpha})\, P_{xy}(\boldsymbol{\alpha}). \tag{6.18}$$

Plugging this decomposition into Eq. 6.14 we find that we need to calculate the following operator terms to resolve the equation:

$$a^\dagger a\, \Lambda(\boldsymbol{\alpha}), \quad \Lambda(\boldsymbol{\alpha})\, a^\dagger a, \quad \left[\left(a + a^\dagger\right), \Lambda(\boldsymbol{\alpha})\right], \quad \left[a^\dagger a, \Lambda(\boldsymbol{\alpha})\right] \quad \text{and} \quad \mathcal{D}[a]\Lambda(\boldsymbol{\alpha}). \tag{6.19}$$

The following subsection is dedicated to calculating these expressions.

6.3.1. Operator identities

Identities about a and $a^\dagger$ acting on bras and kets

The first set of identities that we need to resolve the master equation is

$$a^\dagger |\alpha\rangle = \left(\partial_\alpha + \frac{\alpha^*}{2}\right)|\alpha\rangle, \tag{6.20}$$

$$\langle\beta^*| a = \left(\partial_\beta + \frac{\beta}{2}\right)\langle\beta^*|. \tag{6.21}$$

The proof starts by using the definition of a coherent state 2.12 and applying $a^\dagger$:

$$\begin{aligned} a^\dagger |\alpha\rangle &= e^{-\frac{|\alpha|^2}{2}} \sum_{n=0}^{\infty} \frac{\alpha^n}{\sqrt{n!}} a^\dagger |n\rangle \\ &= e^{-\frac{|\alpha|^2}{2}} \sum_{n=1}^{\infty} \frac{\alpha^{n-1}}{\sqrt{(n-1)!}} \sqrt{n}\, |n\rangle \\ &= e^{-\frac{|\alpha|^2}{2}} \frac{\partial}{\partial\alpha} \left(\sum_{n=0}^{\infty} \frac{\alpha^n}{\sqrt{n}} |n\rangle\right) \\ &= \frac{\partial}{\partial\alpha}|\alpha\rangle - \frac{\partial}{\partial\alpha}\left(e^{-\frac{|\alpha|^2}{2}}\right) \cdot \sum_{n=0}^{\infty} \frac{\alpha^n}{\sqrt{n}} |n\rangle. \end{aligned} \tag{6.22}$$

Here we introduced the *Wirtinger Derivative* $\partial_\alpha \equiv 1/2\,(\partial_x - \mathrm{i}\partial_p)$ which satisfies

$$\frac{\partial \alpha^n}{\partial \alpha} = n\alpha^{n-1} \quad , \quad \frac{\partial \alpha^*}{\partial \alpha} = 0, \tag{6.23}$$

allowing us to treat α and α^* as independent variables. An introduction to Wirtinger calculus can be found in Appendix A. To calculate the second term in the last line of Eq. 6.22, we rewrite the exponent using $|\alpha|^2 = \alpha\alpha^*$. Using the identities 6.23 the derivative can be calculated easily, and we find

$$a^\dagger |\alpha\rangle = \left(\partial_\alpha + \frac{\alpha^*}{2}\right)|\alpha\rangle\,, \tag{6.24}$$

which completes the proof of 6.20. The proof of 6.21 can be performed similarly using the hermitian conjugate of the definition 2.12:

$$\langle\beta^*| = e^{-\frac{|\beta|^2}{2}} \sum_{n=0}^{\infty} \langle n| \frac{\beta^n}{\sqrt{n!}}. \tag{6.25}$$

Applying a from the left and using Wirtinger derivatives then leads to 6.21.

Operator Identities - $\Lambda(\boldsymbol{\alpha})$

Using Eqs. 6.20 and 6.21 we can derive further identities involving the non-diagonal coherent state projection operator $\Lambda(\boldsymbol{\alpha})$ 6.17:[43]

$$\begin{aligned} a\Lambda(\boldsymbol{\alpha}) &= \alpha\Lambda(\boldsymbol{\alpha}) \\ a^\dagger\Lambda(\boldsymbol{\alpha}) &= (\beta + \partial/\partial\alpha)\,\Lambda(\boldsymbol{\alpha}) \\ \Lambda(\boldsymbol{\alpha})a^\dagger &= \beta\Lambda(\boldsymbol{\alpha}) \\ \Lambda(\boldsymbol{\alpha})a &= (\partial/\partial\beta + \alpha)\,\Lambda(\boldsymbol{\alpha}). \end{aligned} \tag{6.26}$$

The proof of the first and third identity follows trivially from the definition of $\Lambda(\boldsymbol{\alpha})$ in Eq. 6.17. The second and fourth ones can be readily calculated using the identities derived in the previous subsection: For the second one we can use Eq. 6.20 and find:

$$\begin{aligned} a^\dagger\Lambda(\boldsymbol{\alpha}) &= \frac{1}{\langle\beta^*|\alpha\rangle}\,(\partial/\partial\alpha + \alpha^*/2)\,|\alpha\rangle\langle\beta^*| \\ &= \partial_\alpha\,(\Lambda(\boldsymbol{\alpha})) - |\alpha\rangle\langle\beta^*| \cdot \partial_\alpha\left(\frac{1}{\langle\beta^*|\alpha\rangle}\right) + \frac{\alpha^*}{2}\,\Lambda(\boldsymbol{\alpha}). \end{aligned} \tag{6.27}$$

Using the formula 2.25 for the scalar product between two coherent states we can calculate the derivative:

$$\partial_\alpha\left(e^{1/2(\beta\beta^* + \alpha\alpha^* - 2\beta\alpha)}\right) = \left(\frac{\alpha^*}{2} - \beta\right)\frac{1}{\langle\beta^*|\alpha\rangle} \tag{6.28}$$

Inserting back into 6.27 yields the second identity of 6.26. The fourth one can be proven in a similar way.

Final Operator identities

Using Eqs. 6.26 we can finally calculate the expressions 6.19 needed to resolve the differential-equation in the positive P-representation:

$$\begin{aligned} a^\dagger a\,\Lambda(\boldsymbol{\alpha}) &= \alpha\beta + \partial_\alpha\Lambda(\boldsymbol{\alpha}) \\ \Lambda(\boldsymbol{\alpha})\,a^\dagger a &= \alpha\beta + \partial_\beta\Lambda(\boldsymbol{\alpha}) \\ \left[\left(a + a^\dagger\right),\,\Lambda(\boldsymbol{\alpha})\right] &= (\partial_\alpha - \partial_\beta)\,\Lambda(\boldsymbol{\alpha}) \\ \left[a^\dagger a,\,\Lambda(\boldsymbol{\alpha})\right] &= \alpha\partial_\alpha\Lambda(\boldsymbol{\alpha}) - \beta\partial_\beta\Lambda(\boldsymbol{\alpha}) \\ \mathcal{D}[a]\Lambda(\boldsymbol{\alpha}) &= -\frac{1}{2}\left[\alpha\partial_\alpha\Lambda(\boldsymbol{\alpha}) + \beta\partial_\beta\Lambda(\boldsymbol{\alpha})\right], \end{aligned} \tag{6.29}$$

which are all straightforward to prove given the previous operator identities.

6.3.2. Solving the differential equation for ρ_{xy}

Now that the necessary expressions 6.29 are calculated, we can use the representation 6.18 for ρ_{xy} on the equation 6.14 and find

$$\begin{aligned}\dot{\rho}_{xy} = \int \Big\{ &- \mathrm{i}\delta\omega_r \Big(\alpha\partial_\alpha\Lambda(\boldsymbol{\alpha}) - \beta\partial_\beta\Lambda(\boldsymbol{\alpha})\Big) - \mathrm{i}\epsilon\big(\partial_\alpha - \partial_\beta\big)\Lambda \\ &+ \big(\mathrm{i}\chi(y) - \mathrm{i}\chi(x)\big)\alpha\beta\Lambda - \mathrm{i}\chi(x)\alpha\partial_\alpha\Lambda + \mathrm{i}\chi(y)\beta\partial_\beta\Lambda \\ &- \frac{\kappa}{2}\left[\alpha\partial_\alpha\Lambda(\boldsymbol{\alpha}) + \beta\partial_\beta\Lambda(\boldsymbol{\alpha})\right]\Big\} P_{xy}(\boldsymbol{\alpha})\,\mathrm{d}^4\boldsymbol{\alpha}.\end{aligned} \tag{6.30}$$

We simplify the notation by introducing

$$\begin{pmatrix} D \\ E \end{pmatrix}\begin{pmatrix} F \\ G \end{pmatrix} \equiv D\cdot F + E\cdot G \tag{6.31}$$

and collecting all terms with a partial derivative. This yields

$$\begin{aligned}\dot{\rho}_{xy} = &\int \begin{pmatrix} -\partial_\alpha\Lambda(\boldsymbol{\alpha}) \\ \partial_\beta\Lambda(\boldsymbol{\alpha}) \end{pmatrix}\begin{pmatrix} \left(\mathrm{i}\delta\omega_r + \mathrm{i}\chi(x) + \frac{\kappa}{2}\right)\alpha + \mathrm{i}\epsilon \\ \left(\mathrm{i}\delta\omega_r + \mathrm{i}\chi(y) - \frac{\kappa}{2}\right)\beta + \mathrm{i}\epsilon \end{pmatrix} P_{xy}(\boldsymbol{\alpha})\,\mathrm{d}^4\boldsymbol{\alpha} \\ &+ \int \Big\{\alpha\beta\big(\mathrm{i}\chi(y) - \mathrm{i}\chi(x)\big)\Big\}\Lambda(\boldsymbol{\alpha})\,P_{xy}(\boldsymbol{\alpha})\,\mathrm{d}^4\boldsymbol{\alpha}\end{aligned} \tag{6.32}$$

for the right-hand side. Employing 6.18 again, the left-hand side takes the form

$$\dot{\rho}_{xy} = \int \Lambda(\boldsymbol{\alpha})\,\dot{P}_{xy}(\boldsymbol{\alpha})\,\mathrm{d}^4\boldsymbol{\alpha}. \tag{6.33}$$

Comparing both sides, we find it tempting to symbolically identify the entries in the second vector in 6.32 as the time derivatives of some functions $\alpha_x(t)$ and $\beta_y(t)$:

$$\dot{\alpha}_x = -\left(\mathrm{i}\delta\omega_r + \mathrm{i}\chi(x) + \frac{\kappa}{2}\right)\alpha - \mathrm{i}\epsilon \tag{6.34}$$

$$\dot{\beta}_y = -\left(\mathrm{i}\delta\omega_r + \mathrm{i}\chi(y) + \frac{\kappa}{2}\right)\beta + \mathrm{i}\epsilon, \tag{6.35}$$

leading to a structure of the right-hand-side somewhat similar to a total time derivative of a function $f(\boldsymbol{\alpha} - \boldsymbol{\alpha}(t))$:

$$\begin{aligned}\dot{\rho}_{xy} = &\int \begin{pmatrix} \partial_\alpha\Lambda(\boldsymbol{\alpha}) \\ \partial_\beta\Lambda(\boldsymbol{\alpha}) \end{pmatrix}\begin{pmatrix} \dot{\alpha}_x \\ \dot{\beta}_y \end{pmatrix} P_{xy}(\boldsymbol{\alpha})\,\mathrm{d}^4\boldsymbol{\alpha} \\ &+ \int \Big\{\alpha\beta\big(\mathrm{i}\chi(y) - \mathrm{i}\chi(x)\big)\Big\}\Lambda(\boldsymbol{\alpha})\,P_{xy}(\boldsymbol{\alpha})\,\mathrm{d}^4\boldsymbol{\alpha}.\end{aligned} \tag{6.36}$$

The similarity can be made more explicit by performing a partial integration. In Appendix A we show that the usual formula for partial integration also holds in this context, where Wirtinger derivatives appear under an integral over the complex plane:

$$\int_D \frac{\partial f}{\partial\alpha}\,g\,\mathrm{d}^2\alpha = -\int_D f\,\frac{\partial g}{\partial\alpha}\,\mathrm{d}^2\alpha \tag{6.37}$$

Application of this formula to Eq. 6.36 leads to the following equation for P_{xy}:

$$\begin{aligned}\int \Lambda(\boldsymbol{\alpha})\,\dot{P}_{xy}(\boldsymbol{\alpha})\,\mathrm{d}^4\boldsymbol{\alpha} \;= &-\int \Lambda(\boldsymbol{\alpha})\begin{pmatrix} \partial_\alpha \\ \partial_\beta \end{pmatrix}\begin{pmatrix} \dot{\alpha}_x P_{xy}(\boldsymbol{\alpha}) \\ \dot{\beta}_y P_{xy}(\boldsymbol{\alpha}) \end{pmatrix}\mathrm{d}^4\boldsymbol{\alpha} \\ &+ \int \Lambda(\boldsymbol{\alpha})\Big\{\alpha\beta\big(\mathrm{i}\chi(y) - \mathrm{i}\chi(x)\big)\Big\}\,P_{xy}(\boldsymbol{\alpha})\,\mathrm{d}^4\boldsymbol{\alpha}.\end{aligned} \tag{6.38}$$

Both sides of this equation have the same structure if two conditions are satisfied:

1. $P_{xy}(\boldsymbol{\alpha})$ is of the form $a_{xy}(t) f_{xy}\big[\alpha - \alpha_x(t), \beta - \beta_y(t)\big]$,
2. α_x, β_y and a_{xy} are independent of $\boldsymbol{\alpha}$.

The first condition ensures that the time derivative of P_{xy} has the form

$$\dot{P}_{xy} = -\dot{\alpha}_x a_{xy}(t)\partial_\alpha f - \dot{\beta}_y a_{xy}(t)\partial_\beta f + \dot{a}_{xy} f, \tag{6.39}$$

while the second condition enables us to commute the partial derivatives past $\dot{\alpha}_x$, $\dot{\beta}_y$, and $a_{xy}(t)$. Both conditions are met if $P_{xy}(\boldsymbol{\alpha})$ is proportional to delta distributions:

$$P_{xy}(\boldsymbol{\alpha}) = a_{xy}(t)\delta^{(2)}\big[\alpha - \alpha_x(t)\big]\delta^{(2)}\big[\beta - \alpha_y^*(t)\big], \tag{6.40}$$

with $\delta^{(2)}[\alpha] = \delta[\operatorname{Re}\alpha]\delta[\operatorname{Im}\alpha]$, since now, the Dirac deltas fixes any occurring $\boldsymbol{\alpha}$ to $(\alpha_x(t), \alpha_y^*(t))$, effectively removing the problematic dependency.

Remark

In case it is not obvious, we can easily see that the identity $\partial_x\left(f(x)\delta(x)\right) = f(0)\partial_x\delta(x)$ holds via the following calculation:

$$\begin{aligned}\int_\infty^\infty g(x)\partial_x\big(f(x)\delta[x]\big)\,\mathrm{d}x &= -\int_\infty^\infty \partial_x\big(g(x)\big)f(x)\delta[x]\,\mathrm{d}x = -\frac{\mathrm{d}g}{\mathrm{d}x}\bigg|_{x=0} f(0)\\ &= f(0)\int_\infty^\infty g(x)\partial_x\delta(x)\,\mathrm{d}x = -f(0)\frac{\mathrm{d}g}{\mathrm{d}x}\bigg|_{x=0},\end{aligned} \tag{6.41}$$

which proves that we can just evaluate $\dot{\alpha}_x(t)$ at $\alpha = \alpha_x$ in Eq. 6.38.

Therefore, using the Ansatz 6.40 for Eq. 6.38 we can identify, by comparing both sides

$$\dot{\alpha}_x = -\left(\mathrm{i}\delta\omega_r + \mathrm{i}\chi(x) + \frac{\kappa}{2}\right)\alpha_x(t) - \mathrm{i}\epsilon \tag{6.42}$$

$$\dot{\beta}_y = -\left(\mathrm{i}\delta\omega_r + \mathrm{i}\chi(y) + \frac{\kappa}{2}\right)\alpha_y^*(t) + \mathrm{i}\epsilon = \dot{\alpha}_y^*(t) \tag{6.43}$$

$$\dot{a}_{xy}(t) = -\mathrm{i}\Big[\big(\chi(x) - \chi(y)\big)\alpha_x\alpha_y^*\Big]\cdot a_{xy}(t). \tag{6.44}$$

Solving these differential equations determines all left unknowns and we find the solution of the master equation 6.7:

$$\rho = \sum_{x,y} a_{xy}(t)\,|x\rangle\langle y| \otimes \frac{|\alpha_x(t)\rangle\langle\alpha_y(t)|}{\langle\alpha_y(t)|\alpha_x(t)\rangle}. \tag{6.45}$$

The coherent states $|\alpha_x(t)\rangle$ re given by

$$\alpha_x(t) = \alpha_x^s + \big[\alpha_x(0) - \alpha_x^s\big]e^{-\mathrm{i}\left(\delta\omega_r + \chi(x) - \mathrm{i}\frac{\kappa}{2}\right)t}, \tag{6.46}$$

with α_x^s being the steady state

$$\alpha_x^s = \frac{-\mathrm{i}\epsilon}{\frac{\kappa}{2} + \mathrm{i}\left(\delta\omega_r + \chi(x)\right)}. \tag{6.47}$$

The coefficients $a_{xy}(t)$ are given by

$$a_{xy}(t) = a_{xy}(0)e^{-\mathrm{i}[\chi(x) - \chi(y)]\int_0^t \alpha_x\alpha_y^*\,\mathrm{d}t'}. \tag{6.48}$$

This concludes the solution of the simplified master equation 6.7.

6.4. The complete solution (No Qubit-Dissipation)

We can now construct the full solution to the master equation 6.5 by combining the solution of the last section with the solution 6.13 obtained for $\mathcal{L}_Q$. As we have seen, the time evolution generated by $\mathcal{L}_Q$ is given by multiplying a factor $\mathcal{L}_Q(x,y)$ (6.10) to the off-diagonal elements of the complete density matrix. The complete solution of the master equation without qubit relaxation is therefore given by:

Solution

$$\rho(t) = \sum_{xy} c_{xy}(t)\,|x\rangle\langle y| \otimes \frac{|\alpha_x(t)\rangle\langle\alpha_y(t)|}{\langle\alpha_y(t)|\alpha_x(t)\rangle}, \tag{6.49}$$

with the coherent states

$$\alpha_x(t) = \alpha_x^s + \left[\alpha_x(0) - \alpha_x^s\right] \exp\left[-\mathrm{i}\left(\delta\omega_r + \chi(x) - \mathrm{i}\frac{\kappa}{2}\right)t\right] \tag{6.50}$$

$$\alpha_x^s = \frac{-\mathrm{i}\epsilon}{\frac{\kappa}{2} + \mathrm{i}\left(\delta\omega_r + \chi(x)\right)} \tag{6.51}$$

and the coefficients

$$c_{xy}(t) = \exp\left[-\mathrm{i}\phi_Q(x,y,t) - \mathrm{i}\phi_m(x,y,t)\right] \exp\left[-\gamma_2(x,y)t - \Gamma_m(x,y,t)\right]. \tag{6.52}$$

The qubit phase ϕ_Q and the measurement induced phase ϕ_m are given by

$$\phi_Q(x,y,t) = \sum_q \frac{\delta\tilde{\omega}_q}{2}\left[Z^q(x) - Z^q(y)\right]t, \tag{6.53}$$

$$\phi_m(x,y,t) = \left[\chi(x) - \chi(y)\right] \mathrm{Re}\left[\int_0^t \alpha_x\alpha_y^*\,\mathrm{d}t'\right]. \tag{6.54}$$

Solution

and the dephasing rate due to pure dephasing $\gamma_2(x,y)$ as well as the dephasing factor due to measurement $\Gamma_m(x,y,t)$ are given by

$$\gamma_2(x,y) = \sum_q \frac{\gamma_{\phi q}}{2}\left[1 - Z^q(x)Z^q(y)\right] \tag{6.55}$$

$$\Gamma_m(x,y,t) = -\left[\chi(x) - \chi(y)\right] \mathrm{Im}\left(\int_0^t \alpha_x\alpha_y^*\,\mathrm{d}t'\right). \tag{6.56}$$

We note that this solution is only valid if the system starts out in a superposition of coherent states at time $t = 0$ of the form

$$\rho(0) \sim \sum_{xy} |x\rangle\langle y| \otimes \frac{|\alpha_x(0)\rangle\langle\alpha_y(0)|}{\langle\alpha_y(0)|\alpha_x(0)\rangle}. \tag{6.57}$$

6.5. Analysis of the result

The first thing we can say about our solution is that compared to the 1-qubit solution obtained in [2] and the 2-qubit solution obtained in [4], the N-qubit solution is a straightforward generalization of those earlier solutions. They only differ in the expectation values $Z^q(x) = \langle x|\sigma_z^q|x\rangle$ and $\chi(x) = \sum_q \langle x|\chi\sigma_z^q|x\rangle$ which are now being evaluated with respect to arbitrary register states $|x\rangle$, instead of just 1- or 2- qubits register states.

It follows that most of the analysis and interpretation of the solution can be directly transferred from these earlier ones. Therefore, we only give a brief review on the meaning and importance of this result.

6.5.1. Formation of coherent states

Assuming the oscillator starts out in the vacuum state $|0\rangle\langle 0|$ at $t = 0$, the system is driven into an entangled superposition of coherent states moving towards the stationary states α_x^s, depending on the respective register state to which the oscillator is coupled:

$$\sum_{x,y} c_{xy}(0)\,|x\rangle\langle y| \otimes |0\rangle\langle 0| \longrightarrow \sum_{x,y} c_{xy}(t)\,|x\rangle\langle y| \otimes \frac{|\alpha_x(t)\rangle\,\langle\alpha_y(t)|}{\langle\alpha_y(t)|\alpha_x(t)\rangle} \qquad (6.58)$$
$$\text{with} \quad \alpha_x(t) = \alpha_x^s \exp\left[-\mathrm{i}\left(\delta\omega_r + \chi(x) - \mathrm{i}\kappa/2\right) t\right].$$

The rate at which this relaxation occurs is given by $\kappa/2$. The final amplitude of the oscillator, given by $|\alpha_x^s|$, crucially depends on ϵ, κ, and the difference between the shifted resonator frequency and the drive frequency:

$$|\alpha_x^s| = \frac{\epsilon}{\sqrt{\kappa^2/4 + \left(\delta\omega_r + \chi(x)\right)^2}}. \qquad (6.59)$$

There are two ways the amplitude can be increased:

1. Choosing the driving frequency ω_d such that $\omega_r - \omega_d + \chi(x) = 0$,
2. increasing the ratio ϵ/κ.

The first option can be used to *distinguish* between certain register states $|x\rangle$. For example, one can choose to maximize the amplitude of all states with $\chi(x) = 0$ by choosing $\omega_d = \omega_r$. Or more generally: Driving resonantly at the *shifted frequency* of the oscillator $\omega_d = \omega_r + \chi(x)$ maximizes the amplitudes of all register states with mean dispersive shift $\chi(x)$ by minimizing the denominator in Eq. 6.59 (see Fig. 6.1). Recalling our analysis of the driven oscillator in section 2.1 this is a physically quite intuitive result.

The second option does not differentiate between different register states and increases the amplitude of all α_x. This however, does spread them out in phase space, which leads to distinguishability between some subspaces eventually. (see Figures 6.2 and 6.3)

6.5.2. Measurement induced dephasing

The formation and separation of coherent states in oscillator phase space is accompanied by a measurement-induced dephasing of the register states. The oscillator starts to "distinguish" between different register subspaces, as the corresponding coherent states increase their distance, thereby becoming more orthogonal to each other. The oscillator and register become *entangled*. This process coincides precisely with the description of measurement and environmental monitoring given in [40] for example. Therefore, the states $|\alpha_x\rangle$ can be identified as *pointer states* of the resonator, acting as a measurement-apparatus for the register [2] [46].

A necessary aspect of any quantum mechanical measurement is the dephasing between those system-subspaces, which are being distinguished by the apparatus [40]. In our case, this is reflected by the presence of $\Gamma_m(x, y, t)$ (Eq. 6.56) in the exponent of the coefficients $c_{xy}(t)$ (Eq.6.52). It is easy to see that this term only induces damping for the off-diagonal elements of the register-state matrix since $\Gamma_m \sim [\chi(x) - \chi(y)]$. I.e. the decohering subspaces are labeled by their respective dispersive shift $\chi(x)$. For times large compared to $1/\kappa$, the rate at which the coherent states form, we can approximate $\alpha_x(t) \sim \alpha_x^s$ in the definition 6.56 of Γ_m and find a fixed rate at which the damping occurs:

$$\Gamma_m(x, y, t) = \underbrace{-\left[\chi(x) - \chi(y)\right] \mathrm{Im}\left[\alpha_x^s (\alpha_y^s)^*\right]}_{\equiv \gamma_m(x,y)} \cdot t. \qquad (6.60)$$

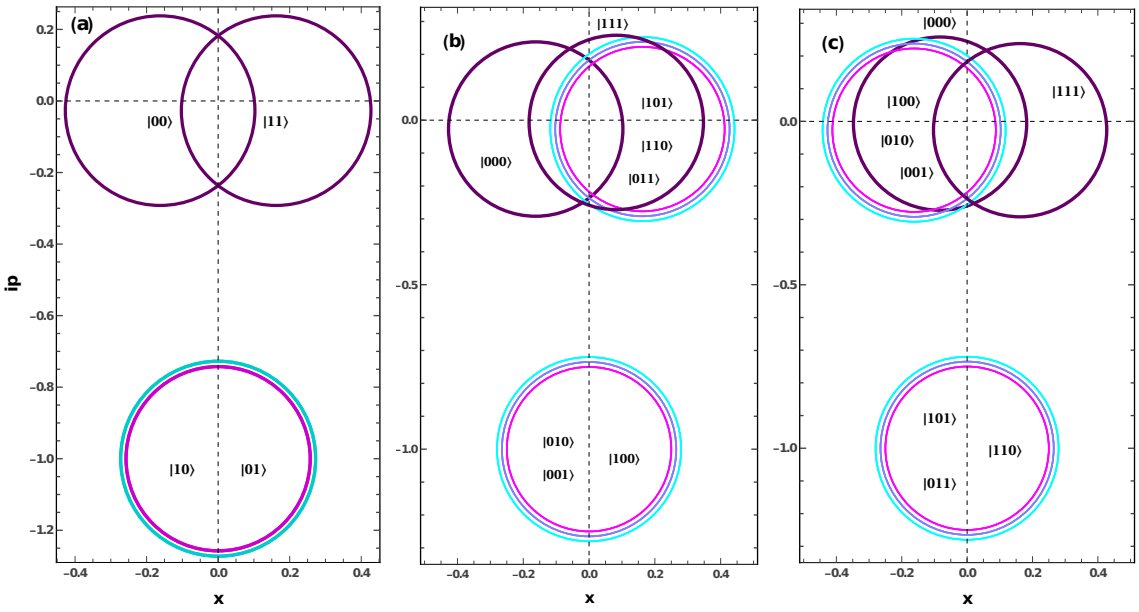

Figure 6.1.: Depiction of coherent states as circles with uncertainty radius 1/4 in phase space. The number of circles around the same center indicates the dimensionality of the subspace, i.e. three circles depict three states centered at that point. In all pictures $\chi = 1.5\kappa$ and $\kappa = 2\epsilon$. **(a)** 2-qubit system driven at bare resonance $\delta\omega_r = 0$. Since $\chi(01) = \chi(10) = 0$, the odd parity states get displaced far from the even ones, which are driven off-resonance. Measuring the p-quadrature of the oscillator only distinguishes between even- and odd-states. [4] **(b)** 3-qubit system driven at $\delta\omega_r = \chi(x)$, in resonance with the two-up one-down states ($n(e) = 2$ and $n(g) = 1$), allowing discrimination between the $n(e) = 2$ states and all others. **(c)** 3-bit system driven at $\delta\omega_r = -\chi$, in resonance with the $n(g) = 2$ states.

Since the imaginary part of $\alpha_x^s(\alpha_y^s)^*$ vanishes, as α_x^s approaches α_y^s, the dephasing rate not only depends on the difference in dispersive shift but also on the distance between α_x^s and α_y^s. This is made explicit by noticing that

$$\mathrm{Im}\left[\alpha_x^s(\alpha_y^s)^*\right] = \frac{1}{2}\,\mathrm{Im}\left[\left(\alpha_x^s - \alpha_y^s\right)\left(\left[\alpha_x^s\right]^* + \left[\alpha_y^s\right]^*\right)\right], \tag{6.61}$$

which reinforces our intuition that the dephasing rate of the register states directly depends on how well the oscillator can distinguish between them.

Reduced master equation for the register

By tracing out the oscillator degrees of freedom from the master equation 6.5, the measurement-induced dephasing can also be found as an explicit effect on the register dynamics caused by the driven oscillator: Using the solution 6.4 we rewrite ρ as

$$\begin{aligned} \rho &= \sum_{x,y} c_{xy}(t)\,|x\rangle\langle y| \otimes \rho_{xy} \\ \text{with} \quad \rho_{xy} &= \frac{|\alpha_x(t)\rangle\langle\alpha_y(t)|}{\langle\alpha_y(t)|\alpha_x(t)\rangle} \end{aligned} \tag{6.62}$$

and note that $Tr_O\left[\rho_{xy}\right] = 1$. Therefore the reduced density matrix of the register ρ_Q is

$$\rho_Q \equiv \mathrm{Tr}_O\left[\rho\right] = \sum_{x,y} c_{xy}(t)\,|x\rangle\langle y|\,. \tag{6.63}$$

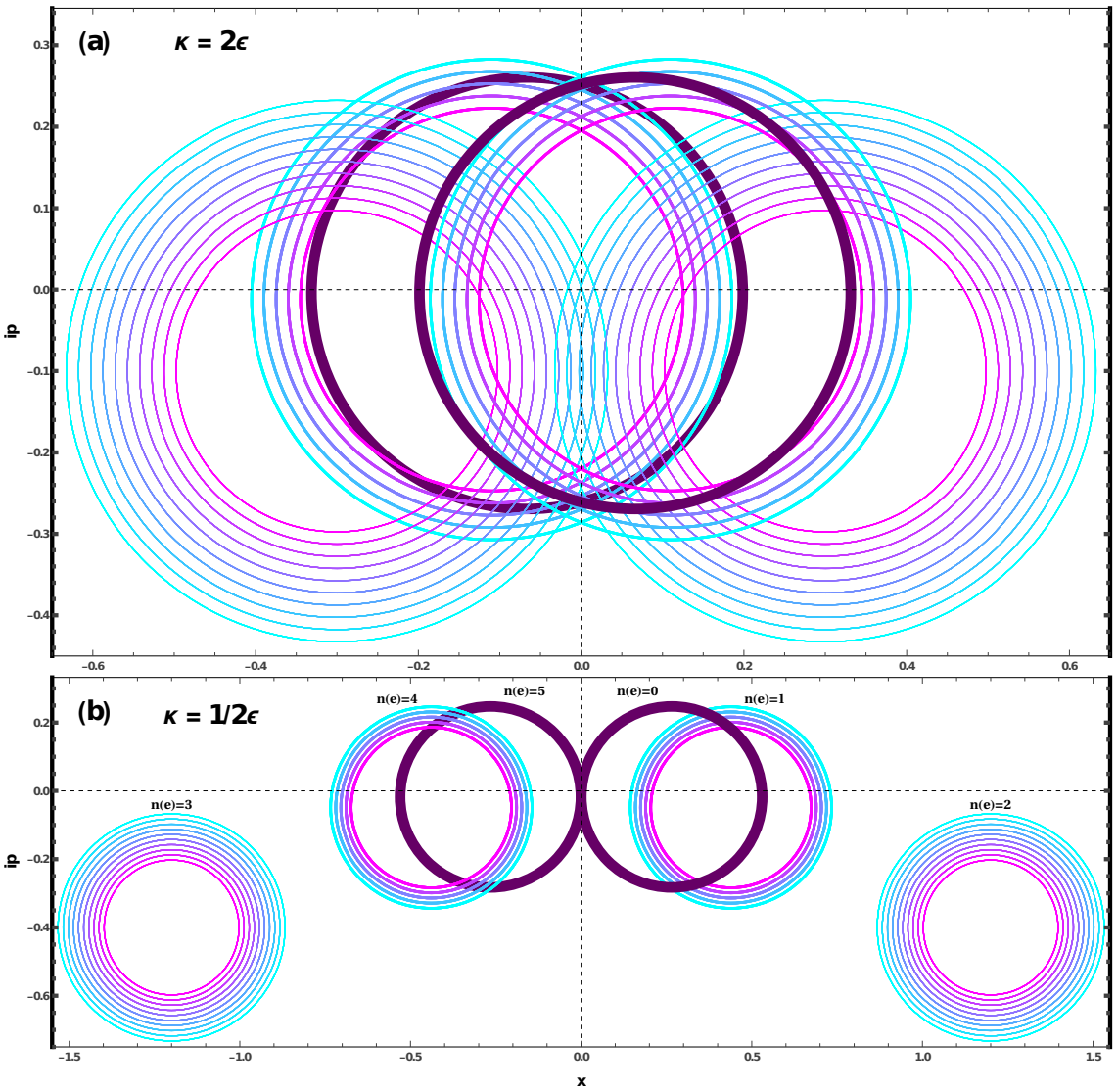

Figure 6.2.: Phase space distribution of coherent states for 5-qubit system, for $\chi = 1.5\kappa$, driven at $\delta\omega_r = 0$, which is resonant with none of the states. **(a)** For a weak drive $\epsilon = 1/2\kappa$ no state-discrimination is possible. **(b)** Increasing the drive to $\epsilon = 2\kappa$ separates the states with $n(e) = 3$ and $n(e) = 2$ from the bulk, since they are closest to resonance. $n(e)$ denotes the number of excited qubits in the corresponding register states.

Now we calculate the terms in the reduced master equation, given by

$$\dot{\rho}_Q = \mathrm{Tr}_O\left[\mathcal{L}\rho\right] = -\mathrm{i}\,\mathrm{Tr}_O\left[H,\rho\right] + \kappa\,\mathrm{Tr}_O\left[\mathcal{D}[a]\rho\right] + \frac{\gamma_{\phi q}}{2}\,\mathrm{Tr}_O\left[\mathcal{D}[\sigma_z^q]\rho\right]. \tag{6.64}$$

First of all, the oscillator dissipator term vanishes:

$$\begin{aligned}\mathrm{Tr}_O\left[\mathcal{D}[a]\rho\right] &= \sum_{x,y} c_{xy}(t)\,|x\rangle\langle y| \cdot \mathrm{Tr}\left\{a\rho_{xy}a^\dagger - \frac{1}{2}\left(a^\dagger a\rho_{xy} + \rho_{xy}a^\dagger a\right)\right\} \\ &= \sum_{x,y} c_{xy}(t)\,|x\rangle\langle y| \cdot \mathrm{Tr}\left\{a\rho_{xy}a^\dagger - \frac{1}{2}\left(a\rho_{xy}a^\dagger + a\rho_{xy}a^\dagger\right)\right\} \\ &= 0.\end{aligned} \tag{6.65}$$

This is a reflection of the fact that the dissipators generate trace-preserving time evolution. For the second dissipator, we use the fact that the trace can be commuted past $\mathcal{D}[\sigma_z^q]$ since

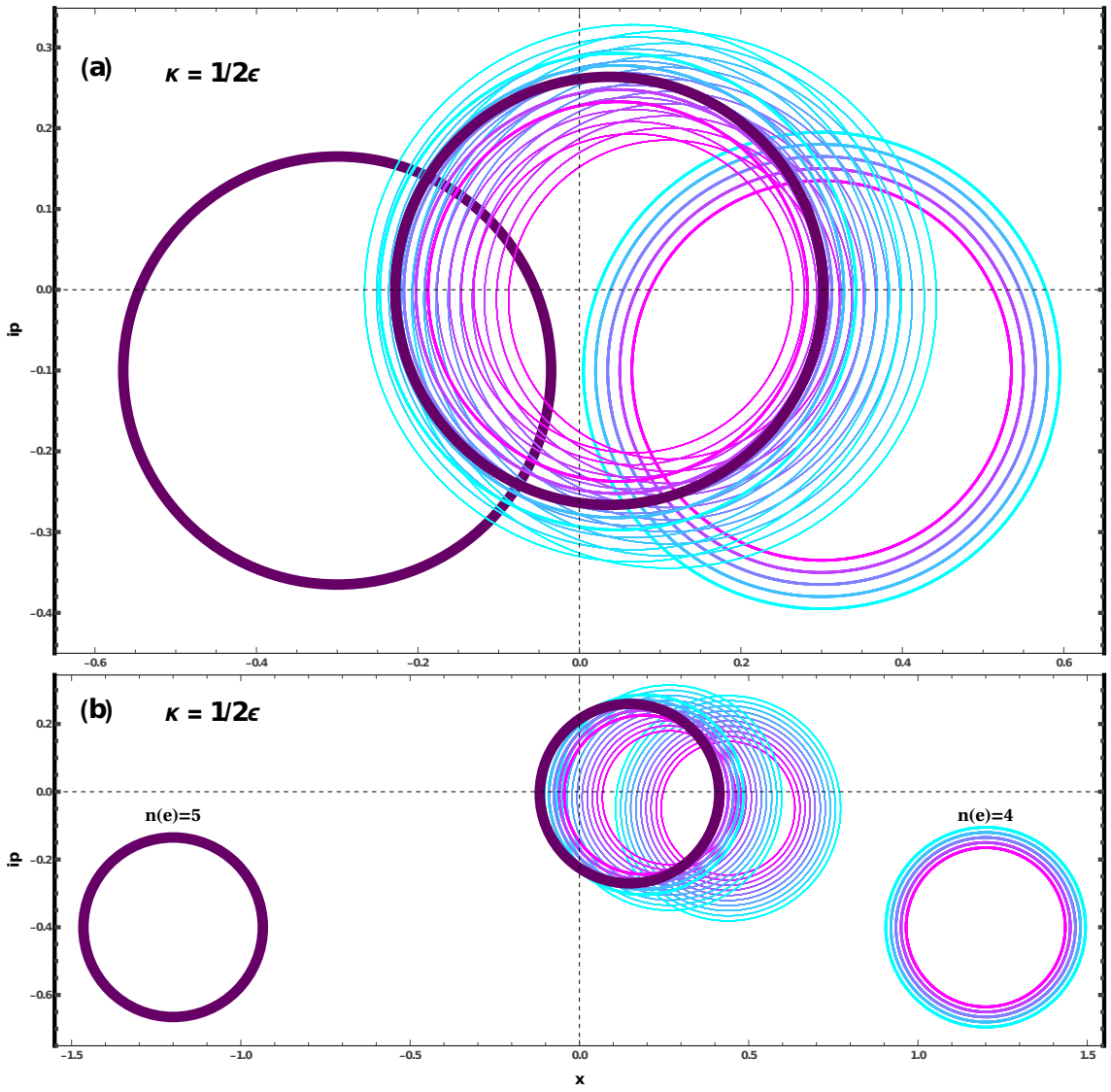

Figure 6.3.: Phase space distribution of coherent states for 5-qubit system, for $\chi = 1.5\kappa$, driven at $\delta\omega_r = -4\chi$, which is also not perfectly resonant with any of the states. **(a)** The weak drive $\epsilon = 1/2\kappa$ leaves all states indistinguishable. **(b)** The strong drive $\epsilon = 2\kappa$ still selects the state $n(e) = 5$, making it possible to measure whether all qubits are excited or not.

the latter only acts on the register states:

$$\mathrm{Tr}_O\left\{\mathcal{D}[\sigma_z^q]\rho\right\} = \mathcal{D}[\sigma_z^q]\rho_Q. \tag{6.66}$$

Finally, for the commutator with H we obtain

$$-\mathrm{i}\,\mathrm{Tr}_O\left[H,\rho\right] = -\mathrm{i}\frac{\delta\tilde{\omega}_q}{2}\left[\sigma_z^q,\rho_Q\right] - \mathrm{i}\chi_q\left[\sigma_z^q,\mathrm{Tr}_O\left\{a\rho a^\dagger\right\}\right]. \tag{6.67}$$

The trace in the second term is given by

$$\begin{aligned}\mathrm{Tr}_O\left\{a\rho a^\dagger\right\} &= \sum_{x,y} c_{xy}(t)\left|x\right\rangle\!\left\langle y\right|\mathrm{Tr}_O\left\{a\rho_{xy}a^\dagger\right\}\\ &= \sum_{x,y} c_{xy}(t)\alpha_x(t)\alpha_y^*(t)\left|x\right\rangle\!\left\langle y\right|\\ &= \sum_{x,y}\alpha_x(t)\alpha_y^*(t)\Pi(x)\rho_Q\Pi(y),\end{aligned} \tag{6.68}$$

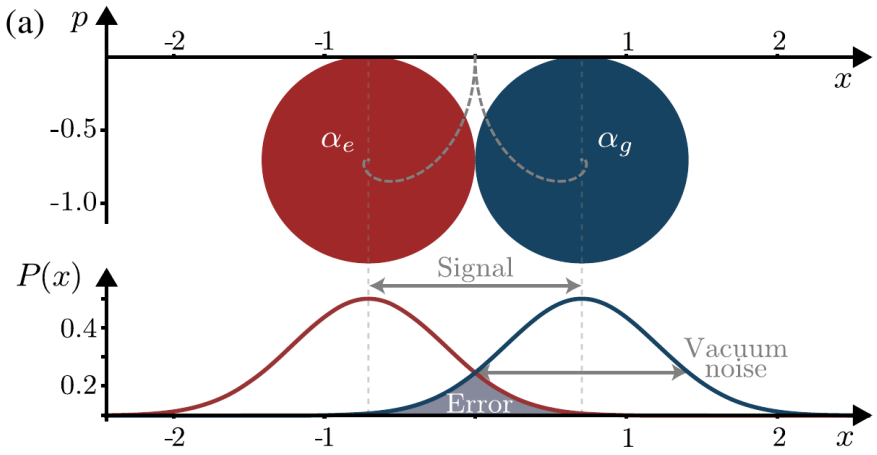

Figure 6.4.: 1 qubit system driven at bare resonance. The overlap "Error" of the coherent states corresponds to a lack of state discrimination and leads to a measurement Error $E_m = \mathrm{erfc}(SNR/2)$.[1] (Figure taken from [1])

yielding the commutator

$$-\mathrm{i}\chi_q \left[\sigma_z^q, \mathrm{Tr}_O\left\{a\rho a^\dagger\right\}\right] = -\mathrm{i}\sum_{x,y}\left[\chi(x)-\chi(y)\right]\alpha_x(t)\alpha_y^*(t)\Pi(x)\,\rho_Q\,\Pi(y), \tag{6.69}$$

which is composed of the time derivatives of the measurement-induced phase $\phi_m(x,y,t)$ and the measurement-induced damping factor $\Gamma_m(x,y,t)$ defined in Box 6.4:

$$-\mathrm{i}\chi_q \left[\sigma_z^q, \mathrm{Tr}_O\left\{a\rho a^\dagger\right\}\right] = -\mathrm{i}\sum_{x,y}\left[\chi(x)-\chi(y)\right]\left\{\dot{\phi}_m(x,y,t) - \mathrm{i}\,\dot{\Gamma}_m(x,y,t)\right\}\Pi(x)\,\rho_Q\,\Pi(y). \tag{6.70}$$

The full reduced master equation is therefore given by

$$\begin{aligned}\dot{\rho}_Q = &-\mathrm{i}\frac{\delta\tilde{\omega}_q}{2}\left[\sigma_z^q,\rho_Q\right] + \frac{\gamma_{\phi q}}{2}\mathcal{D}[\sigma_z^q]\rho_Q \\ &-\mathrm{i}\sum_{x,y}\left[\chi(x)-\chi(y)\right]\left\{\dot{\phi}_m(x,y,t) - \mathrm{i}\,\dot{\Gamma}_m(x,y,t)\right\}\Pi(x)\,\rho_Q\,\Pi(y).\end{aligned} \tag{6.71}$$

This equation describes a qubit register, which additionally to pure dephasing, also suffers from a *measurement induced dephasing* with an instantaneous dephasing rate between the subspaces with dispersive shift $\chi(x)$ and $\chi(y)$ given by $[\chi(x)-\chi(y)]\,\dot{\Gamma}_m(x,y,t)$.

6.5.3. Applications

The formation of coherent states and the corresponding dephasing of register subspaces can be used for various purposes. As explained in [47], [2] and [1] they can be used for single qubit-readout. There the goal is to maximize the distance between the "excited-resonator state" α_e^s and the "resonator-ground state" α_g^s, such that, upon measuring the oscillator using heterodyne- or homodyne- measurement, one can infer the corresponding qubit state, effectively performing a qubit readout. Here, the overlap between the two states $\alpha_{e/g}^s$ is directly correlated to the signal-to-noise ratio (SNR) - the smaller the overlap, the better the SNR (see Fig. 6.4). [1]

In a 2-qubit register, one can record the coherent states to perform parity measurements, as proposed in [4]. The dispersive shifts of all qubits are chosen to be equal (as is done in this thesis as well), resulting in the odd parity states $|eg\rangle$ and $|ge\rangle$ having the same averaged dispersive shift $\chi(eg) = \chi(ge) = 0$. Driving at the bare resonance frequency ω_r then displaces those odd-parity states, while the even parity states $|ee\rangle$ and $|gg\rangle$ stay near

the vacuum state (see Fig. 6.1). Measuring the amplitude or suitable quadrature of the oscillator then reveals the parity of the system with high fidelity [4]. The parity measurements can then be used to generate entangled states, since a perfect parity measurement either results in $|eg\rangle \pm |ge\rangle$ or $|ee\rangle \pm |gg\rangle$, regardless of the initial state.

Another application lies in using the parity measurements in continuous quantum error correction protocols, as experimentally achieved in a 3-qubit system in [6]. In their experiment, they coupled 3-qubits to 2 resonators, performing continuous parity measurements on the qubits. Since the odd-parity states have equal dispersive shifts, they are not distinguished by the resonators, thus effectively forming *decoherence free subspaces* [40]. The scheme can be used to detect errors that propagate the state outside the odd-parity states, which serve as the logical subspace on which information is stored and manipulated.

6.5.4. Limitations

Mean photon number

Although it is theoretically possible to increase the amplitude of the oscillator without limit, by increasing the ratio ϵ/κ, it is not well justified physically when the dispersive Hamiltonian is obtained via a Schrieffer-Wolff transformation of the Jaynes-Cummings model. As discussed in section 3.8 there is an upper limit to the mean photon number in the resonator. If the number of photons is not well below n_{crit} (3.79), the dispersive approximation loses its validity. Since the mean photon number $\langle n\rangle = |\alpha|^2$ for a coherent state, we find with Eq. 6.59 the mean photon number for the register state $|x\rangle$:

$$n_{disp} \equiv \langle n\rangle = \frac{\epsilon^2}{\frac{\kappa^2}{4} + \left(\delta\omega_r + \chi(x)\right)^2} \overset{!}{\ll} \left(\frac{\Delta_q}{2g_q}\right)^2. \tag{6.72}$$

In the tuning scheme presented in Section 3.9 this condition becomes

$$\frac{\epsilon^2}{\frac{\kappa^2}{4} + \left(\delta\omega_r + \chi(x)\right)^2} \overset{!}{\ll} \frac{1}{4}\frac{\delta\omega_1}{\chi}. \tag{6.73}$$

This equation tells us, that we need to either decrease χ or increase $\delta\omega_1$ in order to increase the allowed oscillator amplitude. The problem with the former is, that decreasing χ necessarily decreases the distance between the respective $\alpha_x(t)$ in phase space (since they only differ in their value for $\chi(x) \sim \chi$). The problem with the latter is that the detuning $\delta\omega_1$ cannot be increased indefinitely, since we have already established the relationship

$$\frac{\delta\omega_1}{2\pi} \lesssim \frac{10\,\mathrm{GHz}}{2N} \tag{6.74}$$

in section 3.9 as a rough estimate for when the frequency space will be "too crowded" for the qubit-approximation of the transmons to still hold. Furthermore, increasing $\delta\omega_r$ at constant χ would also require an increase of g^2 by the same amount. Since the coupling cannot be arbitrarily large this is another limitation to maximizing the oscillator amplitude. Sticking to the realistic values $\delta\omega_1 \approx 1\,\mathrm{GHz}$ ([2]) and $g \approx 100\,\mathrm{MHz}$ yields a critical photon number

$$n_{crit} \approx 25 \quad \text{for} \quad \lambda \approx 0.1, \tag{6.75}$$

which is quite high. However, the condition for the dispersive approximation is that the actual photon number needs to be much smaller than n_{crit}, and we will see in the next chapter that the analytic-dispersive solution does indeed depart from the full-numerical solution well below n_{crit}.

In conclusion, it can be said that, as long as the dispersive Hamiltonian used to generate the phase space distributions of coherent states is just the approximation of the Jaynes-Cummings Model as in our case, we are limited in optimizing state discrimination by increasing the distance between any given register-subspace, because the approximation starts to break down as the mean photon number increases alongside the distance between the coherent states.

Qubit relaxation for times large compared to $1/\kappa$

At the beginning of the chapter the qubit relaxation term in the master equation $\gamma_{1q}\mathcal{D}[\sigma_-^q]$ was neglected. It should be clear that this is only physically reasonable for small relaxation rates γ_{1q}. In particular, the qubit relaxation rate γ_{1q} should be much smaller than the resonator dissipation rate κ. Then, on timescales much smaller than $1/\gamma_{1q}$, we can expect the effects of qubit relaxation to be small (only rarely will a qubit relax by sending out a photon to the bath in such a short time interval), and safely neglect the contribution of qubit relaxation. The result is a formation of coherent states at rate κ, while the qubit occupation numbers stay constant at all times - the coefficients $c_{xx}(t)$ for the diagonal elements satisfy $\sum_x c_{xx}(t) = 1$ for all t. For times that approach $1/\gamma_{1q}$ we expect that the qubits start to relax resulting in the decay of all occupation numbers c_{xx} except for the one of the ground state .

Therefore, in order to take qubit relaxation into account, it is tempting to use solution 6.4 as a starting point and modify it slightly as an ansatz for the full master equation 6.1, by allowing the occupation numbers c_{xx} to be dependent on time as well. However, looking at the effect of the qubit dissipator on the time evolution in the $|x\rangle$ basis (Eq. 6.4), we can see that its exact effects can not be so simple:

$$\mathcal{D}[\sigma_-^q]\rho = \sum_{xy} \rho_{xy} \otimes \left\{ |x_{q_-}\rangle\langle y_{q_-}| - \frac{1}{4}\Big[(\mathbb{1} + \sigma_z^q)\,|x\rangle\langle y| + |x\rangle\langle y|\,(\mathbb{1} + \sigma_z^q) \Big] \right\}. \tag{6.76}$$

The structure of the dissipator implies that it also couples different oscillator states with each other, resulting in a deviation of those states from the coherent states found in the relaxation-free solution. To make this more explicit, we can project the dissipator with a fixed $\langle x|$ from the left and $|y\rangle$ from the right to find the effect of γ_{1q} on the time evolution of the oscillator operators ρ_{xy}:

$$\dot{\rho}_{xy} \sim \sum_q \gamma_{1q} \Big\{ \rho_{x_{q+}y_{q+}} - \rho_{xy}\,\frac{1}{4}\big[1 + Z^q(x)\big]\big[1 + Z^q(y)\big] \Big\}. \tag{6.77}$$

The second term describes a "loss of amplitude" for every qubit q that is excited in the register states $|x\rangle$ and $|y\rangle$. This loss of amplitude is proportional to ρ_{xy} itself. The first term describes a "leaking" down of those oscillator states $\rho_{x_{q+}y_{q+}}$ which have the qubit q excited, whenever q is not already excited in $|x\rangle$ and $|y\rangle$. Therefore, the coherent states $|\alpha_x t\rangle$ cannot be the solutions of the full master equation, since, even if the system started in such a state, the different components are mixed by the qubit relaxation, likely resulting in non-coherent oscillator states.

Conclusion

The results obtained are limited, first by the critical photon number condition, constraining the amplitude of the coherent states for which the solution is still a good approximation of the full dynamics.

Secondly, since we neglected the qubit relaxation, they are valid only for $\gamma_{1q} \ll \kappa$ and for time intervals much shorter than $1/\gamma_{1g}$, when the effects of qubit relaxation are expected to become much more relevant.

Therefore, the next chapter is dedicated to finding numerical solutions of the full Jaynes-Cummings dynamics, as well as numerical solutions including γ_{1q}, in order to compare those numerical results with the analytical ones obtained. Especially, we are interested in the effects of the drive strength on the oscillator states, as well as the influence of γ_{1q} on ρ_{xy} and the register occupation numbers $c_{xx}(t)$.

7. Numerical analysis of full master equation

In this chapter numerical solutions to the master equation of the full Jaynes Cummings model is presented, as well as numerical solutions to the master equation of the dispersive Hamiltonian including the qubit-relaxation term.

In the first section, we restrict our analysis to the stationary states of the above models. Those appear as the eigenvectors of the respective vectorized Lindbladians with eigenvalue 0. Next, the stationary solutions are compared to the analytically obtained stationary solution of the previous chapter. The numerical solution of the full Jaynes-Cummings model are compared to the analytic one for different drive strengths and qubit numbers, in order to obtain information about the range of validity of the dispersive approximation. Furthermore, the numerical solutions of the dispersive problem including qubit relaxation are compared to the analytic solution, to check, how γ_{1q} affects the ρ_{xy}.

In the second section, we then continue with a numerical analysis of the dispersive dynamics and the effects of γ_{1q} on the register occupation numbers $c_{xx}(t)$. Here, the complete eigensystem of all Eigenvectors and Eigenvalues of the Lindbladian serve to decompose input states in the eigenbasis, which makes it possible to evolve them numerically in time. The main quantity of interest is then the expectation value of the annihilation operator $\langle a \rangle (t)$, with respect to initial states of the form $|x\rangle\langle x| \otimes |0\rangle\langle 0|$, which for vanishing γ_{1q} would coincide with the $\alpha_x(t)$ found in the previous chapter.

Finally, in the last section, we draw conclusions on the effect that qubit relaxation has on the dynamics for times $t \gg 1/\kappa$ to motivate our further analytical treatment in the next chapter.

7.1. Approach to obtaining the numerical solutions

We start by constructing the matrix representing the Lindbladian of the vectorized master equation. Using Eq. 4.16, the vectorized version of Eq. 7.3 is

$$\begin{aligned}\mathcal{L} = &-\mathrm{i}\Big[H \otimes \mathbb{1} + \mathbb{1} \otimes H^T\Big] + \kappa \left\{ a \otimes a^* - \frac{1}{2}\Big(a^\dagger a \otimes \mathbb{1} + \mathbb{1} \otimes a^T a^*\Big) \right\} \\ &+ \sum_q \frac{\gamma_{\phi q}}{2} \left\{ \sigma_z^q \otimes \sigma_z^q - \frac{1}{2}\Big(\sigma_z^q \sigma_z^q \otimes \mathbb{1} + \mathbb{1} \otimes \sigma_z^q \sigma_z^q\Big) \right\} \\ &+ \sum_q \gamma_{1q} \left\{ \sigma_-^q \otimes \sigma_-^q - \frac{1}{2}\Big(\sigma_+^q \sigma_-^q \otimes \mathbb{1} + \mathbb{1} \otimes \sigma_+^q \sigma_-^q\Big) \right\},\end{aligned} \tag{7.1}$$

where we already applied the properties of the spin matrices σ_z and σ_- in the z-basis where σ_z is diagonal. This Lindbladian can be represented as a finite-dimensional matrix upon truncating the oscillator Hilbert space to finite dimensionality. For example, truncating to the first five energy levels (thus admitting only four photons), the annihilation operator reduces to the 5×5 matrix

$$a \mathrel{\widehat{=}} \begin{pmatrix} 0 & \sqrt{1} & 0 & 0 & 0 \\ 0 & 0 & \sqrt{2} & 0 & 0 \\ 0 & 0 & 0 & \sqrt{3} & 0 \\ 0 & 0 & 0 & 0 & \sqrt{4} \\ 0 & 0 & 0 & 0 & 0 \end{pmatrix}, \tag{7.2}$$

in the energy-eigenbasis $|n\rangle$.

In general, truncating to the n-th energy level of the oscillator, $\mathcal{L}$ is represented by a $(2^N n)^2 \times (2^N n)^2$ -dimensional matrix for a N-qubit register, where all the operators in 7.1 then must be $2^N n \times 2^N n$ dimensional matrices accordingly. This is achieved by taking the Kronecker product of the basic operators of any subspace with the identity matrices of the remaining subspaces in the correct order, similar to how the N-bit-register Pauli matrices σ_x^q are constructed in Eq. 2.29.

Then, *Mathematica* is used to find the numerical eigenvectors and eigenvalues of the matrix $\mathcal{L}$, for a fixed set of parameters. As explained in Section 4.3, the stationary state $\vec{\rho}_s$ is identified as the eigenvector belonging to the eigenvalue 0 with non-vanishing trace.

To study the dynamics generated by $\mathcal{L}$ in Sec. 7.4, the numerically obtained eigensystems are used to find the time evolution of different initial states according to the eigenmode decomposition procedure outlined in Sec. 4.3.2.

The resulting vectors $\vec{\rho}_s$ and $\vec{\rho}(t)$ are then reassembled into matrix form, and are decomposed into the matrices ρ_{xy} conditioned on the register states x and y. Finally, various techniques are used to extract information about the phase space representations of the obtained oscillator density matrices ρ_{xx}, comparing them for different parameters to the analytic solution given in Box 6.4. The details will be explained in the respective section.

7.2. Stationary States: Full Hamiltonian for various ϵ/κ

This section is concerned with numerically obtained *stationary* solutions to the master equation

$$\dot{\rho} = -\mathrm{i}\,[H, \rho] + \kappa \mathcal{D}[a]\rho + \gamma_{1q}\mathcal{D}[\sigma_-^q]\rho + \frac{\gamma_{\phi q}}{2}\mathcal{D}[\sigma_z^q]\rho. \tag{7.3}$$

H is taken to be the full Jaynes Cummings Hamiltonian 3.16.

According to 3.90, we expect that the analytical solutions 6.4 start to deviate from the full Jaynes Cummings dynamics as ϵ is increased and the mean photon number approaches the critical photon number n_{crit}. To verify this, the master equation 7.3 is solved for $H = H_{JC}$ (Eq. 3.16) numerically. The qubit detunings and coupling strengths are chosen in accordance with the scheme presented in section 3.9, to ensure that the dispersive shift χ is equal for every qubit while at the same time minimizing qubit-qubit interactions. The parameters of the master equation are furthermore chosen such that

$$\begin{aligned}
N_{Qubits} &= \{2, 3\} \\
g &= 0.1\,\delta\omega_1 \quad \Rightarrow \quad \lambda = -0.1 \quad \text{and} \quad n_{crit} = 25 \\
\delta\omega_r &= \{0, -\chi\} \quad \text{where} \quad \chi = -0.01\,\delta\omega_1 \\
\kappa &\approx g/1.5 \\
\epsilon/\kappa &= \{0.25, 0.5, 0.75, 1\} \\
\gamma_1 &= 0.0001\,g \\
\gamma_\phi &= 0.001\,g,
\end{aligned} \tag{7.4}$$

where we have assumed that the qubit relaxation rates γ_{1q} as well as the pure dephasing rates $\gamma_{\phi q}$ are equal for all qubits. By truncating the oscillator Hilbert space to 4 photons (i.e. 5 dimensions), which is justified by the expected mean number of photons around ~ 1, the stationary states are obtained as explained in the previous section. Then, the Husimi Q-functions 2.23 of the conditioned oscillator states $\rho_{xx}^s = \langle x|\,\rho^s\,|x\rangle$ are calculated by projecting onto coherent states $|\alpha\rangle$ and normalizing to remove the register weights $\mathrm{Tr}[\rho_{xx}^s]$:

$$Q_x(\alpha) \equiv \frac{1}{\pi}\frac{\langle\alpha|\,\rho_{xx}^s\,|\alpha\rangle}{\mathrm{Tr}[\rho_{xx}^s]}. \tag{7.5}$$

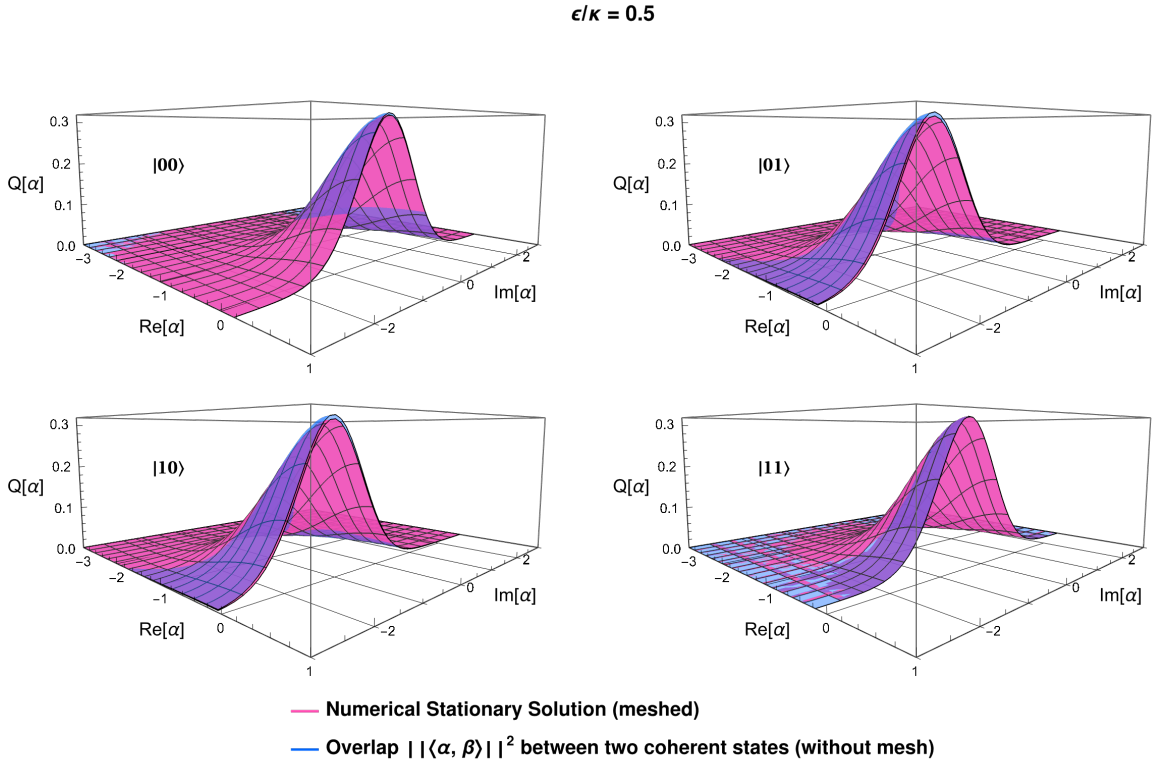

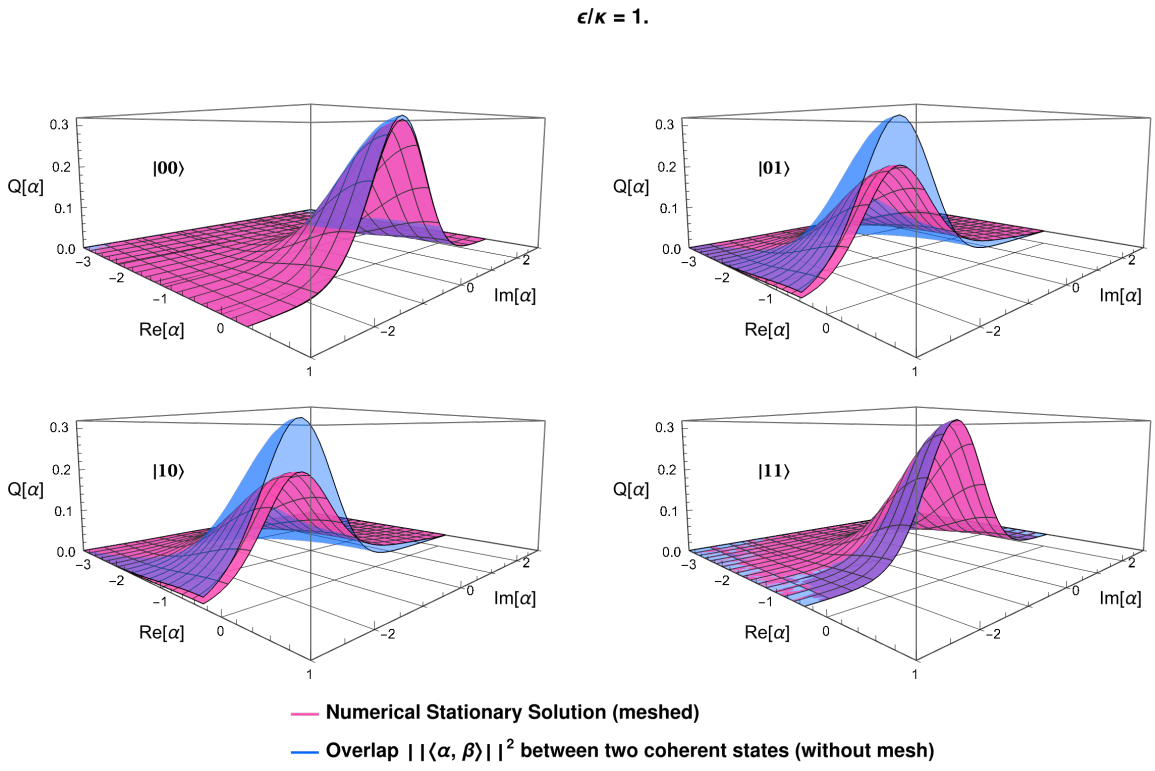

Figure 7.1.: Cross-section of **2-bit Q-functions** of all register-states ρ^s_{xx} for $\epsilon/\kappa = 0.5$ (**top**) and $\epsilon/\kappa = 1$ (**bottom**). The numerical solutions are depicted alongside the Q-function of a coherent pure state $|\beta_x\rangle\langle\beta_x|$ centered around the same respective point in phase space. For $\epsilon/\kappa = 1$ the even parity states $|01\rangle$ and $|10\rangle$ show a significant deviation from ideal coherent states (in accordance with the fact that they are driven resonantly leading to higher photon numbers), while for $\epsilon/\kappa = 0.5$ the deviation is small in all register states. (see Table 7.1 also)

Figure 7.1 shows a cross-section of the Q-functions obtained for $N_{Qubits} = 2$ and $\epsilon/\kappa = 0.5, 1$. To compare the numerically obtained Q-functions with the analytic solutions 6.4, we first evaluate the maxima β_x of the $Q_x(\alpha)$ with respect to α:

$$\beta_x \equiv \max\left[Q_x(\alpha)\right]. \tag{7.6}$$

Then disks of radius 1/4 are plotted, centered around β_x in the complex plane, alongside circles centered around the analytical values of α_x, to visualize their distance in phase space (see Figures 7.2 and 7.3). Finally we estimate the deviations δ_x of the ρ^s_{xx} from coherent states in %, by integrating the difference between $Q_x(\alpha)$ and $|\langle\alpha|\beta_x\rangle|^2$, which is the Q-Function of a pure coherent state $|\beta_x\rangle$:

$$\delta_x \equiv 100 \cdot \int \left| Q_x(\alpha) - |\langle\alpha|\beta_x\rangle|^2 \right| \mathrm{d}\alpha. \tag{7.7}$$

The results of δ_x for $N_{Qubits} = 2$ can be found in Table 7.1, together with the ratios between the numerically obtained photon numbers $n_{num} = |\beta_x|^2$ and the critical photon number, as well as the corresponding ratios of the dispersive photon number n_{disp} 6.72, predicted by the analytical solution, and n_{crit} (in %):

$$n_n \equiv 100 \cdot \frac{n_{num}}{n_{crit}}, \quad n_d \equiv 100 \cdot \frac{n_{disp}}{n_{crit}}. \tag{7.8}$$

ϵ/κ	$\|00\rangle$			$\|01\rangle$			$\|10\rangle$			$\|11\rangle$			**Mean Value**		
	δ	n_n	n_d	δ	n_n	n_d	δ	n_n	n_d	δ	n_n	n_d	δ	n_n	n_d
0.25	0.42	0.030	0.027	0.27	0.96	1.0	0.33	0.99	1.0	0.010	0.028	0.027	0.26	0.5	0.51
0.50	1.09	0.12	0.11	4.4	3.6	4.0	4.5	3.7	4.0	0.035	0.11	0.11	2.5	1.9	2.1
0.75	1.8	0.26	0.24	20.	5.9	9.0	21.	6.0	9.0	0.067	0.25	0.24	11	3.1	4.6
1.0	2.4	0.46	0.43	36.	7.2	16.	38.	7.3	16.	0.100	0.44	0.43	19	3.9	8.2

Table 7.1.: Deviations δ_x for a 2-Qubit system for increasing drive strength, together with the numerical and analytical photon numbers n_n and n_d, in % of n_{crit}.

Interpretation of the results

The analysis of the stationary states supports the theoretical prediction of the breakdown of the dispersive approximation for increased mean photon number. Furthermore, it gives some insight into the possible effects of γ_1 on the evolution of the system.

We note first that normalizing the sub-states ρ^s_{xx} yields density matrices, which for $\epsilon/\kappa \lesssim 1$ correspond to a good approximation to the coherent states $|\alpha^s_x\rangle$ obtained analytically by disregarding γ_1. A possible explanation is, that during the time evolution, the system is initially driven to a state close to the solution 6.4. The relaxation of the qubits then leads to a decay of the resonator weights c_{xx}, while leaving the form of the oscillator matrix intact, resulting in the "imprints" of approximate coherent states $|\beta_x\rangle \approx |\alpha^s_x\rangle$ in the stationary state. Further evidence in favor of this explanation is given in the next section, where the time evolution of initial states $|x\rangle\langle x| \otimes |0\rangle\langle 0|$ is numerically calculated.

Increasing the ratio ϵ/κ beyond 1 quickly leads to noticeable deviations of the imprints from the state $|\alpha^s_x\rangle$. Already for $\epsilon/\kappa = 0.75$, corresponding to $n_{disp}/n_{crit} \approx 5\%$, the mean deviation Mean(δ_x) from coherent states reaches 10% in the 2-Qubit system. The centers β_x in phase space deviate by a distance of approximately 0.35 from α_x for the odd parity states, revealing that the actual amplitude of the oscillator increases more slowly with ϵ/κ than predicted by the non-dissipative dispersive approximation.

For $\epsilon/\kappa \sim 0.5$ a mean deviation Mean(δ_x) = 2.5% is found, combined with distance between β_x and α_x of around 0.15 for the odd parity states, while at the same time offering good state-discrimination between the odd- and even-parity subspaces. We conclude that $\epsilon/\kappa = 0.5$ is a suitable choice for further calculations.

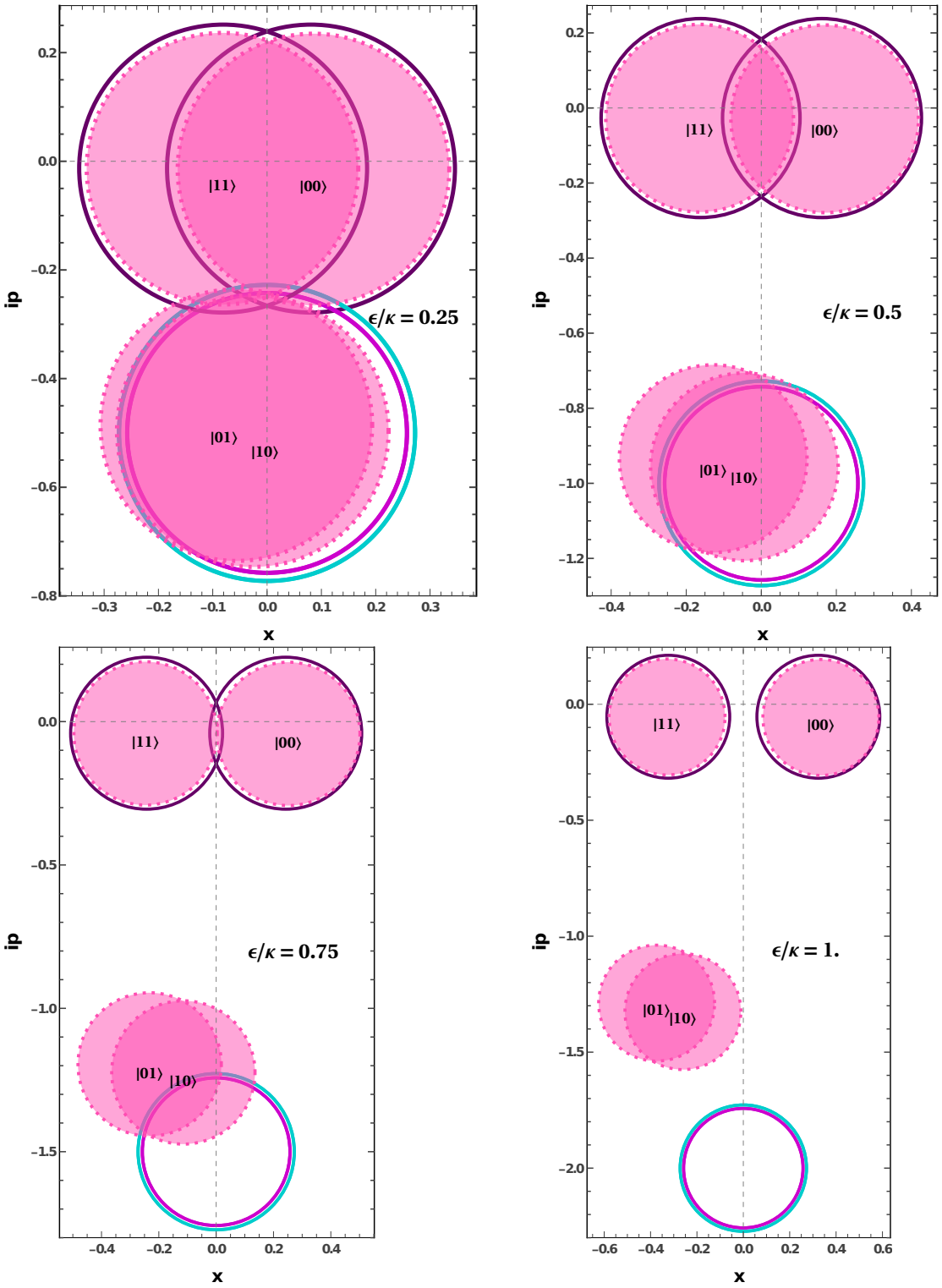

Figure 7.2.: **Comparison of the phase space centers** β_x of ρ^s_{xx} with α^s_x for a 2 qubit register driven at $\delta\omega_r = 0$ and increasing ϵ/κ. The opaque disks are centered around the maxima of the numerical $Q_x(\alpha)$, the solid circles around α^s_x. Increasing the amplitude of the odd parity states leads to noticeable deviation from the analytical positions already beginning at $\epsilon/\kappa \sim 0.5$, corresponding to a ratio n_d between the dispersive photon number n_{disp} 6.72 to the critical photon number n_{crit} of $n_d \sim 1/25$.

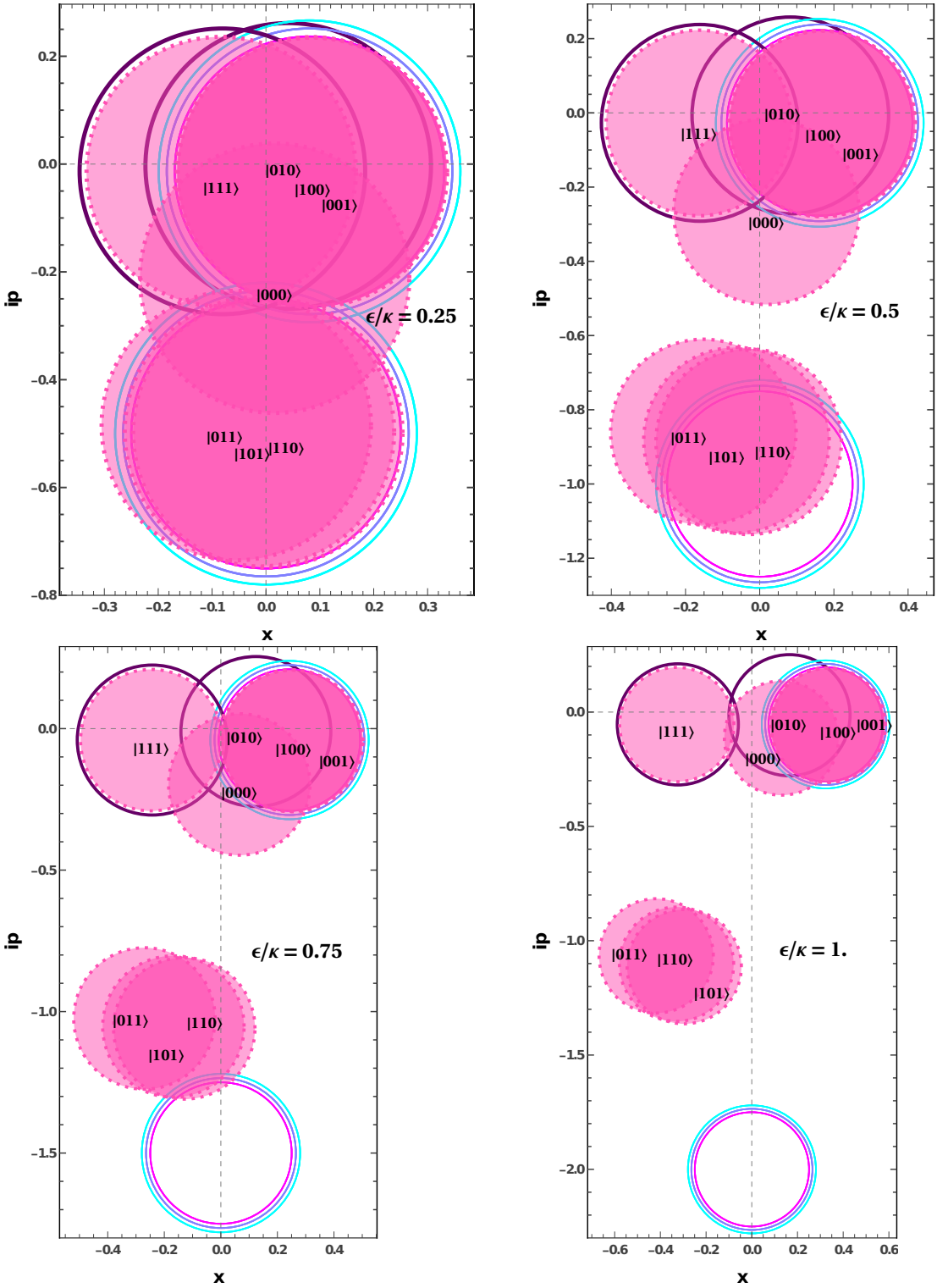

Figure 7.3.: **Comparison of the phase space centers** β_x with α_x^s for a 3-qubit register driven at $\delta\omega_r = -\chi$ and increasing ϵ/κ.

γ_1/g	$\|00\rangle$	$\|01\rangle$	$\|10\rangle$	$\|11\rangle$	**Mean**(δ)
0.0001	0.48	2.1	1.8	0.000020	1.1
0.001	20.	3.0	2.3	0.000022	6.4
0.01	39	26	18	0.000019	21
0.1	530	106	210	0.000023	211

Table 7.2.: Deviations δ_x of the numerical solutions from $|\beta_x\rangle\langle\beta_x|$ in %, for varying γ_1.

7.3. Stationary States: Dispersive Hamiltonian for various γ_1

In this section, the effects of the qubit relaxation are studied by applying the same approach as in the last section, comparing numerical stationary solutions to $|\alpha_x^s\rangle$ for different values of γ_1. In contrast to the last section, $H = H_{disp}$ is chosen as the Hamiltonian. For the calculations underlying the results presented in the section, we used the dispersive Hamiltonian 3.59 including the drive correction term and the flip-flop interaction. However, numerical results obtained by neglecting those correction terms show now significant difference.

The master equation 6.1 is solved for the following parameter values:

$$\begin{aligned} N_{Qubits} &= 2, \\ g &= 0.1\,\delta\omega_1 \quad \Rightarrow \quad \lambda = -0.1 \quad \text{and} \quad n_{crit} = 25, \\ \delta\omega_r &= 0, \quad \text{where} \quad \chi = -0.01\,\delta\omega_1, \\ \kappa &\approx g/1.5, \\ \epsilon/\kappa &= 0.5, \\ \gamma_1 &= \{0.0001\,g, 0.001\,g, 0.01\,g, 0.1\,g\}, \\ \gamma_\phi &= 0.001\,g. \end{aligned} \tag{7.9}$$

Again, the maxima β_x of the Q-functions 7.5 are calculated and plotted together with α_x in phase space (see Fig. 7.4). The deviations δ_x (Eq. 7.7) are calculated and can be found in Tab. 7.2. Plots of $Q_x(\alpha)$ are shown in Fig. 7.5 for $\gamma_1 = \{0.01\,g, 0.1\,g\}$.

Interpretation of the results

The value of γ_1 has a strong effect on the "imprints" left in the stationary state ρ_s. In the regime $\gamma_1 \ll \kappa$, for $\gamma_1/g = 0.0001$ and $\gamma_1/g = 0.001$, the imprints show only very little deviation from the states $|\alpha_x^s\rangle$, with Mean$(\delta) \approx 1 - 6\%$ while being centered around α_x^s in phase space to very good approximation. As γ_1 approaches κ the oscillator states deviate noticeably from coherent states depending on the number of excited qubits in the register. In the regime where $\gamma_1 \approx \kappa$ ($\gamma_1 = 0.1\,g$) the oscillator imprints can no longer be reasonably approximated by coherent states, as is apparent from the bottom plot in Figure 7.5, and their position in phase space deviates widely from α_x^s. This behavior can be qualitatively explained by the action of $\mathcal{D}[\sigma_-]$ on the master equation, as discussed in Subsection 6.5.4. It is further noted that for large γ_1, the β_x's seem to depend chaotically on the precise value of γ_1, meaning that slight changes in γ_1 can lead to apparently random shifts of β_x (see Appendix B).

The solutions for $\gamma_1 = 0.0001\,g$ and $\gamma_1 = 0.001\,g$ are stable however and show good agreement with the analytical solutions $|\alpha_x^s\rangle$, giving further indication that qubit relaxation mostly leads to a decay of the register-weights in the $\gamma_1 \ll \kappa$ regime, while having only little effect on ρ_{xx}.

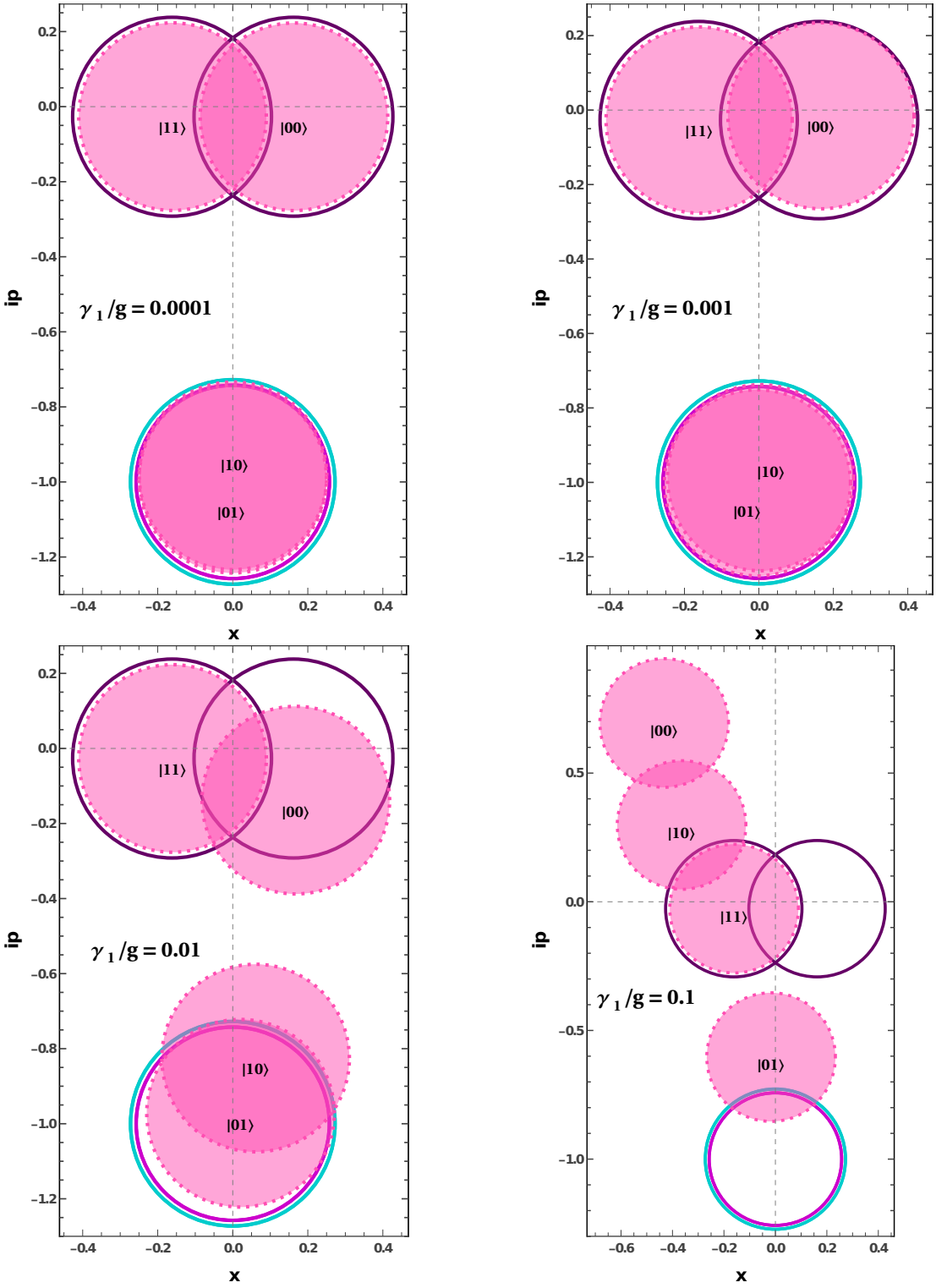

Figure 7.4.: **Comparison of the phase space centers** β_x for varying γ_1. The opaque disks are centered β_x, the solid circles around α_x^s.

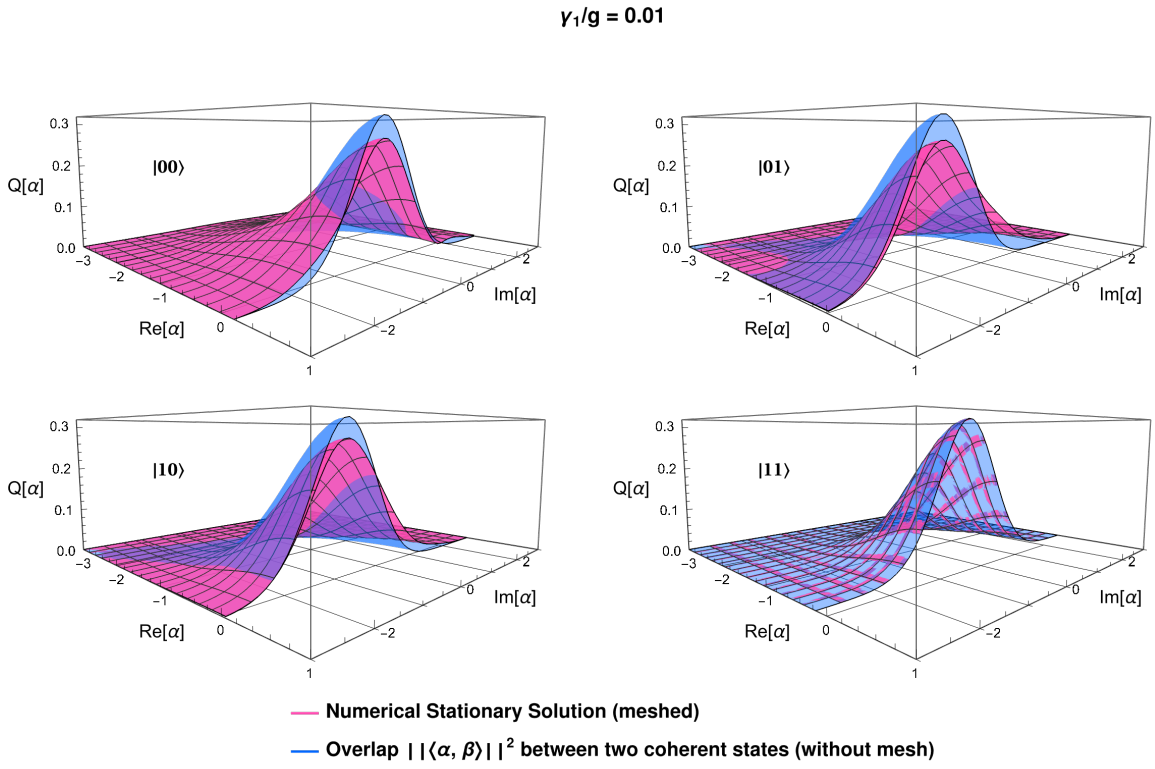

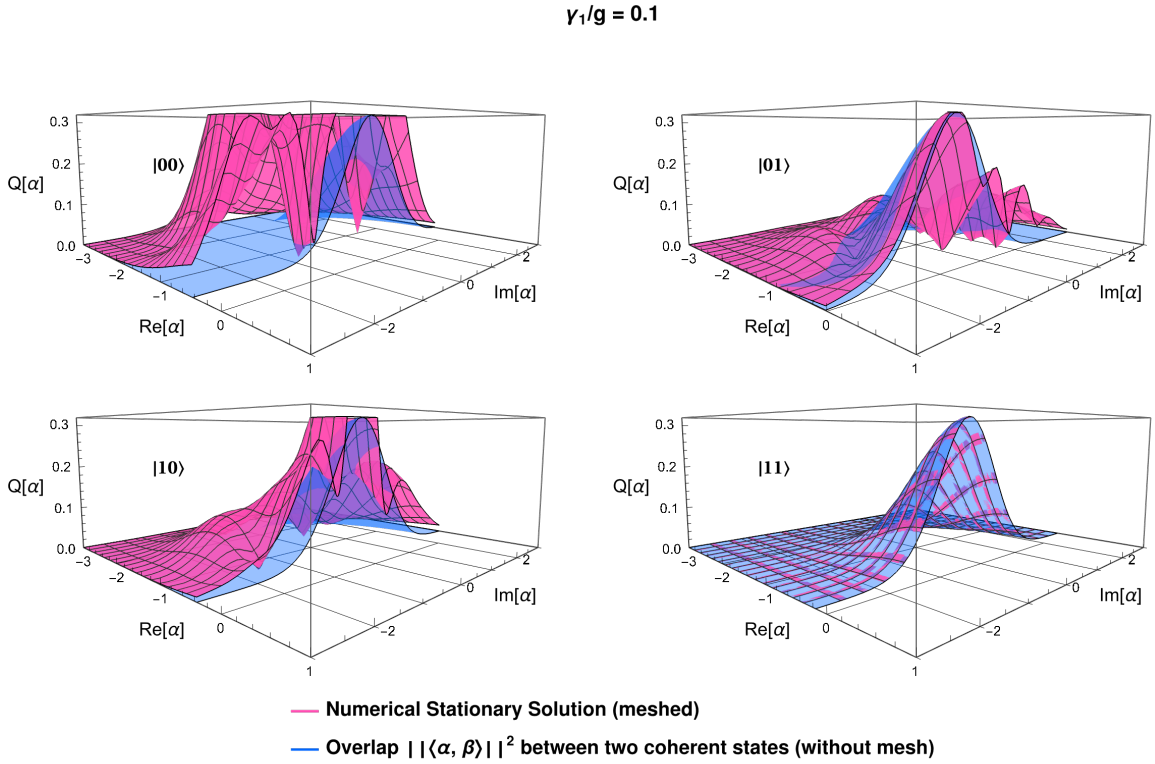

Figure 7.5.: Cross-section of **2-bit Q-functions** of all register-states ρ^s_{xx} for $\gamma_1/g = 0.01$ (**top**) and $\gamma_1/g = 0.1$ (**bottom**).

7.4. Numerical analysis of dissipative dynamics

In this section we go beyond the analysis of the stationary states by applying the protocol presented in Sec. 4.3.2 to decompose initial state vectors into a linear combination of the eigenvectors of $\mathcal{L}$. Each term in the linear combination is then multiplied with $\exp(\lambda_i t)$ to obtain the time-evolved state

$$\rho(t) = \sum_i c_i(0) e^{\lambda_i t} v_i, \tag{7.10}$$

where v_i is the i-th eigenmode of $\mathcal{L}$. As initial states, we choose states of the form

$$\rho(x,0) = |x\rangle\langle x| \otimes |0\rangle\langle 0|\,, \tag{7.11}$$

i.e. we are interested in the time evolution of register eigenstates coupled to a ground-state oscillator initially. For the parameters entering $\mathcal{L}$, we again choose the same set of values as in 7.9.

We start by calculating the trajectories of the oscillator states $\rho_{xx}(t)$ in phase space. For a time-dependent coherent state $|\alpha_x(t)\rangle\langle\alpha_x(t)|$, the trajectories can be obtained by taking the expectation value of the annihilation operator:

$$\alpha_x(t) = \mathrm{Tr}\left[a\,|\alpha_x(t)\rangle\langle\alpha_x(t)|\,\right]. \tag{7.12}$$

Adopting this method we define a coherent parameter $\beta(x_0,t)$ for the more general, numerically obtained density matrices as

$$\beta(x_0,t) = \mathrm{Tr}[a\rho(x_0,t)], \tag{7.13}$$

where $\rho(x_0,t)$ is the time-evolved initial state $|x_0\rangle\langle x_0| \otimes |0\rangle\langle 0|$ and is not to be confused with the conditional oscillator state $\rho_{yy}(x_0,t)$:

$$\rho(x_0,t) = \sum_{x,y} c_{xy}(x_0,t)\,|x\rangle\langle y| \otimes \rho_{xy}(x_0,t), \tag{7.14}$$

with the register weights $c_{xx}(x_0,t)$ and $\rho_{xx}(x_0,t)$ normalized to 1. Furthermore, to get a measure of the width of the states $\rho(x,t)$ the variance of the quadratures p and x are calculated:

$$\Delta X_x^2(t) = \frac{1}{4}\,\mathrm{Tr}\Big[(a+a^\dagger)^2\rho(x,t)\Big] - \frac{1}{4}\left(\mathrm{Tr}\Big[(a+a^\dagger)\rho(x,t)\Big]\right)^2 \tag{7.15}$$

$$\Delta P_x^2(t) = -\frac{1}{4}\,\mathrm{Tr}\Big[(a-a^\dagger)^2\rho(x,t)\Big] + \frac{1}{4}\left(\mathrm{Tr}\Big[(a-a^\dagger)\rho(x,t)\Big]\right)^2. \tag{7.16}$$

$$\tag{7.17}$$

The results are plotted as ellipses with semi-axes given by $\Delta X/2$ and $\Delta P/2$ centered around $\beta_x(t)$ in the complex plane. Figure 7.6 shows the trajectories of the states $|x\rangle\langle x| \otimes |0\rangle\langle 0|$ with $x = \{00, 01, 10, 11\}$ compared to the stationary states α_x^s for a relaxation rate $\gamma_1 = 0.0015\kappa \ll \kappa$. In this case, the oscillator is first driven close to the α_x^s (from $t = 0$ to $t \sim 15/\kappa$) before slowly starting to relax into the ground-state (from $t = 15/\kappa$ to $t \sim 2000/\kappa$). In the relaxation phase the variance of the quadratures x and p show significant deviation from the variance expected from a coherent state - being "squeezed" along the direction of the ground-state.

The trajectories for $\gamma_1 = 0.015\kappa$ plotted in Fig. 7.7 show the same qualitative behavior. Overall the relaxation happens much quicker, as expected, with the ground-state being reached by every initial state around $t \sim 240/\kappa$. However, the time-span between the formation and separation of the different register states and the onset of relaxation is also shorter, with the excited state $|00\rangle$ decaying already before the odd-parity states reach the

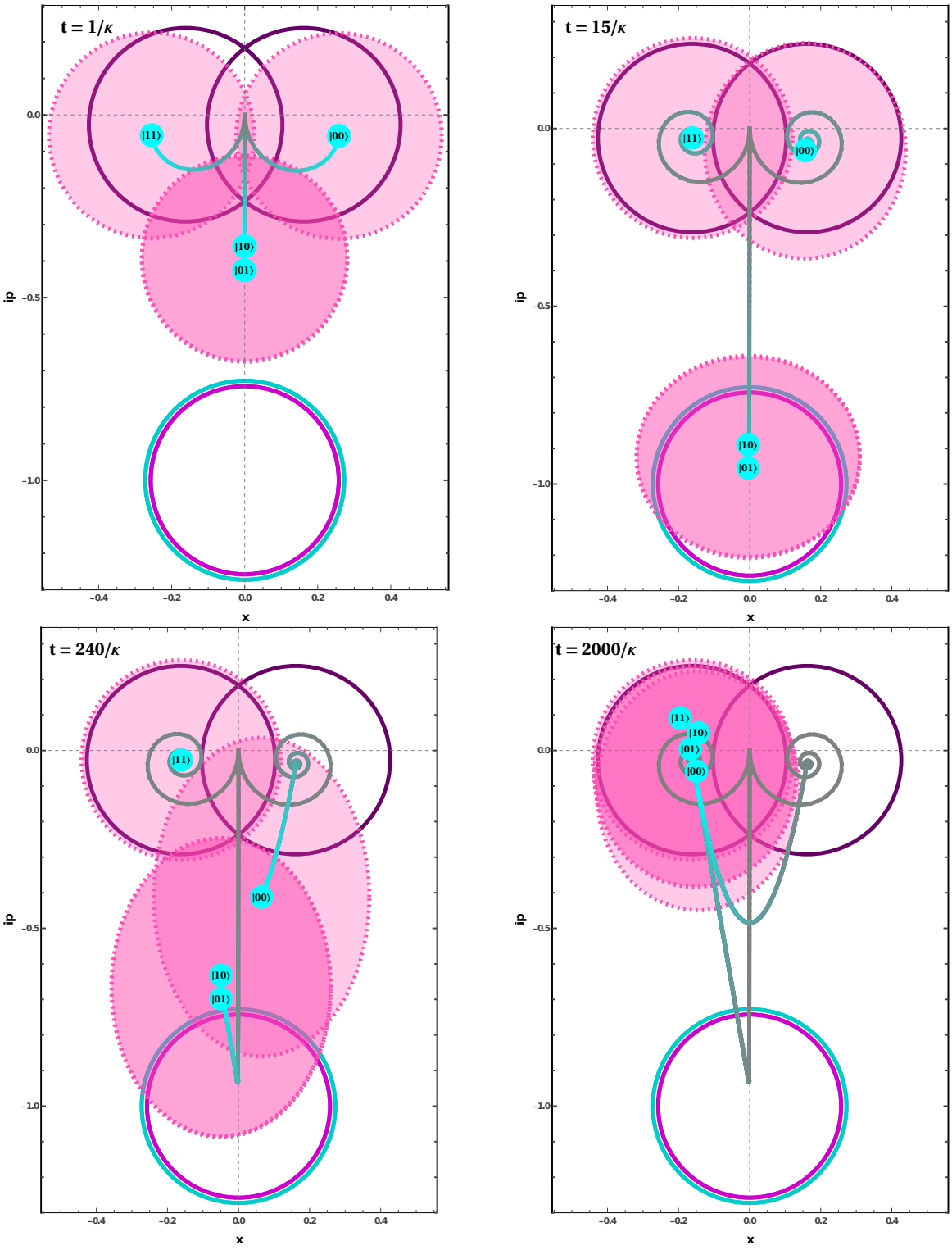

Figure 7.6.: **Trajectories of initial states for $\gamma_1 = 0.0015\kappa$**: The opaque ellipses are centered around $\beta(x_0, t)$ for the initial register states $|x_0\rangle$. The solid gray/cyan line shows the trajectory of the respective register-state up to the given point in time. t is measured in units of $1/\kappa$. The solid circles are centered around α_x^s. The odd parity states reach their maximum amplitudes around $t \sim 5/\kappa$. At $t \sim 15/\kappa$ the excited state $|00\rangle$ starts to decay and drift towards the odd-parity states. At $t \sim 2000/\kappa$ all initial states decayed into the ground-state $|11\rangle$.

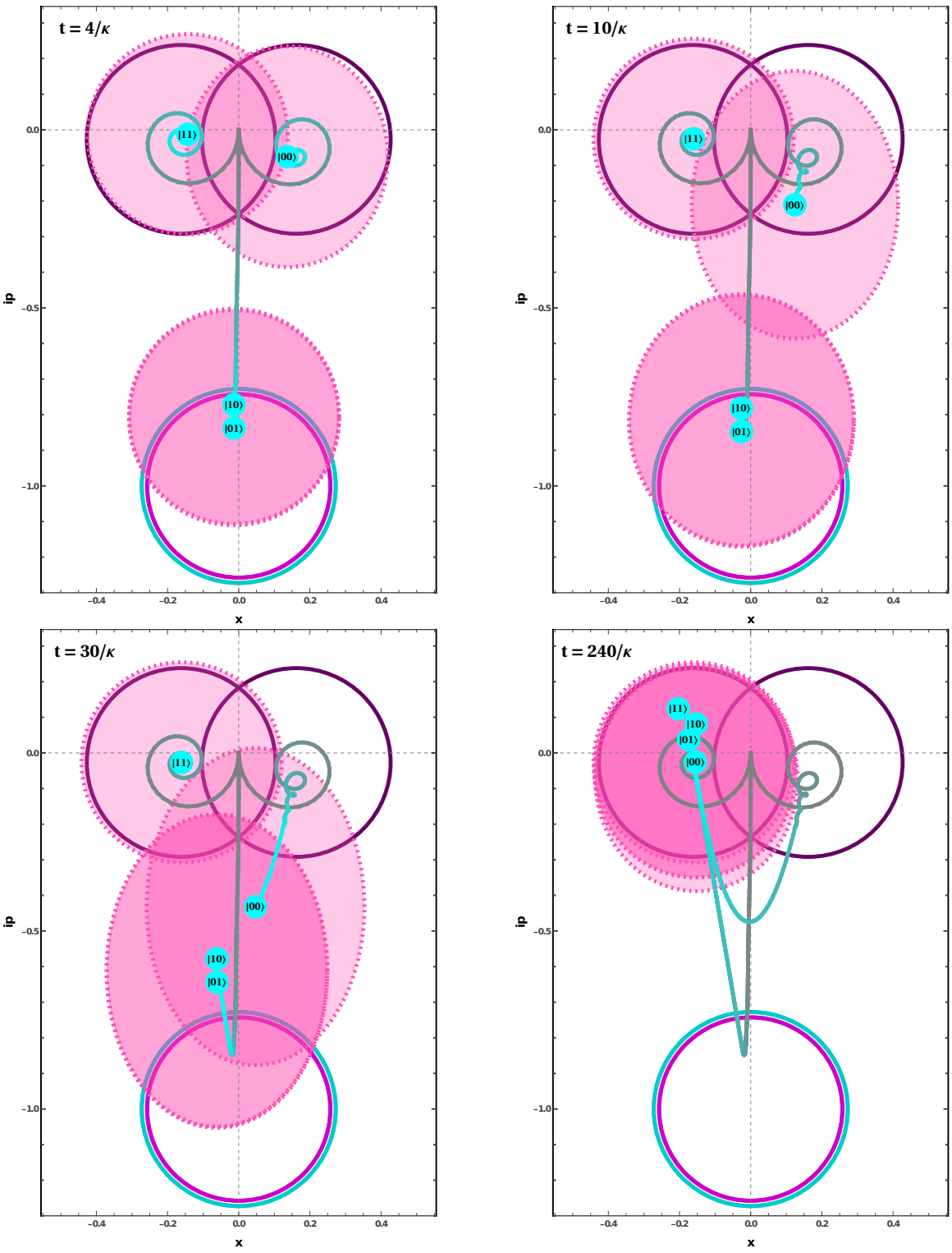

Figure 7.7.: **Trajectories of initial states for $\gamma_1 = 0.015\kappa$**: The excited state $|00\rangle$ starts to dissipate before the odd parity states reach α_x^s. The final amplitude is significantly smaller than in the case without relaxation.

full amplitude that would be expected without relaxation. Therefore, this ratio between γ_1 and κ would experimentally already be much less favorable for carrying out parity measurements for example.

Finally, Fig. 7.8 shows the trajectories for $\gamma_1 = 0.15\kappa$ and $\gamma_1 = 1.5\kappa$, are clearly not satisfying $\gamma_1 \ll \kappa$ anymore. As expected, the trajectories show large deviations from the analytic solutions. Here, the oscillator never starts to distinguish any of the register states, since they all start to drift toward the ground-state instead of being driven into clear separation first.

At this point, there are several different possible explanations of how the observed trajectories emerge. One possibility is that the apparent motion in the complex plane is mostly due to a decay of the register-weights $c_{xx}(x_0, t)$ while the oscillator states $\rho_{yy}(x_0, t)$ stay roughly the same, and are given to good approximation by coherent states at all times. To further investigate and show whether this really is the case, we continue the analysis by examining the conditional states $\rho_{xx}(x_0, t)$. Specifically, the temporal evolutions of three quantities are calculated:

- The phase space distance $d_x(x_0, t)$ between $\rho_{xx}(x_0, t)$ and α_x^s,
- the register weights $c_{xx}(x_0, t) = \mathrm{Tr}[\langle x| \rho(x_0, t) |x\rangle]$,
- the deviations $\delta_x(x_0, t)$ of $\rho_{xx}(x_0, t)$ from coherent states.

More precisely, $d_x(x_0, t)$ and $\delta_x(x_0, t)$ are defined as follows: denoting the Q-function of $\rho_{xx}(x_0, t)$ as

$$Q_x(x_0, t, \alpha) \equiv \frac{1}{\pi} \langle \alpha| \rho_{xx}(x_0, t) |\alpha\rangle \tag{7.18}$$

and its maximum in the complex plane as $\beta_x(x_0, t) \equiv \max_{\alpha\in\mathbb{C}}[Q_x(x_0, t, \alpha)]$, we define the phase space difference $d_x(x_0, t)$ via

$$d_x(x_0, t) \equiv \left|\beta_x(x_0, t) - \alpha_x^s\right| \tag{7.19}$$

and deviation δ from a coherent state $|\beta_x(x_0, t)\rangle$ by the following integral:

$$\delta_x(x_0, t) \equiv \int \left|Q_x(x_0, t, \alpha) - \left|\langle \alpha|\beta_x(x_0, t)\rangle\right|^2\right| \mathrm{d}\alpha. \tag{7.20}$$

For brevity, the analysis of these quantities is restricted to the initial state $|00\rangle$ for the four different values of γ_1. Figure 7.9 shows the time evolutions of $\delta_x(00, t)$, $d_x(00, t)$ and $\mathrm{Tr}[\langle x| \rho(00, t) |x\rangle]$ for $\gamma_1 = 0.0015\kappa$. For the other 3 values of γ_1 we find the same qualitative behavior. Their plots can be found in Appendix C.

As expected for the weights, we can see that the initial excited state decays with a rate $\sim \gamma_1$ into the odd-parity states $|01\rangle$ and $|10\rangle$ first, followed by a decay of all three into the ground-state $|11\rangle$. Looking at the distances $d_x(00, t)$, we can see that $\rho_{00,00}(00, t)$ quickly ($\sim 1/\kappa$) arrives at α_{00}^s and then stays there at all times. The odd parity states that are being populated by the decay of $|00\rangle$, quickly get into close vicinity of their respective α_x^s and stay at a distance of ~ 0.05. For the deviations $\delta_x(00, t)$, we find that the initial excited state stays very close to a coherent state at all times. The odd parity states show a deviation around 5% throughout the evolution, while the ground-state quickly drops from a deviation around 8% to zero, as it is being populated.

In summary, we note that throughout the time evolution, notable deviations of conditional states mostly occur together with low weight: The deviation of the ground-state vanishes as it acquires notable weight, and the deviations of the odd parity states peak at around $t \sim 1\gamma_1$, playing little role before and after due to their small weight.

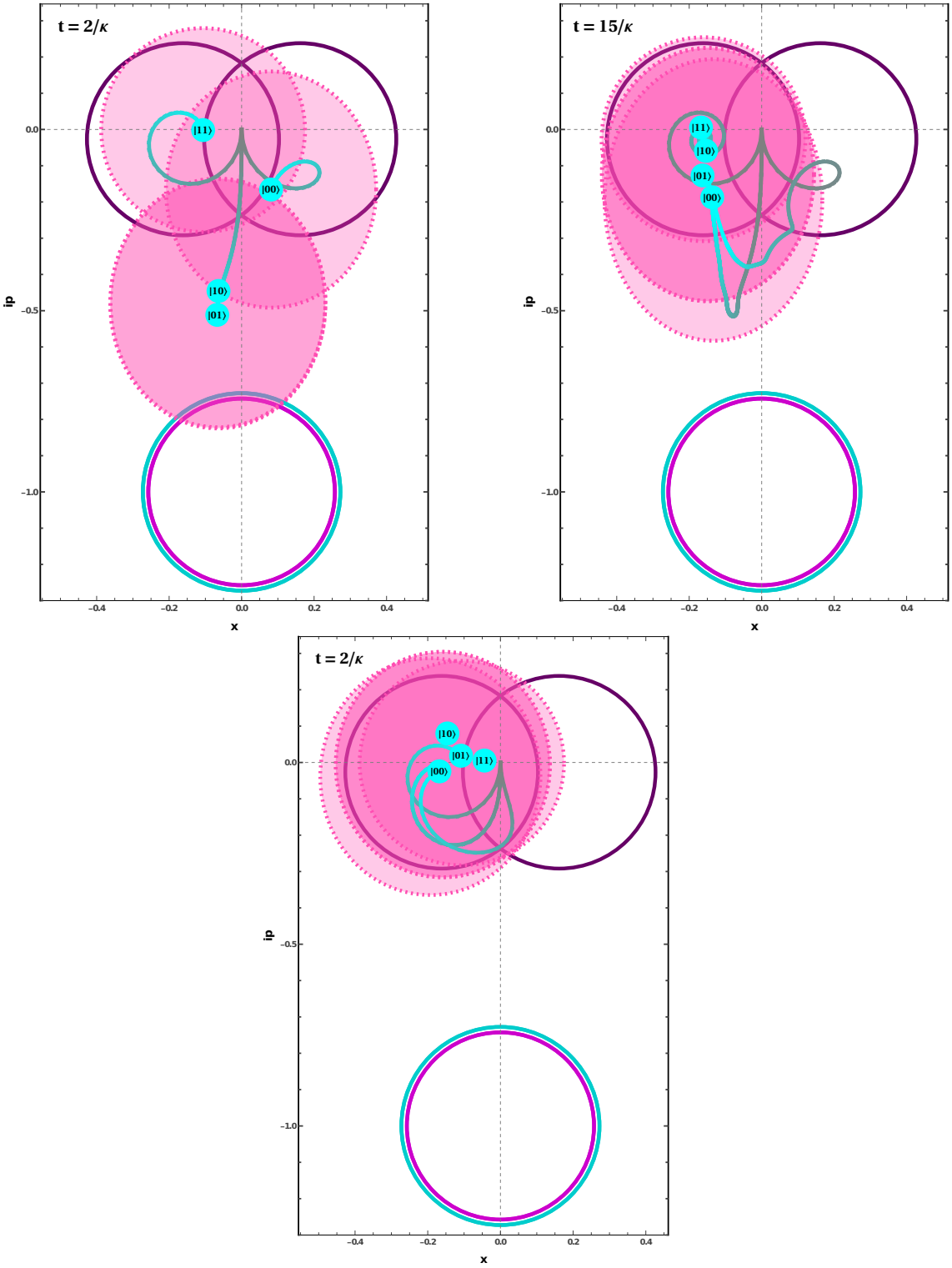

Figure 7.8.: **Trajectories for $\gamma_1 = 0.15\kappa$ (top)** and **$\gamma_1 = 1.5\kappa$ (bottom)**: The condition $\gamma_1 \ll \kappa$ is satisfied in neither of these cases, resulting in large deviations from the analytical solutions, to the point where the oscillator never clearly distinguishes between the odd- and the even-parity subspaces.

7.5. Results of numerical analysis and conclusion

The numerical data indicates that qubit relaxation affects the time evolution of the system as follows: the conditional oscillator states ρ_{xx} are mostly unaffected by the relaxation, meaning that their time evolution follows to good approximation the coherent states $|\alpha_x(t)\rangle$, especially for times very large compared to $1/\kappa$. The weights $c_{xx}(t)$ decay with a rate $\sim \gamma_1$, driving all initial states to the ground-state $|\alpha_{11}^s\rangle$ eventually. The trajectories of the system in phase space can be explained by this mechanism, which amounts to making the following Ansatz for the solution $\rho(t)$ of the master equation including qubit relaxation:

$$\rho(t) = \sum_{xy} \tilde{c}_{xy}(t)\, |x\rangle\langle y| \otimes \frac{|\alpha_x(t)\rangle\langle\alpha_y(t)|}{\langle\alpha_y(t)|\alpha_x(t)\rangle}, \tag{7.21}$$

where the weights $\tilde{c}_{xx}(t)$ now contain additional factors decaying with rates $\sim \gamma_1$ compared to the analytical solution 6.4.

In the next chapter, we show how this Ansatz can be motivated by theoretic considerations alone.

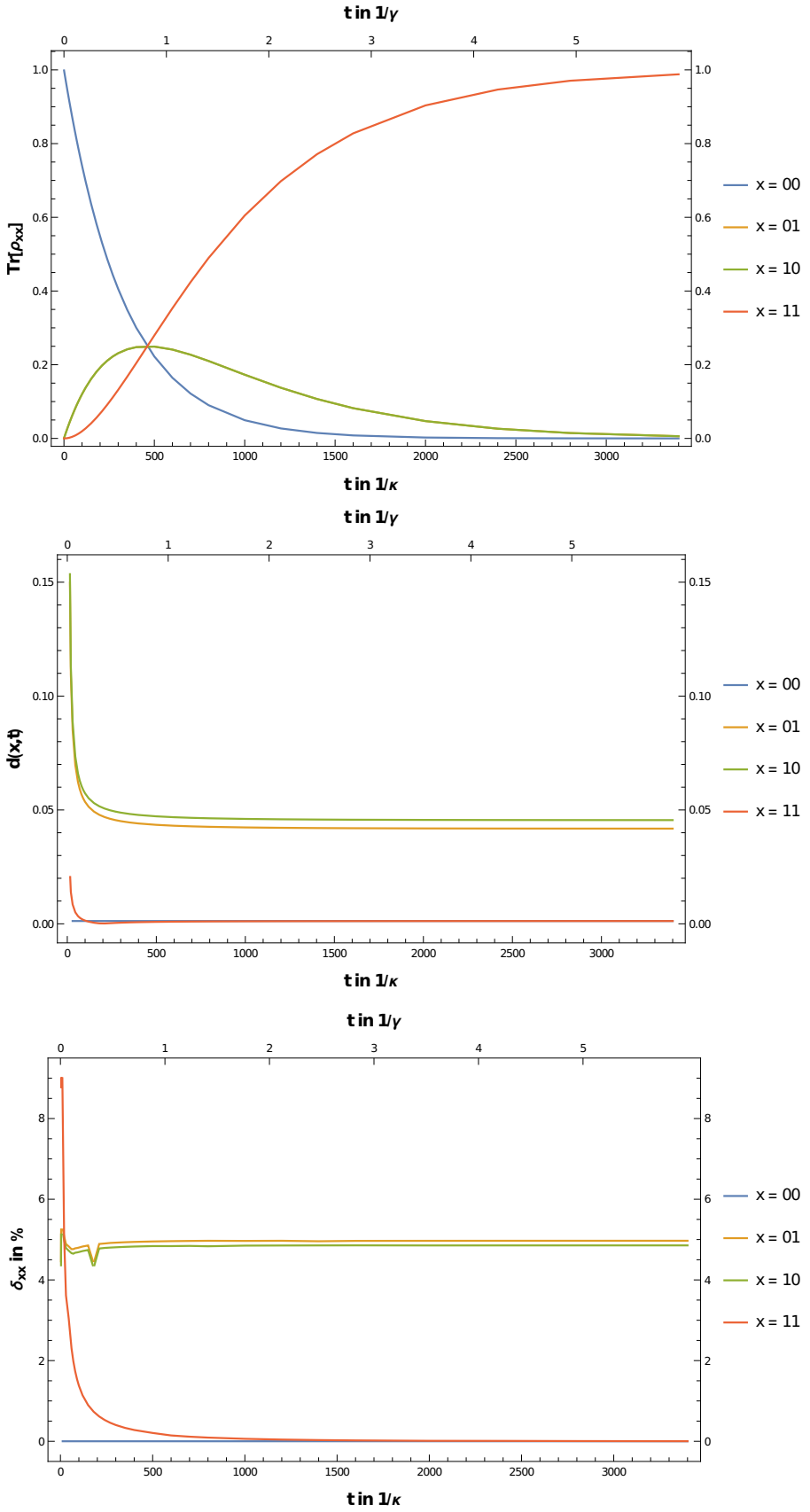

Figure 7.9.: Plots of **weights, distances and deviations** (from top to bottom) for $\gamma_1 = 0.0015\kappa$:

8. Analytic treatment of the master equation for $\gamma_1 \neq 0$

In this chapter, a perturbation solution to the full master equation 6.1 is presented for the class of initial states

$$\rho(0) = \sum_{x,y} a_{xy}(0)\,|x\rangle\langle y| \otimes \frac{|\alpha_x(0)\rangle\langle\alpha_y(0)|}{\langle\alpha_y(0)|\alpha_x(0)\rangle}, \tag{8.1}$$

which leads to a theoretic justification of solving the master equation approximately in the limit $\gamma_1 \ll \kappa$ and $t \gg 1/\kappa$ with the Ansatz proposed in the previous chapter:

$$\rho(t) = \sum_{x,y} \tilde{c}_{xy}(t)\,|x\rangle\langle y| \otimes \frac{|\alpha_x(t)\rangle\langle\alpha_y(t)|}{\langle\alpha_y(t)|\alpha_x(t)\rangle}, \tag{8.2}$$

with $\alpha_x(t)$ given by Eqs. 6.50 and 6.51 from the solution of the relaxation-free master equation. Furthermore, the perturbative solution enables us to derive the master equation for the reduced register-density matrix in a much simpler fashion than presented in [2].

Finally, the chapter is closed by explicitly calculating the weights $\tilde{c}_{xx}(t)$ in 8.2 and comparing the solution to the numerical trajectories from Section 7.4.

8.1. Perturbative solution and interpretation

The main idea to obtain a perturbative solution of the master equation 6.1 is to derive a Dyson series similar to the one obtained from time-dependent perturbation theory in standard quantum mechanics [48]. We start by splitting the Lindbladian into a "known" part and a perturbation given by the qubit-dissipation jump-term:

$$\mathcal{L}\rho = \underbrace{-\mathrm{i}\,[H,\rho] + \kappa\mathcal{D}[a]\rho + \frac{\gamma_{\phi q}}{2}\mathcal{D}[\sigma_z^q]\rho - \frac{\gamma_{1q}}{2}\left\{\sigma_+^q\sigma_-^q,\rho\right\}}_{\mathcal{L}_0\rho} + \underbrace{\gamma_{1q}\sigma_-^q\rho\sigma_+^q}_{\mathcal{L}_1\rho}. \tag{8.3}$$

Here $\mathcal{L}_0$ deviates from the Dissipation-free Lindbladian just by the anti-commutator term, which is diagonal in the z-basis (see Eq. 6.4). Therefore, recalling the approach of Section 6.2 we find the time evolution generated by $\mathcal{L}_0$ by simply adding the z-basis representation of $\{\sigma_+\sigma_-,\cdot\}$ to $\mathcal{L}_Q(x,y)$. The resulting time propagation of states 8.1 due to $\exp(\mathcal{L}_0 t)$ is given by

$$e^{\mathcal{L}_0 t}\left[|x\rangle\langle y| \otimes \frac{|\alpha_x(0)\rangle\langle\alpha_y(0)|}{\langle\alpha_y(0)|\alpha_x(0)\rangle}\right] = e^{\mathcal{L}_Q(x,y)t} a_{xy}(t)\,|x\rangle\langle y| \otimes \frac{|\alpha_x(t)\rangle\langle\alpha_y(t)|}{\langle\alpha_y(t)|\alpha_x(t)\rangle}, \tag{8.4}$$

where

$$\begin{aligned}\mathcal{L}_Q(x,y) = \sum_q \Bigg(&-\mathrm{i}\frac{\delta\tilde{\omega}_q}{2}\left[Z^q(x) - Z^q(y)\right] - \frac{\gamma_{\phi q}}{2}\left[1^q - Z^q(x)Z^q(y)\right] \\ &- \frac{\gamma_{1q}}{4}\left[2 + Z^q(x) + Z^q(y)\right]\Bigg),\end{aligned} \tag{8.5}$$

and $a_{xy}(t)$ as in Eq. 6.48. This propagation rule is the basis for obtaining the perturbative series. Note that the last term in $\mathcal{L}_Q(x,y)$ reduces to $\gamma_1 N_e(x)$ for $x = y$ and $\gamma_{1q} = \gamma_1$ - with $N_e(x)$ the number of excited qubits in the register state $|x\rangle$, therefore representing

register relaxation at the rate $\gamma_1 N_e(x)$. Next, we follow the usual procedure of performing time-dependant perturbation theory by introducing the "interaction picture" via

$$\rho_I(t) \equiv e^{-\mathcal{L}_0 t}\rho(t). \tag{8.6}$$

Although we do not know how $e^{-\mathcal{L}_0 t}$ acts on a general state (or whether it is even defined for arbitrary states), it is still possible to reverse the time evolution of any density matrix of the form $\sim |x\rangle\langle y| \otimes |\alpha_x(t)\rangle\langle\alpha_y(t)|$ back to $t = 0$ if $\alpha_x(0)$ is known. In this interaction frame, the Lindblad equation is transformed to

$$\dot{\rho}_I = \mathcal{L}_1^I(t)\rho_I(t), \tag{8.7}$$

with the interaction picture Lindbladian

$$\mathcal{L}_1^I(t) \equiv e^{-\mathcal{L}_0 t}\mathcal{L}_1 e^{\mathcal{L}_0 t}. \tag{8.8}$$

Integration of 8.7 and iteration leads to the formal Dyson series

$$\rho_I(t) = \rho_I(0) + \int_0^t \mathcal{L}_1^I(s)\rho_I(0)\,\mathrm{d}s + \int_0^t\int_0^s \mathcal{L}_1^I(s)\mathcal{L}_1^I(s')\rho_I(0)\,\mathrm{d}s'\,\mathrm{d}s + \dots. \tag{8.9}$$

This series still contains propagators backward in time of the form $\exp(-\mathcal{L}_0 t)$. To remove them, we transform back to the "Schrödinger picture" by applying $\exp(\mathcal{L}_0 t)$:

$$\begin{aligned}\rho(t) &= e^{\mathcal{L}_0 t}\rho(0) + e^{\mathcal{L}_0 t}\int_0^t \mathcal{L}_1^I(s)\rho_I(0)\,\mathrm{d}s + e^{\mathcal{L}_0 t}\int_0^t\int_0^s \mathcal{L}_1^I(s)\mathcal{L}_1^I(s')\rho_I(0)\,\mathrm{d}s'\,\mathrm{d}s + \dots \\ &= e^{\mathcal{L}_0 t}\rho(0) + \int_0^t e^{\mathcal{L}_0(t-s)}\mathcal{L}_1 e^{\mathcal{L}_0 s}\rho(0)\,\mathrm{d}s \\ &\quad + \int_0^t\int_0^s e^{\mathcal{L}_0(t-s)}\mathcal{L}_1 e^{\mathcal{L}_0(s-s')}\mathcal{L}_1 e^{\mathcal{L}_0 s'}\rho_I(0)\,\mathrm{d}s\,\mathrm{d}s' + \dots.\end{aligned} \tag{8.10}$$

Now, for the terms propagating forward in time, we use Eq. 8.4 to find the expressions in the integrands if $\rho(0)$ is of the form 8.1:

$$\begin{aligned}e^{\mathcal{L}_0(t-s)}\mathcal{L}_1 e^{\mathcal{L}_0 t}\rho(0) &= \sum_{x,y,q} a_{xy}(t)\gamma_{1q}\, e^{\mathcal{L}_Q(x,y)t}\, e^{\mathcal{L}_0(t-s)}\left[\sigma_-^q\,|x\rangle\langle y|\,\sigma_+^q \otimes \frac{|\alpha_x(s)\rangle\langle\alpha_y(s)|}{\langle\alpha_y(s)|\alpha_x(s)\rangle}\right] \\ &= \sum_{x,y,q} a_{xy}(t)\gamma_{1q}\, e^{\mathcal{L}_Q(x,y)t} e^{\mathcal{L}_0(t-s)}\left[|x_{q-}\rangle\langle y_{q-}| \otimes \frac{|\alpha_x(s)\rangle\langle\alpha_y(s)|}{\langle\alpha_y(s)|\alpha_x(s)\rangle}\right].\end{aligned} \tag{8.11}$$

The second propagator $\exp[\mathcal{L}_0(t-s)]$ again acts on a state of the form 8.1 and can therefore be calculated. To find a compact and precise expression we introduce the notation for the propagated coherent parameter

$$\alpha_{x\to x_{q-}}^{s\to t} \equiv \alpha_{x_{q-}}^s + \left[\alpha_x(s) - \alpha_{x_{q-}}^s\right]\exp\!\left[-\mathrm{i}\left(\delta\omega_r + \chi(x) - \mathrm{i}\frac{\kappa}{2}\right)(t-s)\right]. \tag{8.12}$$

This just the formula for $\alpha_{x_{q-}}(t)$ with initial state $\alpha_x(s)$. For the propagated coefficient $a_{xy}(t)$ we write

$$a_{xy\to[xy]_{q-}}^{s\to t} \equiv a_{xy}(s)\, e^{-\mathrm{i}[\chi(x_{q-})-\chi(y_{q-})]\int_s^{t-s}\alpha_{x\to x_{q-}}^{s\to\tau}\left[\alpha_{y\to y_{q-}}^{s\to\tau}\right]^*\mathrm{d}\tau} \tag{8.13}$$

$$\Rightarrow \quad a_{xy}(t) \mathrel{\widehat{=}} a_{xy\to xy}^{0\to t}, \tag{8.14}$$

which is derived from Eq. 6.48. Further defining the symbol

$$c_{xy\to[xy]'}^{s\to t} \equiv a_{xy\to[xy]'}^{s\to t}\, e^{\mathcal{L}_Q(x',y')(t-s)}\, e^{\mathcal{L}_Q(x,y)s}, \tag{8.15}$$

leads to

$$e^{\mathcal{L}_0(t-s)}\mathcal{L}_1 e^{\mathcal{L}_0 t}\rho(0) = \sum_{x,y,q} \gamma_{1q}\, c^{s\to t}_{xy\to[xy]_{q-}}\ |x_{q-}\rangle\langle y_{q-}| \otimes \frac{\left|\alpha^{s\to t}_{x\to x_{q-}}\right\rangle\left\langle\alpha^{s\to t}_{y\to y_{q-}}\right|}{\left\langle\alpha^{s\to t}_{y\to y_{q-}}\middle|\alpha^{s\to t}_{x\to x_{q-}}\right\rangle}. \tag{8.16}$$

Using this result yields the perturbation series

$$\begin{aligned}\rho(t) = e^{\mathcal{L}_0 t}\rho(0) &+ \sum_{x,y,q} \gamma_{1q}\int_0^t c^{s\to t}_{xy\to[xy]_{q-}}\ |x_{q-}\rangle\langle y_{q-}| \otimes \frac{\left|\alpha^{s\to t}_{x\to x_{q-}}\right\rangle\left\langle\alpha^{s\to t}_{y\to y_{q-}}\right|}{\left\langle\alpha^{s\to t}_{y\to y_{q-}}\middle|\alpha^{s\to t}_{x\to x_{q-}}\right\rangle}\,\mathrm{d}s \\ &+ \sum_{x,y,q,p} \gamma_{1q}\gamma_{1p}\int_0^t\int_0^s \Bigg\{ c^{s'\to s\to t}_{xy\to[xy]_{q-}\to[xy]_{qp-}} \cdot |x_{qp-}\rangle\langle y_{qp-}| \\ &\qquad \otimes \frac{\left|\alpha^{s'\to s\to t}_{x\to x_{q-}\to x_{qp-}}\right\rangle\left\langle\alpha^{s'\to s\to t}_{y\to y_{q-}\to y_{qp-}}\right|}{\left\langle\alpha^{s'\to s\to t}_{y\to y_{q-}\to y_{qp-}}\middle|\alpha^{s'\to s\to t}_{x\to x_{q-}\to x_{qp-}}\right\rangle}\Bigg\}\,\mathrm{d}s\,\mathrm{d}s' + \dots\,,\end{aligned} \tag{8.17}$$

where $|x_{qp-}\rangle \equiv \sigma^p_-\sigma^q_-\,|x\rangle$. The integrand of the first order correction can be interpreted as follows: From $t = 0$ to $t = s$ the system evolves according to the relaxation-free solution 6.4. At $t = s$ the qubit register undergoes a relaxation induced by σ^q_- and jumps from $|x\rangle$ to $|x_{q-}\rangle$. The correlated oscillator state $|\alpha_x(s)\rangle$ adjusts its trajectory and begins to drift towards the stationary state $|\alpha^s_{x_{q-}}\rangle$. By integrating over s all possible points in time at which the σ^q_- jumps could have occurred are considered. The higher-order terms can be interpreted similarly. For example, the second-order term considers all possible trajectories where one qubit relaxes at $t = s'$ followed by a second one at $t = s$, with the oscillator reacting to the register changes accordingly.

We note that the time it takes for the oscillator states to adjust to the register and reach the corresponding α^s_x, is of the magnitude $1/\kappa$. Therefore, when $t \gg 1/\kappa$, a majority of the possible trajectories leave the system in a state of the form $|x\rangle \otimes |\alpha^s_x\rangle$, since the oscillator had enough time to "follow" the register and reach its stationary state. In that case, the perturbation series can be simplified to

$$\begin{aligned}\rho(t) \approx e^{\mathcal{L}_0 t}\rho(0) &+ \sum_{x,y,q} \gamma_{1q}\,|x_{q-}\rangle\langle y_{q-}| \otimes \frac{\left|\alpha^s_{x_{q-}}\right\rangle\left\langle\alpha^s_{y_{q-}}\right|}{\left\langle\alpha^s_{y_{q-}}\middle|\alpha^s_{x_{q-}}\right\rangle}\int_0^t c^{s\to t}_{xy\to[xy]_{q-}}\,\mathrm{d}s \\ &+ \sum_{x,y,q,p} \gamma_{1q}\gamma_{1p}\,|x_{qp-}\rangle\langle y_{qp-}| \otimes \frac{\left|\alpha^s_{x_{qp-}}\right\rangle\left\langle\alpha^s_{y_{qp-}}\right|}{\left\langle\alpha^s_{y_{qp-}}\middle|\alpha^s_{x_{qp-}}\right\rangle}\int_0^t\int_0^s c^{s'\to s\to t}_{xy\to[xy]_{q-}\to[xy]_{qp-}}\,\mathrm{d}s\,\mathrm{d}s' \\ &+ \dots .\end{aligned} \tag{8.18}$$

Now in the case where furthermore $\gamma_{1q} \ll \kappa$, we can also neglect the effects of γ_{1q} for times $t \sim 1/\kappa$, since then the relaxation of the register happens over timescales large compared to $1/\kappa$. This enables us to write the oscillator state as $|\alpha_x(t)\rangle$ not only in the limit of large t, but for small t as well. Effectively, the oscillator will be in the states $\sim |\alpha_x(t)\rangle$ *at all times* of the time evolution, if $\gamma_{1q} \ll \kappa$ is true. The solution $\rho(t)$ is then given by

$$\rho(t) \approx \sum_{x,y} \tilde{c}_{xy}(t)\,|x\rangle\langle y| \otimes \frac{|\alpha_x(t)\rangle\langle\alpha_y(t)|}{\langle\alpha_y(t)|\alpha_x(t)\rangle}. \tag{8.19}$$

The coefficients $\tilde{c}_{xy}(t)$ satisfy the equation

$$\sum_{xy} \tilde{c}_{xy}(t)\,|x\rangle\langle y| = \sum_{x,y} a_{xy}(t)\,e^{\mathcal{L}_Q(x,y)t}\,|x\rangle\langle y| + \sum_{x,y,q} \gamma_{1q}\,|x_{q-}\rangle\langle y_{q-}| \int_0^t c^{s\to t}_{xy\to[xy]_{q-}}\,\mathrm{d}s + \dots, \tag{8.20}$$

which is obtained by tracing out the oscillator degrees of freedom of Eq. 8.18.

8.2. Reduced master equation for the register density matrix

The structure of the perturbative solution 8.17 and the insight in the physical processes encoded in it, can be used to derive the reduced master equation for the register density matrix. This master equation was given exactly in Ref. [2] for one qubit and as an approximation in the case $\gamma_1 \ll \kappa$ for two qubits in [4]. The derivation based on a Polaron type transformation presented there for one qubit is quite technical and does not provide physical intuition. For the two-qubit case, the resulting master equation is presented without an explanation of why it is only an approximation valid for $\gamma \ll \kappa$, as opposed to the one-qubit case, and without a calculation about how it was obtained. In this section, we will derive the same reduced master equation, while also providing insight in why it is an exact equation only for the one qubit case.

8.2.1. Single qubit reduced master equation

To trace out the oscillator from the full master equation 6.1 we follow Sec. 6.5.2 where the reduced master equation is derived for $\gamma_1 = 0$. First $\rho(t)$ is decomposed in the z-basis as

$$\rho(t) = \sum_{xy} \tilde{c}_{xy}(t) \left|x\right\rangle\!\left\langle y\right| \otimes \rho_{xy}, \tag{8.21}$$

with ρ_{xy} being a normalized operator on the resonator space. The reduced density matrix is then given by

$$\rho_Q(t) = \sum_{x,y} \tilde{c}_{xy}(t) \left|x\right\rangle\!\left\langle y\right|. \tag{8.22}$$

Taking the partial trace of the master equation leads to

$$\begin{aligned} \dot{\rho}_Q(t) = &-\mathrm{i}\frac{\tilde{\omega}}{2}\left[\sigma_z, \rho_Q\right] + \frac{\gamma_\phi}{2}\mathcal{D}[\sigma_z]\rho_Q + \gamma_1\mathcal{D}[\sigma_-]\rho_Q \\ &- \mathrm{i}\chi \sum_{x,y} \left[Z(x) - Z(y)\right] \tilde{c}_{xy}(t) \left|x\right\rangle\!\left\langle y\right| \mathrm{Tr}\Big[a\rho_{xy}a^\dagger\Big]. \end{aligned} \tag{8.23}$$

The last term is interesting since the trace can only be calculated if the action of a on ρ_{xy} is known. We note that for $x = y$ the term does not contribute - therefore the diagonal elements ρ_{xx} need not be known. Regarding the off-diagonal elements, we can look at the perturbative solution 8.17: for $N_{Qubits} = 1$ it is straightforward to see, that γ_1 does not contribute to the evolution of the off-diagonal elements $\left|x\right\rangle\!\left\langle y\right|$. This is because the integrals are multiplied with states of the form $\left|x_{q-}\right\rangle\!\left\langle y_{q-}\right|$. In the case of one qubit, the only two off-diagonals are given by $\left|e\right\rangle\!\left\langle g\right|$ and $\left|g\right\rangle\!\left\langle e\right|$. Applying the lowering operator to these states from both sides will always annihilate the state, thus the correction integrals vanish, and the off-diagonal elements evolve under the relaxation-free Lindbladian. It can therefore be safely assumed that the off-diagonal operators ρ_{xy} are given by

$$\rho_{xy} = \frac{\left|\alpha_x(t)\right\rangle\!\left\langle\alpha_y(t)\right|}{\left\langle\alpha_y(t)|\alpha_x(t)\right\rangle}, \tag{8.24}$$

if the system started in a state $\sim \left|x\right\rangle \otimes \left|\alpha_x(0)\right\rangle$. The trace is then given by

$$\mathrm{Tr}\Big[a\rho_{xy}a^\dagger\Big] = \alpha_x(t)\alpha_y(t)^*, \tag{8.25}$$

leading to the reduced master equation

$$\begin{aligned} \dot{\rho}_Q(t) = &-\mathrm{i}\frac{\tilde{\omega}}{2}\left[\sigma_z, \rho_Q\right] + \frac{\gamma_\phi}{2}\mathcal{D}[\sigma_z]\rho_Q + \gamma_1\mathcal{D}[\sigma_-]\rho_Q \\ &- \mathrm{i}\chi \sum_{x,y} \left[Z(x) - Z(y)\right] \tilde{c}_{xy}(t) \left|x\right\rangle\!\left\langle y\right| \alpha_x(t)\alpha_y(t)^*. \end{aligned} \tag{8.26}$$

This equation is equivalent to the one derived in Ref. [2]. It is now clear that this equation is exact in the one qubit case precisely because the γ_1 off-diagonal corrections vanish, since the states $|x_{q-}\rangle\langle y_{q-}|$ with $x \neq y$ do not exist for a single qubit. That γ_1 does not act on the off-diagonal states can also be straightforwardly seen by looking at the action of $\mathcal{D}[\sigma_-]$ on ρ in the z-basis (see Eq. 6.4). Therefore, this derivation does not need the perturbative series as a tool and is arguably much simpler than the one given in [2].

8.2.2. Multi-qubit case

Furthermore, we can immediately see how this result is generalized to multi-qubit systems to obtain the equation presented in [4], while also identifying the precise approximation needed to achieve this extension. The crucial assumption that goes into the derivation is that the ρ_{xy} are of the form 8.24. As we have seen in the previous section, for $N_{Qubits} > 1$ this is an assumption that will approximately be true for $\gamma_1 \ll \kappa$. It is now straightforward to write down the reduced master equation for a multi-qubits register. Extending Eq. 8.26 leads to

$$\begin{aligned}\dot{\rho}_Q(t) = &-\mathrm{i}\frac{\delta\tilde{\omega}_q}{2}\left[\sigma_z^q, \rho_Q\right] + \frac{\gamma_{\phi q}}{2}\mathcal{D}[\sigma_z^q]\rho_Q + \gamma_{1q}\mathcal{D}[\sigma_-^q]\rho_Q \\ &- \mathrm{i}\chi\sum_{x,y}\left[Z^q(x) - Z^q(y)\right]\tilde{c}_{xy}(t)\,|x\rangle\langle y|\,\alpha_x(t)\alpha_y(t)^*,\end{aligned} \tag{8.27}$$

which is equivalent to the equation given in [4]. This concludes the derivation of the register equation. In the next section, the weights $\tilde{c}_{xx}(t)$ are calculated explicitly by Eq. 8.27 for the diagonal states.

8.3. Determining the weights $\tilde{c}_{xx}$ analytically

The reduced master equation 8.27 does not contain terms coupling off- to on-diagonal elements. Hence, to solve for the weights $\tilde{c}_{xx}$ the equation can be restricted to

$$\sum_x \dot{\tilde{c}}_{xx}(t)\,|x\rangle\langle x| = \sum_{x,q}\gamma_{1q}\tilde{c}_{xx}(t)\left(-\frac{1}{2}\left[1 + Z^q(x)\right]|x\rangle\langle x| + \sigma_-^q\,|x\rangle\langle x|\,\sigma_+^q\right). \tag{8.28}$$

Since $\sum_x c_x\sigma_-^q\,|x\rangle\,\langle x|y_{q+}\rangle = c_{y_{q+}}\,|y\rangle$, multiplying with a register ket $|y\rangle$ from the right gives

$$\dot{\tilde{c}}_{yy}(t)\,|y\rangle = \sum_q \gamma_{1q}\left(-\frac{1}{2}\left[1 + Z^q(y)\right]\tilde{c}_{yy}(t)\,|y\rangle + \tilde{c}_{y_{q+}y_{q+}}(t)\,|y\rangle\right), \tag{8.29}$$

with $\tilde{c}_{y_{q+}y_{q+}}(t) = 0$ if $\sigma_+^q\,|y\rangle = 0$. Because the $|y\rangle$ form an orthonormal basis, we can sum over all y to obtain the equivalent equation

$$\sum_y \dot{\tilde{c}}_{yy}(t)\,|y\rangle = \sum_{y,q}\gamma_{1q}\left(-\frac{1}{2}\left[1 + Z^q(y)\right]\tilde{c}_{yy}(t)\,|y\rangle + \tilde{c}_{y_{q+}y_{q+}}(t)\,|y\rangle\right) \tag{8.30}$$

The last term on the right-hand-side can be rewritten employing an index shift:

$$\begin{aligned}\sum_{y,q}\tilde{c}_{y_{q+}y_{q+}}(t)\,|y\rangle &= \sum_{y,q}\tilde{c}_{yy}(t)\,|y_{q-}\rangle \\ &= \sum_{y,q}\tilde{c}_{yy}\sigma_-^q\,|y\rangle\,.\end{aligned} \tag{8.31}$$

By using the notation $|\psi_Q(t)\rangle \equiv \sum_x \tilde{c}_{xx}(t)\,|x\rangle$, Eq. 8.30 can be written as the non hermitian Schrödinger equation

$$|\dot{\psi}\rangle_Q = \sum_q \gamma_{1q}\left(\sigma_-^q - \frac{1}{2}\left[\mathbb{1} + \sigma_z^q\right]\right)|\psi_Q(t)\rangle\,. \tag{8.32}$$

To calculate the associated time evolution operator we rewrite $\sigma_-^q = 1/2(\sigma_x^q - \mathrm{i}\sigma_y^q)$ to find

$$|\dot{\psi}\rangle_Q = \sum_q \frac{\gamma_{1q}}{2} \left(\sigma_x^q - \mathrm{i}\sigma_y^q - \sigma_z^q - \mathbb{1}\right) |\psi_Q(t)\rangle \,. \tag{8.33}$$

or, equivalently, by introducing the normalized vector $\vec{n} \equiv (1, -\mathrm{i}, -1)^T$:

$$|\dot{\psi}\rangle_Q = \sum_q \frac{\gamma_{1q}}{2} \left(\vec{n} \cdot \vec{\sigma}^q - \mathbb{1}\right) |\psi_Q(t)\rangle \,. \tag{8.34}$$

This equation is solved by

$$|\psi_Q(t)\rangle = e^{-\sum_q \frac{\gamma_{1q}}{2} t} e^{\sum_q \frac{\gamma_{1q}}{2} \vec{n}\cdot\vec{\sigma^q}\, t} |\psi_Q(0)\rangle \,, \tag{8.35}$$

where $\tilde{c}_{xx}(0) = \langle x|\psi_Q(0)\rangle$. The second exponential has the typical form of a rotation operator in qubit space, rotating around the axis $\vec{n}$. However, $\vec{n}$ is a complex vector, and does not correspond to a rotation but to a decay of excited modes. Still the usual method of evaluating the exponential as a sum of *sin* and *cos* can be applied, since the necessary calculation only relies on the $\vec{\sigma}$ property

$$(\vec{n} \cdot \vec{\sigma})^2 = \mathbb{1}\,(\vec{n} \cdot \vec{n})^2 = \mathbb{1}, \tag{8.36}$$

which is still satisfied in this case. We find for the exponential

$$\begin{aligned} e^{\sum_q \frac{\gamma_{1q}}{2} \vec{n}\cdot\vec{\sigma^q}\cdot t} &= \prod_q e^{\frac{\gamma_{1q}}{2} \vec{n}\cdot\vec{\sigma^q}\cdot t} \\ &= \prod_q \left[\sum_k \frac{\left(\frac{\gamma_{1q}}{2} t\right)^{2k}}{(2k)!} \mathbb{1} + \left[\vec{n} \cdot \vec{\sigma^q}\right] \sum_k \frac{\left(\frac{\gamma_{1q}}{2} t\right)^{2k+1}}{(2k+1)!} \right] \\ &= \prod_q \left[\cosh\left(\frac{\gamma_{1q}}{2} t\right) \mathbb{1} + \left[\sigma_-^q - \sigma_z^q\right] \sinh\left(\frac{\gamma_{1q}}{2} t\right) \right]. \end{aligned} \tag{8.37}$$

The weights $\tilde{c}_{xx}(t)$ are therefore implicitly given by

$$\begin{aligned} \tilde{c}_{xx}(t) &= \langle x|\psi_Q(t)\rangle \\ &= \langle x| \prod_q e^{-\frac{\gamma_{1q}}{2} t} \left[\cosh\left(\frac{\gamma_{1q}}{2} t\right) \mathbb{1} + \left[\sigma_-^q - \sigma_z^q\right] \sinh\left(\frac{\gamma_{1q}}{2} t\right) \right] |\psi_Q(0)\rangle \,, \end{aligned} \tag{8.38}$$

where $|\psi_Q(0)\rangle$ is the vector containing the initial weights $\tilde{c}_{xx}(0)$.

8.4. Comparison of numeric results with analytic results

Using the formula 8.38 for the register weights, we conclude this thesis by plotting the trajectories $\mathrm{Tr}[a\,\rho(x0,t)]$ of initial register states $|x0\rangle$, with $\rho(t)$ as defined in Eq. 8.20, and comparing them against the numerical trajectories $\beta_x(x0,t)$ obtained in the previous chapter. The deviations ΔX and ΔP (see Eq. 7.15) are depicted as the semi-axes of ellipses centered around $\mathrm{Tr}\{a\,\rho(x0,t)\}$ for various time values t. (see Figs. 8.1, 8.2 and 8.3) All physical parameters are chosen as in the previous chapter (Eqs. 7.9).

Furthermore, Fig. 8.4 presents the analytically calculated weights $\tilde{c}_{xx}(t)$ alongside the numerically determined ones for the initial state $|00\rangle$ at relaxation rates $\gamma_{1q} = 0.0015\kappa,\ 0.015\kappa$ and 1.5κ.

Overall, the trajectories show a high degree of concordance between the numerical and analytical results at all times for the smaller relaxation rates 0.0015κ and 0.015κ. At higher rates, when the condition $\gamma_{1p} \ll \kappa$ no longer applies, the trajectories diverge notably around $t \approx 1/\gamma_{1q}$. Regarding the register-weights, the data indicate that $\tilde{c}_{xx}(t)$ as given

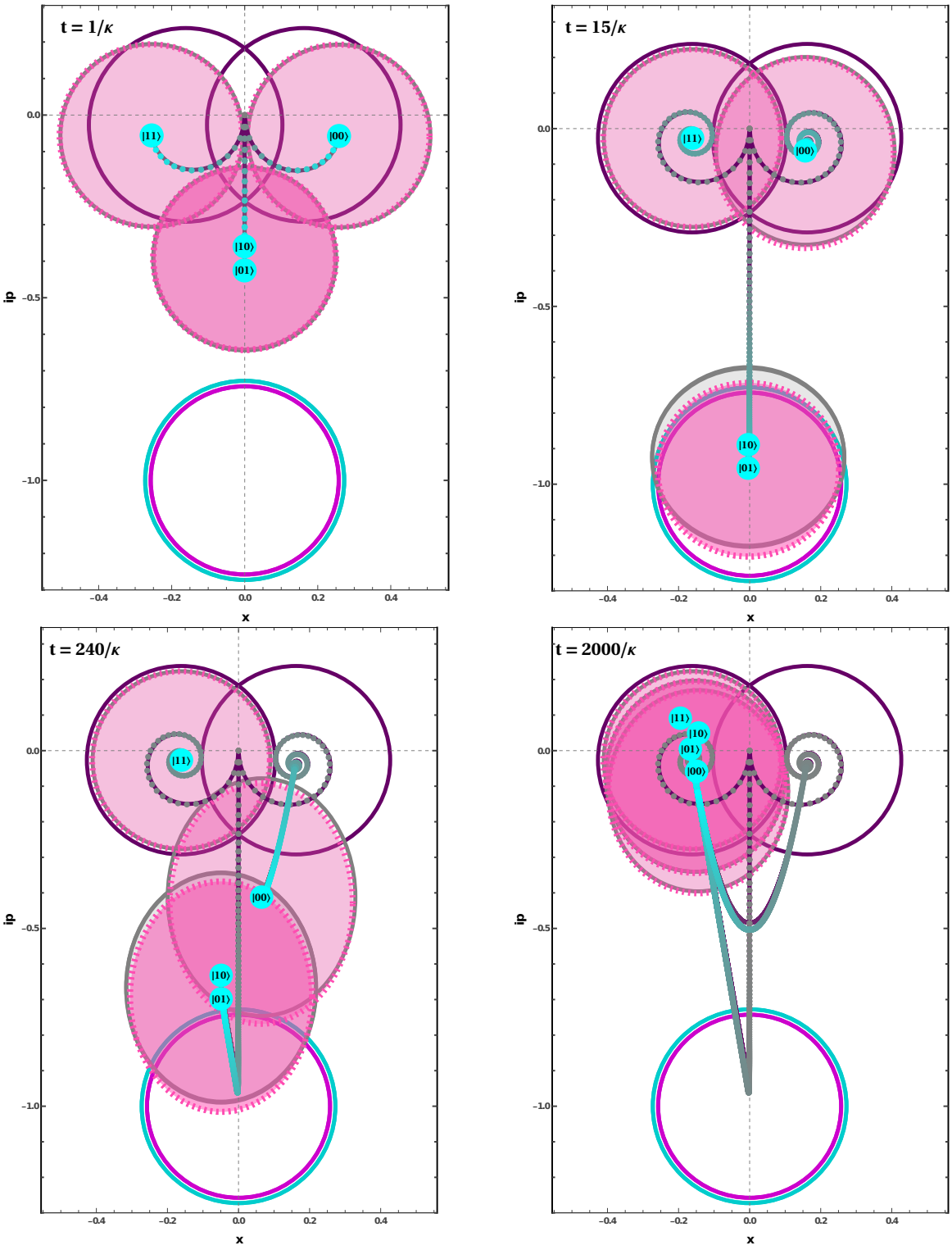

Figure 8.1.: **Numerical and analytic trajectories of initial states $|x\rangle$ for $\gamma_1 = 0.0015\kappa$**: The analytic trajectories (dotted gray/cyan lines) and states at time t (pink opaque discs with dashed contour centered around $\alpha_x(t)$) are plotted against the numerical solutions (solid-lined trajectory and gray opaque discs with solid contour). The length of the semi-axis of the opaque discs is given by the deviations ΔX and ΔY of the respective solutions.

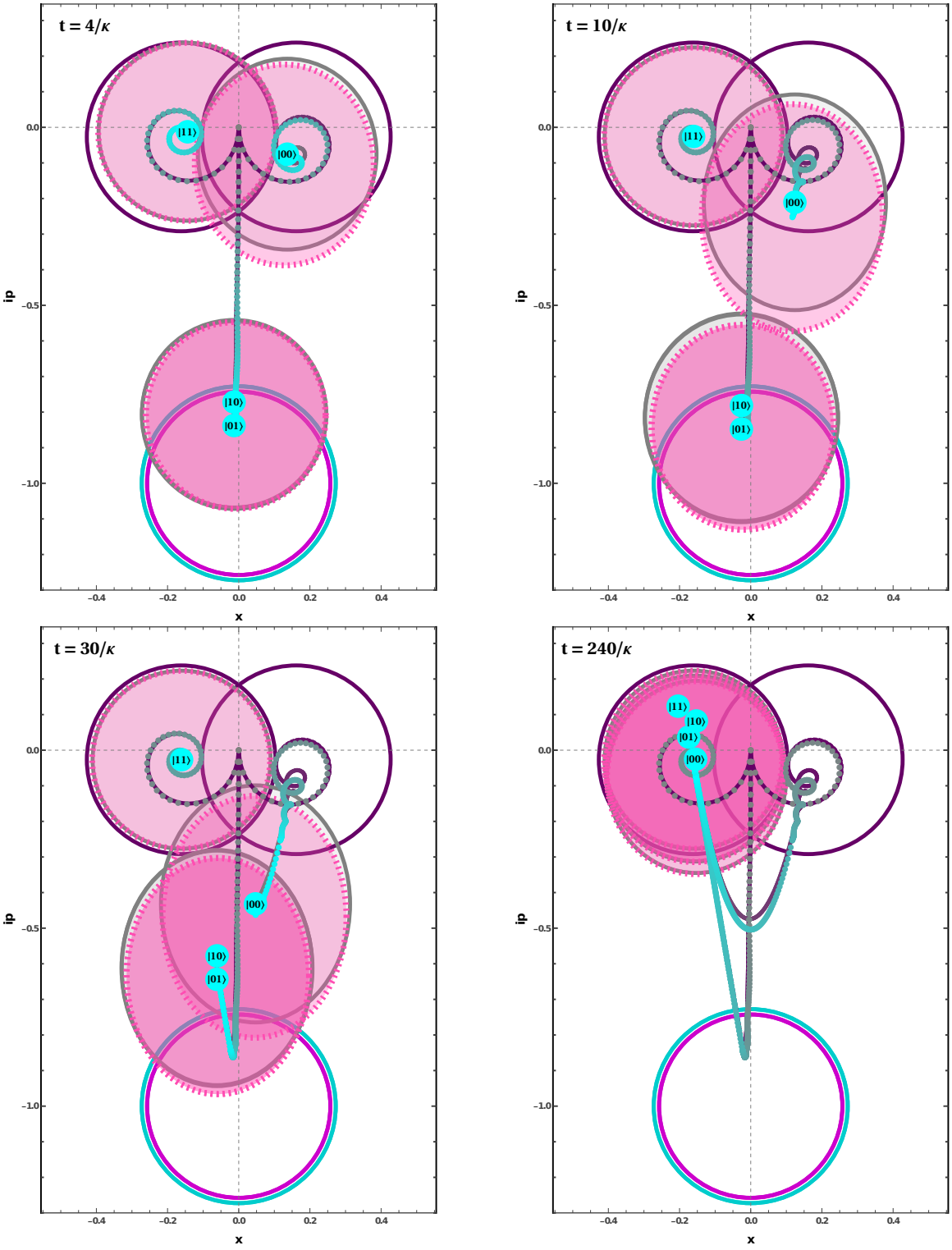

Figure 8.2.: **Numerical and analytic trajectories of initial states $|x\rangle$ for $\gamma_1 = 0.015\kappa$.**

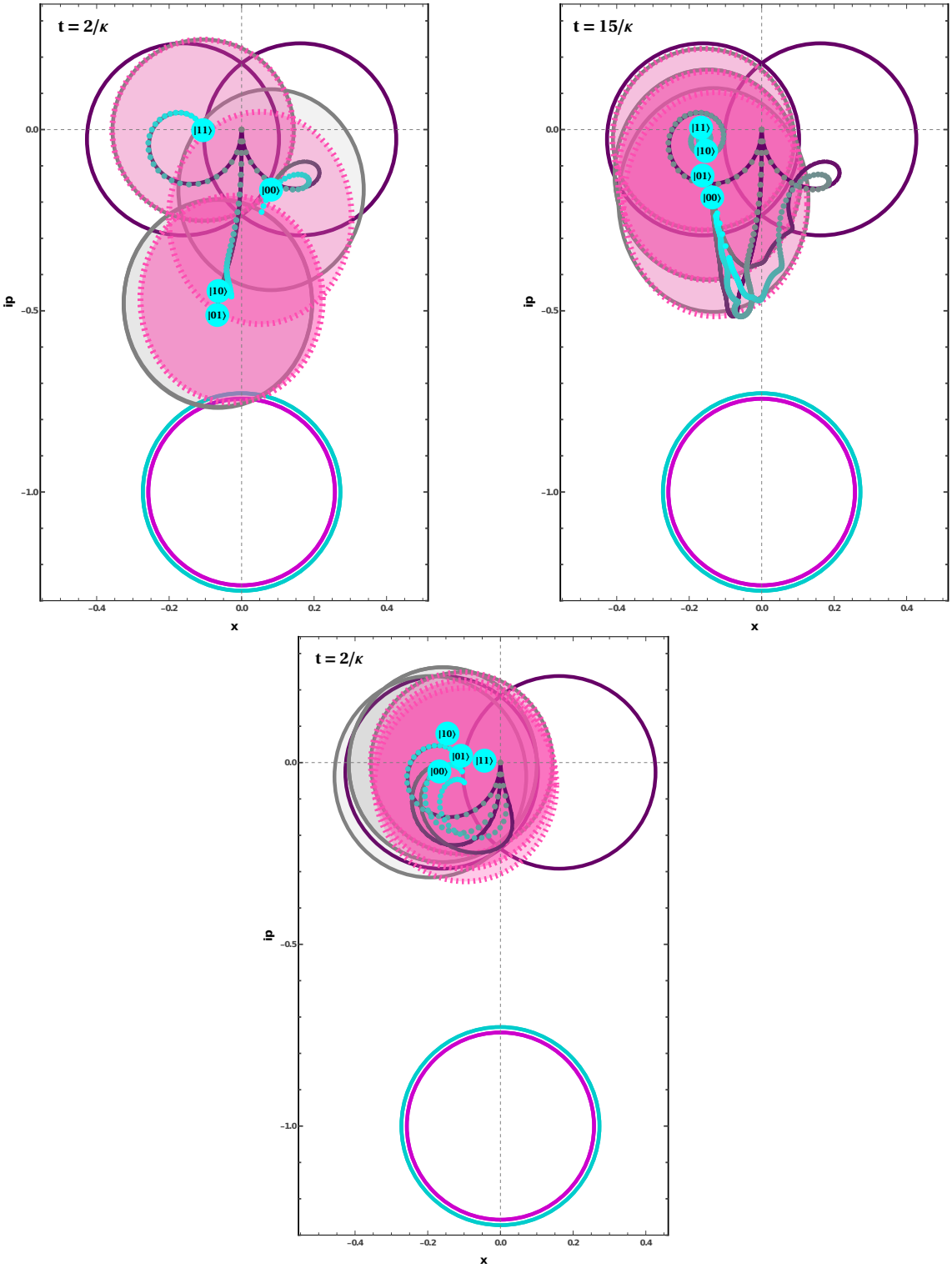

Figure 8.3.: **Numerical and analytic trajectories for $\gamma_1 = 0.15\kappa$ (top)** and **$\gamma_1 = 1.5\kappa$ (bottom).**

by Eq. 8.38 aligns closely with the numerical findings at all times and across all values of γ_{1q}.

In conclusion, the expectation that for $\gamma_{1q} \ll \kappa$ the full solution of the master equation can be approximated by the relaxation-free solution, with modified register weights $\tilde{c}_{xx}(t)$ accounting for qubit decay at rate γ_{1q}, is confirmed by both numerical evidence and analytical arguments.

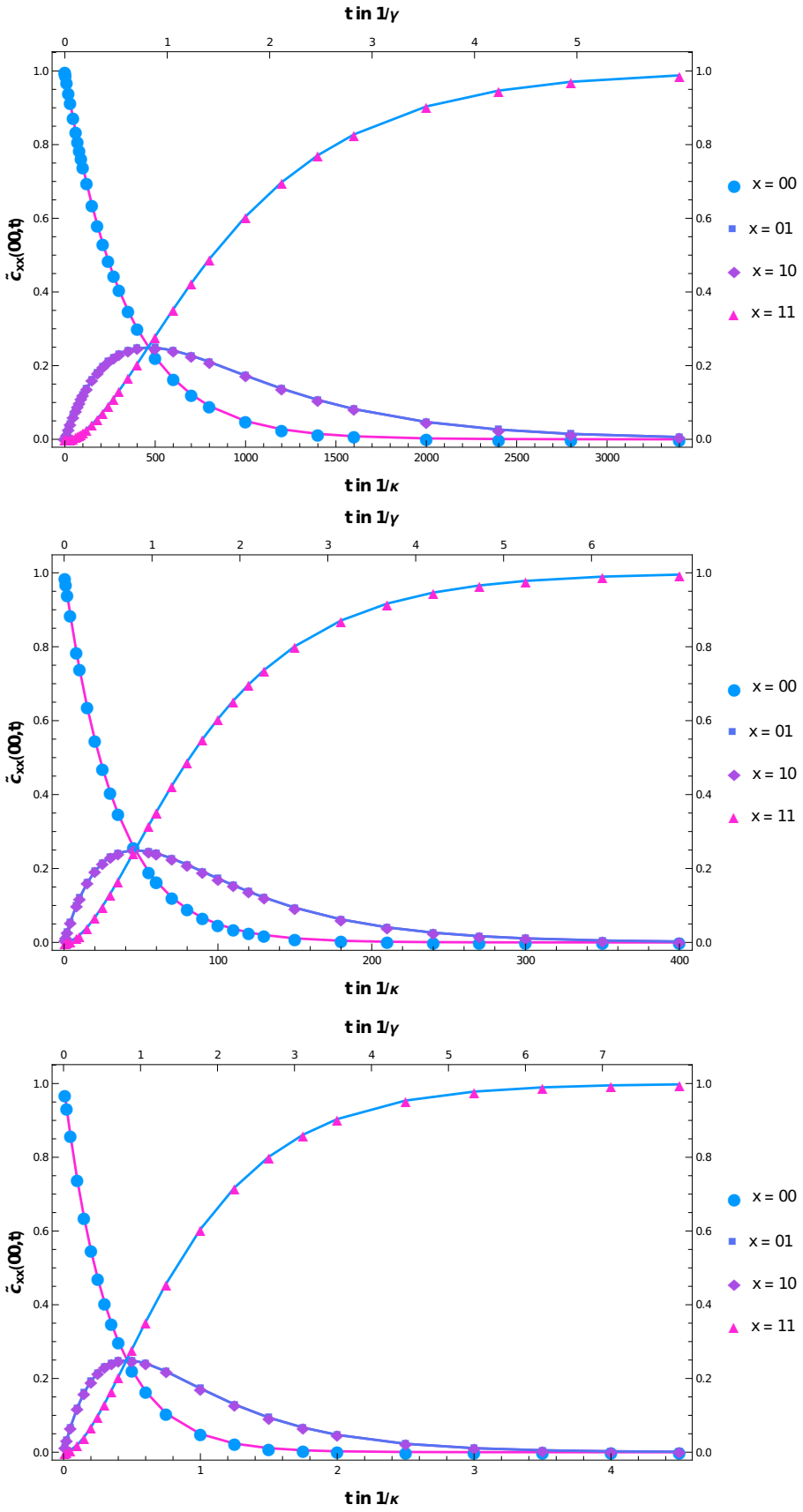

Figure 8.4.: Plots of **weights** for $\boldsymbol{\gamma_1 = 0.0015\kappa,\ 0.015\kappa,\ 1.5\kappa}$ (from top to bottom). The solid lines are the numerical results, the markers the analytical ones. All three pictures show the evolution of the register weights for the **initial register state** $\boldsymbol{|00\rangle}$.

9. Summary and outlook

9.1. Summary

In this thesis, we have provided a detailed derivation of the dispersive hamiltonian, including a short derivation of the transmon hamiltonian coupled to a resonator transmission line, the RWA and multiple Schrieffer Wolff transformations to obtain the dispersive shift as well as to remove the emerging flip-flop interaction between the register qubits. Additionally, we provided a microscopic derivation of the master equation for the coupled system, explicitly taking the structure of the driven dispersive Hamiltonian into account to obtain the jump operators. After observing that different density matrix subspaces probe the environment at different frequencies, we managed to show how the equation reduces to the typical Lindblad form usually postulated for the coupled system.

Further we demonstrated that the extension of the master equation's solution to N qubits is straight forward. A satisfying contribution of this work is the simplified derivation of the effective register equation, aswell as providing a clearer physical intuition regarding the circumstances under which this effective equation accurately describes the register dynamics, compared to [4].

In conclusion, the present thesis might provide valuable resources for students familiar with open system-quantum mechanics, who are interested in learning about the theoretical and physical basics of dispersive qubit readout.

9.2. Limitations and outlook

The analytic solutions obtained in this thesis (aswell as the papers of Blais et al.) are only valid given specific initial states of the form $\sim |x\rangle\langle y| \otimes |\alpha_x(0)\rangle\langle\alpha_y(0)|$. From a theoretic point of view, this is not completely satisfying. Further efforts towards finding the time evolution of arbitrary initial states and maybe even finding a closed solution of the propagator could improve the understanding of dispersive dynamics further.

Moreover, the modifications to the master equation due to the coupling and oscillator drive have neither been analyzed analytically, nor numerically. Doing so could also help refining experimental architectures for more realistic environments, to make them more suitable for practical quantum computing applications.

The role of multi-drive setups in multi-qubit systems is another area worth investigating further. Since multi-drive setups are necessary to properly carry out parity measurements for $N > 2$ systems, understanding their dynamics is crucial to move towards larger scaled quantum registers.

Finally, since multi-transmon chips are already being produced on a semi-commercial basis, examining the possibility of using a transmon as a nonlinear oscillator to perform parity measurements on other transmons coupled to it (similar to the research presented in [7]), might be interesting.

Appendices

A. Wirtinger calculus

A.1. Wirtinger derivatives

The Wirtinger derivatives encountered in Sec. 6.3 when calculating $a^\dagger |\alpha\rangle$, are a type of partial derivatives of functions of complex variables. Consider a complex variable $\alpha = x + \mathrm{i}p$ with x and p real numbers. The essential idea now is to define [49]

$$\frac{\partial}{\partial \alpha} \equiv \frac{1}{2}\left(\frac{\partial}{\partial x} - \mathrm{i}\frac{\partial}{\partial y}\right), \tag{A.1}$$

$$\frac{\partial}{\partial \alpha^*} \equiv \frac{1}{2}\left(\frac{\partial}{\partial x} + \mathrm{i}\frac{\partial}{\partial y}\right). \tag{A.2}$$

These definitions enable us to treat α and α^* as effectively independent variables when differentiating. For example, it is straightforward to show that the differential of a function of x and p can be rewritten as

$$\mathrm{d}f = \frac{\partial f}{\partial x}\mathrm{d}x + \frac{\partial f}{\partial p}\mathrm{d}p = \frac{\partial f}{\partial \alpha}\mathrm{d}\alpha + \frac{\partial f}{\partial \alpha^*}\mathrm{d}\alpha^*, \tag{A.3}$$

where the complex differentials $\mathrm{d}\alpha$ and $\mathrm{d}\alpha^*$ are defined formally via

$$\mathrm{d}x = \frac{1}{2}\left(\mathrm{d}\alpha + \mathrm{d}\alpha^*\right) \quad \text{and} \quad \mathrm{d}p = \frac{\mathrm{i}}{2}\left(\mathrm{d}\alpha^* - \mathrm{d}\alpha\right). \tag{A.4}$$

Moreover, it can be shown that the Wirtinger derivatives are linear and satisfy the product rule. A straightforward calculation using the definitions of α and ∂_α yields

$$\frac{\partial \alpha}{\partial \alpha} = 1 \quad , \quad \frac{\partial \alpha^*}{\partial \alpha} = 0, \tag{A.5}$$

which can be generalized to the usual differentiation rules for products of independent variables using the linearity and the product rule of the Wirtinger derivatives.

A.2. Integration in Wirtinger calculus

Using the Wirtinger differential A.3 and Stokes Theorem, we can show that the usual rule for partial integration also holds in Wirtinger calculus. For two functions $g(\alpha)$ and $f(\alpha)$, denoting the surface of integration as ∂D, where D is some domain in the complex plane, we can write [50]

$$\int_{\partial D} f(\alpha) g(\alpha)\, \mathrm{d}\alpha = \int_D \mathrm{d}\left[f(\alpha) g(\alpha)\, \mathrm{d}\alpha\right], \tag{A.6}$$

which is just Stokes theorem in the complex plane $\mathbb{C}$. Formally, the term in the brackets on the right-hand side is a 1-form, and $\mathrm{d}[\dots]$ denotes the exterior derivative of this 1-form. The exterior derivative of a 1-form $\omega = f\mathrm{d}x^j$, where $\mathrm{d}x^j$ is the differential of the jth variable, is defined by [51]

$$\mathrm{d}\omega \equiv \mathrm{d}f \wedge \mathrm{d}x^j = \sum_i \frac{\partial f}{\partial x_i}\, \mathrm{d}x^i \wedge \mathrm{d}x^j, \tag{A.7}$$

where "$\wedge$" denotes the exterior product between two differentials. Using the Wirtinger representation A.3 for $d(f \cdot g)$ leads to

$$\begin{aligned} \mathrm{d}\left[f(\alpha)g(\alpha)\,\mathrm{d}\alpha\right] &= \sum_{x=\alpha,\alpha^*} \frac{\partial(f\cdot g)}{\partial x}\,\mathrm{d}x \wedge \mathrm{d}\alpha \\ &= \frac{\partial(f\cdot g)}{\partial \alpha^*}\,\mathrm{d}\alpha^* \wedge \mathrm{d}\alpha \\ &= \left[\frac{\partial f}{\partial \alpha^*}\,g + f\,\frac{\partial g}{\partial \alpha^*}\right]\,\mathrm{d}\alpha^* \wedge \mathrm{d}\alpha, \end{aligned} \tag{A.8}$$

where we have used the anti-symmetry of the exterior product $\mathrm{d}x^i \wedge \mathrm{d}x^j = -\mathrm{d}x^j \wedge \mathrm{d}x^i$ in the second line, and the product rule in the third. Plugging into Eq. A.6 and rearranging yields:

$$\int_D \frac{\partial f}{\partial \alpha^*}\,g\,\mathrm{d}\alpha^* \wedge \mathrm{d}\alpha = \int_{\partial D} f(\alpha)g(\alpha)\,\mathrm{d}\alpha - \int_D f\,\frac{\partial g}{\partial \alpha^*}\,\mathrm{d}\alpha^* \wedge \mathrm{d}\alpha. \tag{A.9}$$

A similar calculation gives:

$$\int_D \frac{\partial f}{\partial \alpha}\,g\,\mathrm{d}\alpha \wedge \mathrm{d}\alpha^* = \int_{\partial D} f(\alpha)g(\alpha)\,\mathrm{d}\alpha^* - \int_D f\,\frac{\partial g}{\partial \alpha}\,\mathrm{d}\alpha \wedge \mathrm{d}\alpha^*. \tag{A.10}$$

These relations are useful since the 2-form $\mathrm{d}\alpha \wedge \mathrm{d}\alpha^*$ is proportional to the usual 2-form $\mathrm{d}^2\alpha = \mathrm{d}(\mathrm{Re}\,\alpha) \wedge \mathrm{d}(\mathrm{Im}\,\alpha)$ used for integrating over a domain in $\mathbb{C}$: Using Eq. A.4 we find

$$\begin{aligned} \mathrm{d}(\mathrm{Re}\,\alpha) \wedge \mathrm{d}(\mathrm{Im}\,\alpha) &= \frac{1}{2}\,(\mathrm{d}\alpha + \mathrm{d}\alpha^*) \wedge \frac{\mathrm{i}}{2}\,(\mathrm{d}\alpha^* - \mathrm{d}\alpha) \\ &= \frac{\mathrm{i}}{2}\,\mathrm{d}\alpha \wedge \mathrm{d}\alpha^*. \end{aligned} \tag{A.11}$$

Defining $(x,p) \equiv \big(\mathrm{Re}(\alpha), \mathrm{Im}(\alpha)\big)$, we identify i/2 as the determinant of the Jacobian $\mathcal{J}$ belonging to the change of integration variables $(x,p) \to \big(\alpha,\alpha^*\big)$:

$$\left\|\mathcal{J}_{(x,p)}(\alpha,\alpha^*)\right\| = \frac{\mathrm{i}}{2} \tag{A.12}$$

For vanishing boundary terms we can perform partial integration in $\mathbb{C}$ using the formula

$$\int_D \frac{\partial f}{\partial \alpha}\,g\,\mathrm{d}^2\alpha = -\int_D f\,\frac{\partial g}{\partial \alpha}\,\mathrm{d}^2\alpha, \tag{A.13}$$

where $\mathrm{d}^2\alpha$ can mean both $\mathrm{d}x\,\mathrm{d}p$ or $\mathrm{d}\alpha\,\mathrm{d}\alpha^*$, since the Jacobian determinant cancels in Eq. A.10. Note that the derivation does not depend on the fact that we defined f and g as functions of α only. Therefore, Eq. A.13 can also be used for functions depending on both α and α^*

A.3. Delta distributions in Wirtinger calculus

When encountering a Delta-Distribution of the variables (x,p) in an integral over the complex plane of the form

$$\int \mathrm{d}x\mathrm{d}p\,\delta\big(x-x_0\big)\delta\big(p-p_0\big) \equiv \int \mathrm{d}x\mathrm{d}p\,\delta^{(2)}\big(\alpha-\alpha_0\big) = 1, \tag{A.14}$$

with $\mathrm{d}^2\alpha = \mathrm{d}x\mathrm{d}p$ we can perform a change in variables by introducing the Dirac Distribution for Wirtinger variables. We define the Wirtinger delta distribution by

$$\int \mathrm{d}\alpha\,\mathrm{d}\alpha^*\,\delta\big(\alpha-\alpha_0\big)\delta\big(\alpha^*-\alpha_0^*\big) \equiv \int \mathrm{d}\alpha\,\mathrm{d}\alpha^*\,\delta_w^{(2)}\big(\alpha-\alpha_0\big) = 1. \tag{A.15}$$

Since $\mathrm{d}x\,\mathrm{d}p = \mathrm{i}/2\,\mathrm{d}\alpha\,\mathrm{d}\alpha^*$ we can deduce that

$$\delta_w^{(2)}(\alpha - \alpha_0) = -\mathrm{i}2\,\delta^{(2)}(\alpha - \alpha_0) = \mathcal{J}_{(x,p)}^{-1}(\alpha, \alpha^*)\delta^{(2)}(\alpha - \alpha_0) \tag{A.16}$$

must hold. For integrating an arbitrary function $f(x, p)$ we therefore find the identity

$$\int f(x,p)\,\delta^{(2)}(\alpha - \alpha_0)\,\mathrm{d}x\,\mathrm{d}p = \int f(\alpha, \alpha^*)\,\delta_w^{(2)}(\alpha - \alpha_0)\,\mathrm{d}\alpha\,\mathrm{d}\alpha^*. \tag{A.17}$$

By combining Eqs. A.10 and A.17 we can now use the usual rule for integrating over a Wirtinger derivative of a delta distribution:

$$\int f(x,p)\partial_\alpha\delta^{(2)}(\alpha - \alpha_0)\,\mathrm{d}x\,\mathrm{d}p = -\partial_\alpha f(\alpha, \alpha^*). \tag{A.18}$$

Essentially, we have shown that in most cases we can treat the Wirtinger derivative ∂_α as the usual derivative. especially we are allowed to do so, when integrating in the complex plane with respect to the variables (x, p), since here we can easily change integration variables.

B. Chaotic behavior of β_x for large γ_1

In Chapter 7 the Q-functions of numerical solutions to the dissipative master equation were calculated for $\gamma_1/g = \{0.0001, 0.001, 0.01, 0.1\}$. The position of their maxima β_x in the complex plane shows emerging chaotic behaviour for $\gamma_1/g = \{0.01, 0.1\}$. Here, small variations in γ_1 can lead to noticeable shifts in β_x. For $\gamma_1/g = 0.01$ these shifts are relatively small and mostly restricted to the odd-parity (large amplitude) states (see Fig. B.2), while for $\gamma_1/g = 0.1$ they seem to remove any correlation between the register states and β_x, except for the register-ground-state (see Fig. B.1). This may be attributed to the fact, that in the $\gamma_1 \approx \kappa$ regime, the oscillator states ρ_{xx} are "leaking" into each other due to qubits relaxing, resulting in large deviations of the ρ_{xx} from coherent states. This renders the coherent state basis, and thus the Husimi Q-function, increasingly inadequate to analyse the system in a fruitful manner. It might also just be an artifact of the definition of β_x as the maximum of the Q-representation. A more stable choice might be to define it as the "center of mass", as the expectation value $\mathrm{Tr}[a\rho_{xx}]$.

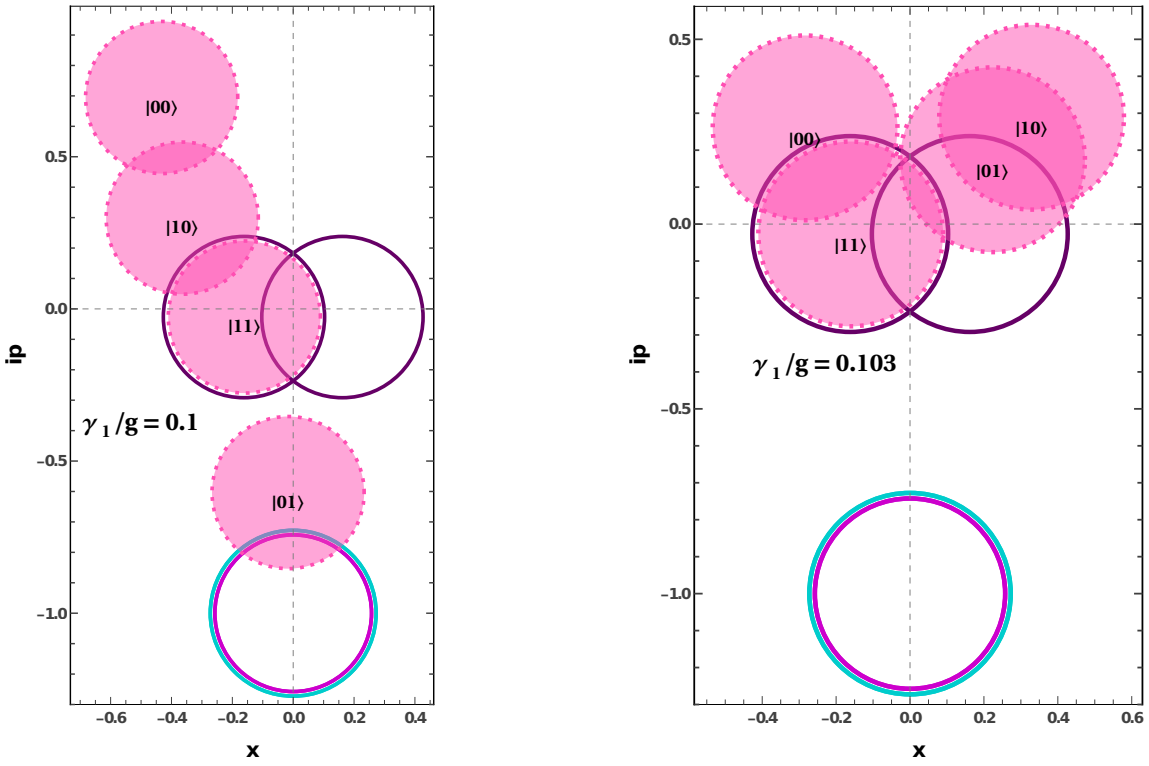

Figure B.1.: Strong chaotic behavior of β_x (centers of opaque disks) for small changes in γ_1

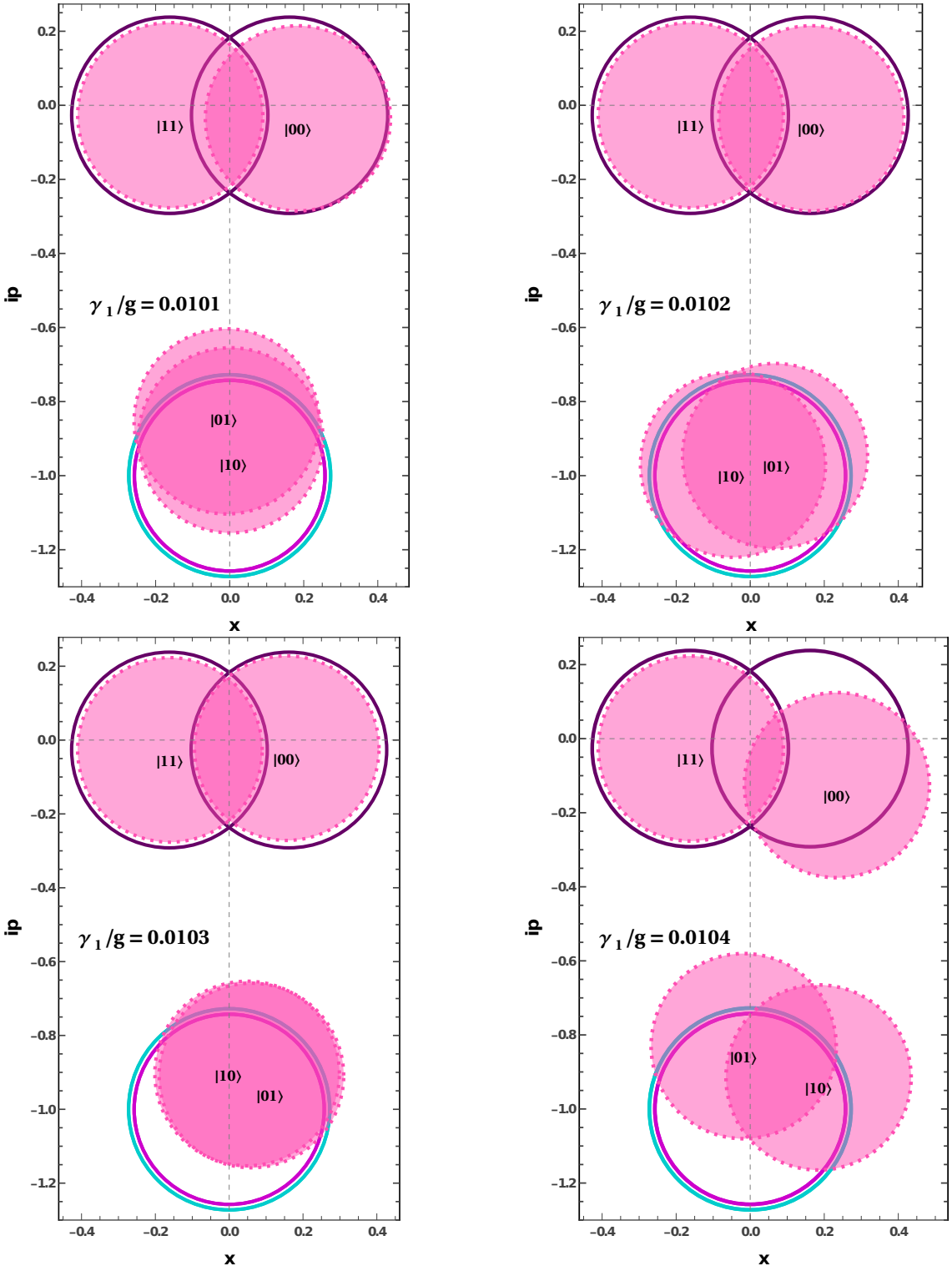

Figure B.2.: Weak chaotic behavior of β_x (centers of opaque disks) for small changes in γ_1

C. Time evolution plots of weights, distances and deviations

This appendix contains additional plots of the weights, distances and deviations discussed in Sec. 7.4, for various values of γ_1.

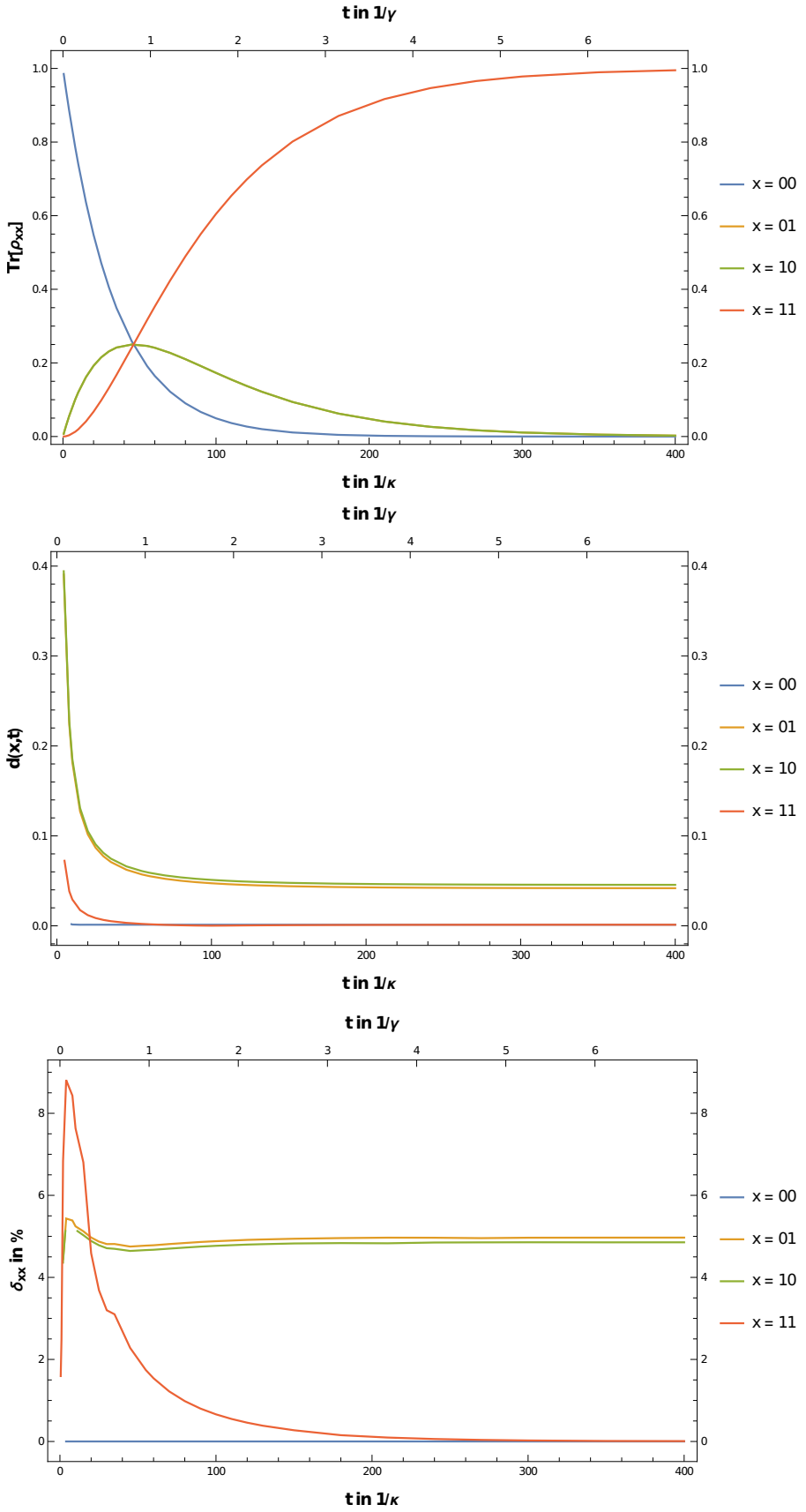

Figure C.1.: Plots of **weights, distances and deviations** (from top to bottom) for $\boldsymbol{\gamma_1 = 0.015\kappa}$:

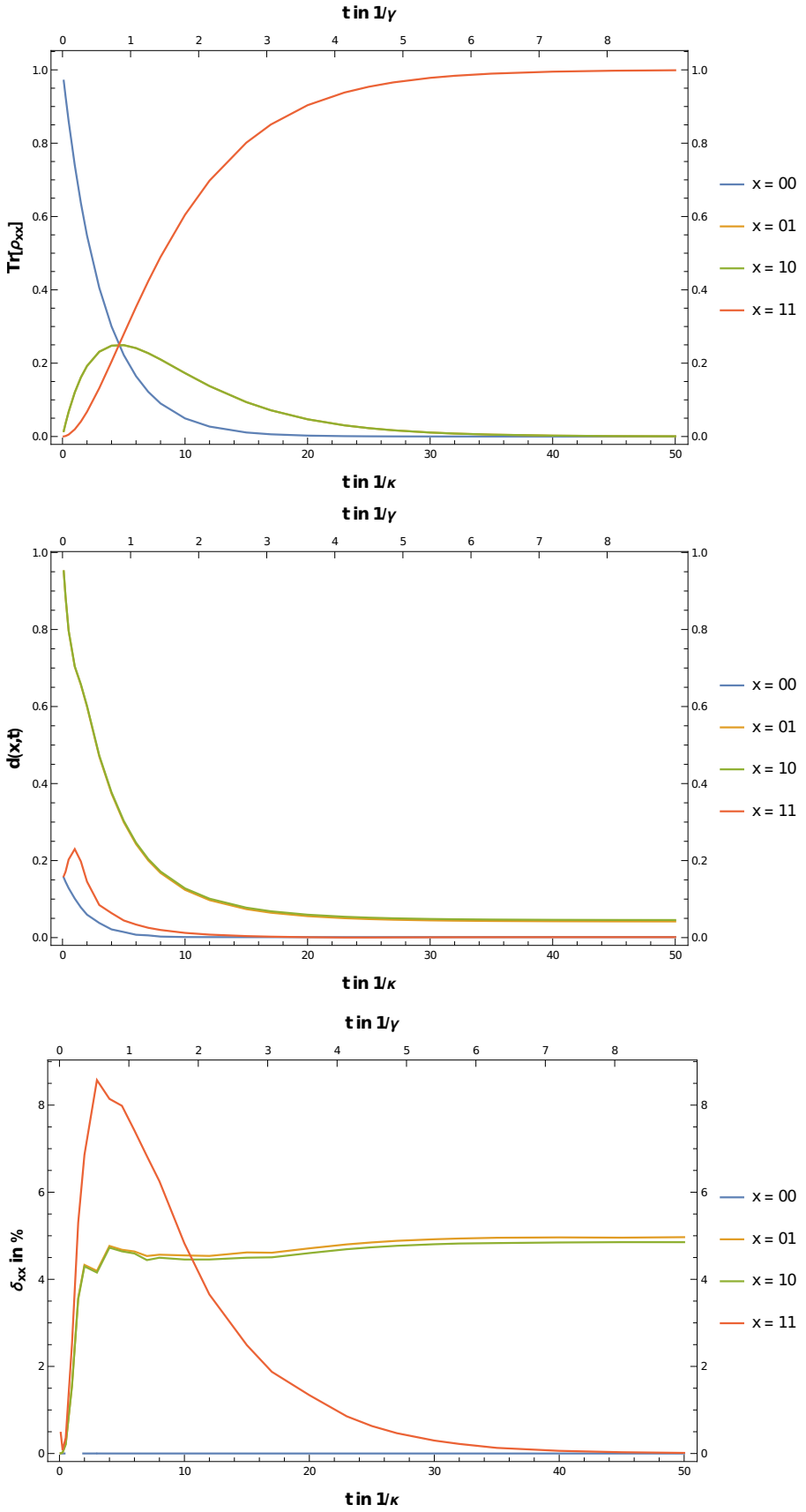

Figure C.2.: Plots of **weights, distances and deviations** (from top to bottom) for $\boldsymbol{\gamma_1 = 0.15\kappa}$:

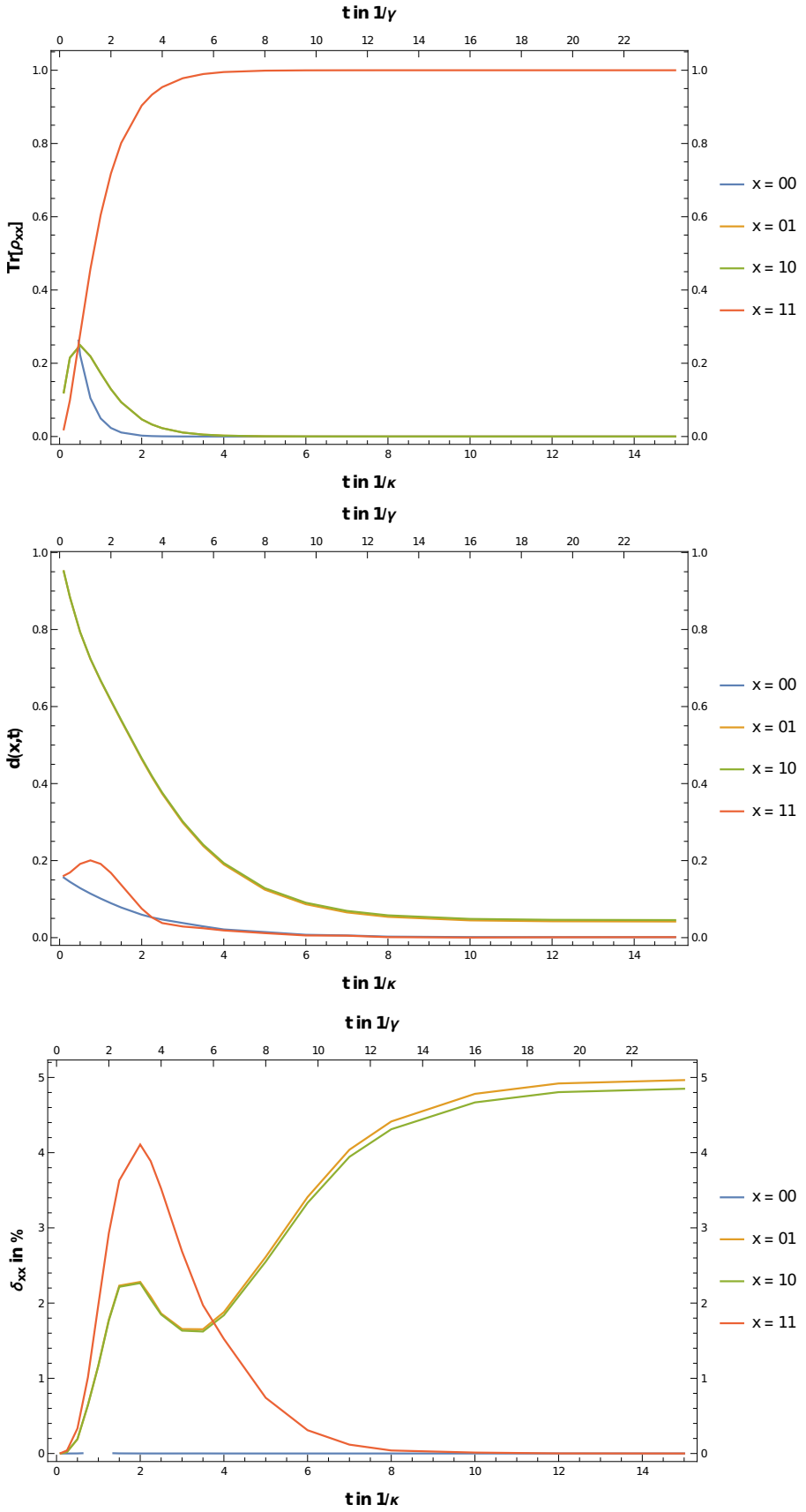

Figure C.3.: Plots of **weights, distances and deviations** (from top to bottom) for $\boldsymbol{\gamma_1 = 1.5\kappa}$:

D. Mathematica Code

D.1. Solving the Lindblad Equation Numerically

The program solving the Lindbladian numerically as outlined in Sec. 7.1 is split into three functions:

- **GetEigenSystem**: This function takes an an input a string specifying the Hamiltonian (full Jaynes Cummings, dispersive with or without drive correction terms), a boolean used to turn flip-flop interaction on or of, and a list of all physical parameters going into the Lindbladian: the number of qubits in the register, the number of photons at which the oscillator Hilbert space is to be truncated and all other parameters present in Eq. 3.91 and 6.1. It outputs the eigensystem of the Lindbladian, a nested list containing the vectorized eigenmodes and corresponding eigenvalues. Furthermore, the input parameters are outputted aswell, so that functions analysing the solutions "know" how they were calculated.
- **buildOperators**: This function is loaded and called by GetEigenSystem and builds the necessary operators going into the Hamiltonian
- **buildLindbladian**: This function is also called and loaded by GetEigenSystem, to build the Lindbladian from the Hamiltonian constructed using the operators build via buildOperators

GetEigenSystem Function

```
GetEigenSystem[h_, f_, jq_, param_] := (
   (* this function calculates the eigenvectors of the
      lindbladian equation for driven oscillator coupled
      jaynes-cummings style to qubits. the paramters are
      chosen such that the resulting dispersive shift is
      equal for all qubits*)
   (*****************************************)
   (*h is the string type of hamiltonian:
        "full" = "Full" Jaynes Cummings hamiltonain, driven
            in RWA approx
         "h1"  =  Dispersive hamiltonian of the first type
                    (where the driving term was considered
                       in finding the transformation
                       generator S)
        "h2"   =  Dispersive hamiltonian with driving term
           neglected at first and tranformed "later"
    "h3"   =  Dispersive hamiltonian without correction of
       driving terms

   f is a function f[q_]:= Subscript[\[Omega], q] that
      gives the qubits detunings (it should have  f(1) =
      -1..., every other quantity will be measured with
      regards to this!)
   jq is boolean: 1 is flip-flop on, 0 is off
        In my calculations I used f[q_]:= -q

   param are the other parameters of the problem:
```

```
param= {Nqubit,Nphoton,Subscript[\[Omega], r],\[Epsilon
    ],\[Kappa], g,Subscript[\[Gamma], 1],Subscript[\[
    Gamma], \[Phi]]}*)

ref = Abs@f[1];     (*this should be "1" and is be the
    reference w.r.t.w. everything else is measured*);

nq = param[[1]];    (*number of qubits in the array*)
nph = param[[2]];   (*number of photons at which we
    truncate*)
Subscript[\[Omega], r] = param[[3]]*ref; (*this is the
    RWA freq.
of the oscillator: its bare freq. - the drive freq.*)
\[Epsilon] = param[[4]]*ref;
\[Kappa] = param[[5]]*ref;
g = param[[6]]*ref;
\[Gamma]1 = param[[7]]*ref;  (* I assume that all qubits
     dissipate equally*)
\[Gamma]\[Phi] = param[[8]]*ref;

MaxPhotons = nph;
NQubits = nq;
DimOsc = MaxPhotons + 1;
DimQubits = 2^(NQubits);
Dim = DimOsc*DimQubits;

(*Define Parameters*)

(*put qubit detunings (before dispersive approx -
    without lambshift)  into an array*)
fq = Array[f, NQubits];

(*define basic parameters*)
gq = Sqrt[(fq - Subscript[\[Omega], r])/(fq[[1]] -
    Subscript[\[Omega], r])]*g;(**)
\[Chi] = ConstantArray[g^2/(fq[[1]] - Subscript[\[Omega
    ], r]), NQubits];
\[Omega]q = fq + \[Chi]; (*lambshifted dispersive-qubit
    frequencies!*);
\[CapitalDelta]q = \[Omega]q - Subscript[\[Omega], r];
J[Q_, P_] := gq[[Q]] gq[[P]]*(1/\[CapitalDelta]q[[Q]] +
    1/\[CapitalDelta]q[[P]])/2;

Subscript[J, qq] = N*g/(fq[[1]] - Subscript[\[Omega], r
    ]); (*constant that is added to H in dispersive
    approx*);

If[jq == 1,
 Jb = 1,
 Jb = 0;
 ];  (* will be used to turnflip-flop on or off: jq=1
     means flip-flop=on*)


(*Print Parameters and Check Conditions*)
Print@StringForm[" +++ For `` Qubits coupled to
    resonator with `` photons: +++", param[[1]], param
    [[2]]];
Print["Build Hamiltonian ", h, " with Flip-Flop
    Interaction set to jq=" , jq, "..."];
```

```
Subscript[\[CapitalDelta], min] = Min@Abs@\[CapitalDelta
   ]q;
Subscript[n, crit] =  1/4 * Abs@((Subscript[\[
   CapitalDelta], min])*(fq[[1]] - Subscript[\[Omega], r
   ])/(g^2));
Subscript[n, disp] = 4*\[Epsilon]^2/(\[Kappa]^2); (*
   number of photons in oscillator for drive at
   resonance*)
Print["---*---The main Parameters of this Hamiltonian
   :---*--"];
Print["fq = ", MatrixForm@fq, "the RWA qubit frequencies
   "];
Print["gq = ", MatrixForm@gq, "the coupling of the qth
   Qubit"];
Print["\[Omega]q = ", MatrixForm@\[Omega]q, "the
   lambshifted RWA-qubit energies"];
Print["\[Chi] = ", MatrixForm@\[Chi], "dispersive
   coupling strengths"];
Print["-----------------CHECK--CONDITIONS
   :------------------"];
Print["for the Qubit Frequency closest to Resonance we
   have "];
Print["             \!\(\*SubscriptBox[\(\[CapitalDelta
   ]\), \(min\)]\) = ", Abs@Sqrt[(Subscript[\[
   CapitalDelta], min])*(fq[[1]] - Subscript[[Omega], r
   ])], " >> g = ", g, " ?"];(*this is the condition for
    the dispersive regime*)
Print["The lowest critical photon numer "];
Print["            \!\(\*SubscriptBox[\(n\), \(crit\)]\)
    = ", Subscript[n, crit]  , " >> \!\(\*SubscriptBox
   [\(n\), \(disp\)]\) ~ ", Subscript[n, disp], " ?"];


(*Build Hamiltonian*)

Get["buildOperators.m"];
Get["buildlindbladian.m"];

Print["-----------------------------------------------"];

buildOperators[DimOsc, NQubits]; (*
builds the operators that are needed to build
   hamiltonian and \lindbladian*)

(* mach jetzt fallunterscheidung jenachdem welcher
   hamiltonian angegeben wurde*)
(*Full Hamiltonian (that is: Driven Jaynes Cummings in
   RWA))*)
If[h == "full",
 PrintTemporary["Building Full Hamiltonian..."];
 (*Oscillator-Hamiltonian: *)
 HRWA = Subscript[\[Omega], r]*Num  + \[Epsilon]*(A +
    Adagger);
 (*Qubit Hamiltonian:*)
 Subscript[H, Q ] = If[NQubits == 0,
                       {{0}},
                       Sum[(fq[[n]]/2)*Z[n], {n,
                          NQubits}]
                   ];
 (*Interaction Hamiltonain:*)
```

```
 Subscript[H, I] = If[NQubits == 0,
   ConstantArray[0, {DimOsc, DimOsc}],
   Sum[
    gq[[j]]*(KroneckerProduct[SubMinus[\[Sigma]][j],
       Adagger] +
       KroneckerProduct[SubPlus[\[Sigma]][j], A]), {j,
          NQubits}]
   ];
 (*Total Hamiltonian: *)
 H = KroneckerProduct[IdQ, HRWA] +
   KroneckerProduct[Subscript[H, Q], IdO] + Subscript[H,
       I];
 ];

(*First Corrected Dispersive hamiltonian*)
If[h == "h1",
     Print[
      "Building Dispersive Hamiltonian of 1. kind, with
         Flip-Flop turned to ", jq, "..."];
     Subscript[H, RWA] = Subscript[\[Omega], r]*Num  +
        \[Epsilon]*(A + Adagger); (*Oscillator-
        Hamiltonian: *)
     Subscript[H, Q ] = If[(*Qubit Hamiltonian:*)
       NQubits == 0,
        {{0}},
       Sum[\[Omega]q[[n]]/2 * Z[n], {n, NQubits}] + Jb*
          Sum[J[o, p]*(SubPlus[\[Sigma]][o] . SubMinus
          [\[Sigma]][p] + SubPlus[\[Sigma]][p] .
          SubMinus[\[Sigma]][o]) Boole[o > p], {o, 1,
          NQubits}, {p, 1, NQubits}]
       ];
     Subscript[H, I] = If[  (*Interaction Hamiltonain:*)
       NQubits == 0,
       ConstantArray[0, {DimOsc, DimOsc}],
       KroneckerProduct[Sum[\[Chi][[u]]*Z[u], {u,
          NQubits}], Num] +  (*dispersive shift*)
        \[Epsilon]*Sum[\[Chi][[q]]/(2*fq[[q]])*
           KroneckerProduct[Z[q], A + Adagger], {q, 1,
           NQubits}] (*correction bec. of drive*)
       ];
     H = KroneckerProduct[IdQ, Subscript[H, RWA]] +
       KroneckerProduct[Subscript[H, Q], IdO] +
       Subscript[H, I]; (*Total Hamiltonian: *)
 ];

(*Second Corrected Dispersive Hamiltonian*)
If[h == "h2",
     PrintTemporary["Building Dispersive Hamiltonian of
        1. kind, with Flip-Flop turned to ", jq, "..."];
     Subscript[H, RWA] =
      Subscript[\[Omega], r]*Num  + \[Epsilon]*(A +
         Adagger); (*Oscillator-Hamiltonian: *)
     Subscript[H, Q ] = If[(*Qubit Hamiltonian:*)
       NQubits == 0,
        {{0}},
       Sum[\[Omega]q[[n]]/2 * Z[n], {n, NQubits}] + Jb*
          Sum[J[o, p]*(SubPlus[\[Sigma]][o] . SubMinus
          [\[Sigma]][p] + SubPlus[\[Sigma]][p] .
          SubMinus[\[Sigma]][o]) Boole[o > p], {o, 1,
          NQubits}, {p, 1, NQubits}]
       ];
```

```
      Subscript[H, I] = If[  (*Interaction Hamiltonain:*)
        NQubits == 0,
        ConstantArray[0, {DimOsc, DimOsc}],
        KroneckerProduct[Sum[\[Chi][[u]]*Z[u], {u,
            NQubits}], Num] + (*dispersive shift*)
        \[Epsilon]*Sum[\[Chi][[q]]/gq[[q]]*
            KroneckerProduct[SubPlus[\[Sigma]][q] +
            SubMinus[\[Sigma]][q], IdO], {q, 1, NQubits}]
            (*correction bec. of drive*)
        ];
      H = KroneckerProduct[IdQ, Subscript[H, RWA]] +
        KroneckerProduct[Subscript[H, Q], IdO] +
            Subscript[H,
        I]; (*Total Hamiltonian: *)
      ];

     (*Uncorrected Dispersive Hamiltonian*)
     If[h == "h3",
      PrintTemporary["Building Dispersive Hamiltonian of
          1. kind, with Flip-Flop \turned to ", jq, "..."
          ];
      Subscript[H, RWA] =
       Subscript[\[Omega], r]*Num  + \[Epsilon]*(A +
          Adagger); (*Oscillator-Hamiltonian: *)
      Subscript[H, Q ] = If[(*Qubit Hamiltonian:*)
        NQubits == 0,
        {{0}},
        Sum[\[Omega]q[[n]]/2 * Z[n], {n, NQubits}] + Jb*
            Sum[J[o, p]*(SubPlus[\[Sigma]][o] . SubMinus
            [\[Sigma]][p] + SubPlus[\[Sigma]][p] .
            SubMinus[\[Sigma]][o]) Boole[o > p], {o, 1,
            NQubits}, {p, 1, NQubits}]
        ];
      Subscript[H, I] = If[  (*Interaction Hamiltonain:*)
        NQubits == 0,
        ConstantArray[0, {DimOsc, DimOsc}],
        KroneckerProduct[Sum[\[Chi][[u]]*Z[u], {u,
            NQubits}], Num] (*dispersive shift*)
        ];
      H = KroneckerProduct[IdQ, Subscript[H, RWA]] +
        KroneckerProduct[Subscript[H, Q], IdO] +
            Subscript[H, I]; (*Total Hamiltonian: *)
 ];

L1 = buildlindbladian[H, NQubits ];

(*************************************)
(*Calculate Solution*)
PrintTemporary["Calculate EigenSystem...."];
EigSys = Eigensystem[L1];
PrintTemporary["Eigensystem found!"];
PrintTemporary[
 "Sort Eigensystem s.th. stationary state is 1st and
    then decreasing decay frequencies from there..."];
EigSys =
 Transpose[
  Sort[Transpose[EigSys],
   Re[#1[[1]]] > Re[#2[[1]]] & ]];(*this orders the
      eigensystem by the real part of the eigenvalues in
       descending order: since they should all be
      negative this casts the stationary state at 1*)
```

```
        (*sAVE dATA*)
        (*a= StringSplit[ToString[\[Gamma]1i],"."][[2]];
        b= StringSplit[ToString[\[Gamma]\[Phi]i],"."][[2]];*)

        (*define new string that will be used in naming the
           output file*)
        If[Subscript[\[Omega], r] == 0,
         wr = "Res", (*resonant drive*)
         wr = "Det"; (*drive detuned from bare osc. freq.*)
         ];

        filename =
         ToString[
          StringForm["sol``_``Q``Ph_Jq``_``_Gamma1=``.mx", h,
             NQubits, MaxPhotons, jq, wr, \[Gamma]1]];
        Print["+++++++ D O N E +++++++++"];
        Print[filename];
        out = {EigSys, {h, f, jq}, param};
        Export[filename, out];
        Print["
           ================================================================
           "];
        Return[out];
        );
(*Save Function as file*)
Export["GetEigenSystem.m", FullDefinition[GetEigenSystem]]
```

buildOperators Function

```
    buildOperators[dimosc_, nqub_] :=
  Module[{DimOsc, NQubits, DimQubits, Dim},
   (*takes the dimensionality of the oscillator hilbertspace and
      number of qubits as input. *)

   DimOsc = dimosc;
   NQubits = nqub;
   DimQubits = 2^NQubits;
   Dim = DimOsc*DimQubits; (*total dimensionality of product
      hilbert space*)

   (*define the identiy operators on the hilbert-spaces*)
   IdO = IdentityMatrix[DimOsc];
   IdQ = IdentityMatrix[DimQubits];
   Id = IdentityMatrix[Dim];

   (*Creation and annihilation operators:*)
   A = ConstantArray[0, {DimOsc, DimOsc}];
   Adagger = A;
   For[i = 1, i < DimOsc, i++,
    A[[i]][[i + 1]] = Sqrt[i];
    ];
   Adagger = ConjugateTranspose[A];
   Num = Adagger . A; (*number operator*)


   (*Build Spin-Operators*)
   (*define the kronecker product of n-qubit identity-matrices:*)
   nId[ne_] := IdentityMatrix[2^ne];
   (*and the pauli matrices for one spin:*)
   z = {{1, 0}, {0, -1}};
   y = {{0, -I}, {I, 0}};
   x = {{0, 1}, {1, 0}};

   (* Spinoperators on the product space -> register operators*)
   (*Z[n] is then the pauli z matrix of the nth qubit on the
      register space*)
   Z[ne_] := KroneckerProduct[nId[ne - 1], z, nId[NQubits - ne]];
   Y[ne_] := KroneckerProduct[nId[ne - 1], y, nId[NQubits - ne]];
   X[ne_] := KroneckerProduct[nId[ne - 1], x, nId[NQubits - ne]];
   (*Pauli Ladder operators on the registerspace:*)
   SubPlus[\[Sigma]][ne_] := 1/2 * (X[ne] + I*Y[ne]);
   SubMinus[\[Sigma]][ne_] := 1/2 * (X[ne] - I*Y[ne]);
   (*++++++++++++++++++++++++++++++++++++++++++++++++++++++++++++*)
   ];
Export["buildOperators.m", FullDefinition[buildOperators]];
```

buildLindbladian Function

```
    buildlindbladian[ham_, nqube_] :=
  (

   H = ham;
   NQubits = nqube;
   (*Dissipator D[A] of operator A: *)
   Diss[A_] :=
    KroneckerProduct[A, Transpose[ConjugateTranspose[A]]] - 1/2 * (
       KroneckerProduct[ConjugateTranspose[A] . A, Id] +
       KroneckerProduct[Id, Transpose[ConjugateTranspose[A] . A]]);
   (*REMARK: Only operators on the full-product space can be taken
      as a input of D[.]!*)

   (*Lindbladian:*)
   PrintTemporary["Building Lindbladian..."];
   L  = -I*(KroneckerProduct[H, Id] -
        KroneckerProduct[Id, Transpose[H]]) + Sum[\[Gamma]1*Diss[
           KroneckerProduct[SubMinus[\[Sigma]][ni], IdO]], {ni,
           NQubits}] + Sum[\[Gamma]\[Phi]*Diss[KroneckerProduct[Z[
           ni], IdO]], {ni, NQubits}] + \[Kappa]*Diss[
           KroneckerProduct[IdQ, A]];
   PrintTemporary["Lindbladian built!"];
   Return[L];
   );
Export["buildlindbladian.m", FullDefinition[buildlindbladian]];
```

D.2. Eigenmode decomposition of initial vectors and time evolution

This section contains the Mathematica code used to decompose initial states into the eigenmodes given in the output of the GetEigenSystem function. The main function is the"dynSys" function. Below are also the additional functions used by "dynSys"

dynSys function

This function takes the output of GetEigenSystem as input. Its output is a list "dynρ0, where the xth entry corresponds to the density matrix $\rho(t)$ evolved from the initial state $|x\rangle\langle x|\otimes|0\rangle\langle 0|$, at an un-evaluated time t. The matrices $\rho(t)$ are constructed via the method presented in Sec. 4.3.2.

```
dynSys[sol_] :=
  Module[{out, rvecs, rvals, lvecs, lvals, h, f, jq,
     param, nq, nph, dimq, dimo, dim, \[Rho]0, u, v, \[
     Tau], dyn\[Rho]0, c, schranke, temp},

   (*read out input and define dimension paramteres*)
   {rvals, rvecs} = sol[[1]];
   {h, f, jq} = sol[[2]];
   param = sol[[3]];

   nq = param[[1]];
   nph = param[[2]];
   dimq = 2^nq;
   dimo = nph + 1;
   dim = dimq*dimo;
```

```
(*load functions*)

Get["GetLeftEV.m"];
Get["MakeZBasisState.m"];
Get["generiereBitString.m"];
Get["bereinigeMatrix.m"];

(*Create Subscript[\[Rho], 0]states whose dynamics
   shall be calculated*)

\[Rho]0 = {};
For[i = 1, i <= dimq, i++,
 bit = generiereBitString[nq, i];
 AppendTo[\[Rho]0, MakeZBasisState[bit, nph]];
 ];          (* now \[Rho]0[[1]] = 00 state, \[Rho
    ]0[[2]] = 001 state and so on, but as a
    vectorized density matrix!*)


(*now get lefteigenvectors of input eigensystem*)
{lvals, lvecs} = GetLeftEV[sol][[1]];
PrintTemporary["Done getting lefteigensystem"];

(* and define the matrices v = Rvec matrix and u =
   leftvec matrix to do the decomposition*)
v = Transpose@rvecs;
u = lvecs;

(*find timedependant coeffs c= u*\[Rho]0*)
c = {};
PrintTemporary["Calculating coeffs c..."];
For[i = 1, i <= dimq, i++,
 AppendTo[c, Exp[rvals*t]*(u . \[Rho]0[[i]])];
 ];
PrintTemporary["Dimensions c: ", Dimensions@c];

(*reconstruct the dynamical matrix dyn\[Rho]0*)
dyn\[Rho]0 = {};

For[i = 1, i <= dimq, i++,
 PrintTemporary["ReConstructing ", i, "th dyn.
    Density Matrix..."];
 temp = ArrayReshape[v . c[[i]], {dim, dim}]; (*
    reshaping to matricize - the state-vector! It
    gives out a density MATRIX*)
 schranke = dim^(-5); (*all terms in dynrho smaller
    than this will be thrown away*)
 PrintTemporary["Bereinige ", i, "te dyn-dens.
    matrix, werfe alles kleiner als " , schranke, "
    weg..."];
 temp = bereinigeMatrix[temp, t, schranke]; (*this
    function "cleans" the matrix by throwing away
    small elements, smaller than "schranke"*)
 AppendTo[dyn\[Rho]0, temp];
 ];
 (*dynRho[[x]] is now the timedependant density
    matrix evolved from the initial state |x><x
    |*|0><0|*)
Print["Done
   ----------------------------------------------------------------
   "];
```

```
    \[Tau] = Abs[1/Re[rvals[[2]]]]; (*lifetime of the
       longest living, nonstationary mode*)

    out = {dyn\[Rho]0, {h, f, jq}, param, \[Tau]};
    Return[out]];
  Export["dynSys.m", FullDefinition[dynSys]]
```

GetLeftEV function

Takes output of GetEigenSystem (which includes the system of right-sided eigenvectors of $\mathcal{L}$) as input and calculates the left-sided eigensystem, as explained at the end of Chapter 4.

```
GetLeftEV[sol_] :=
  Module[{rvals, rvecs, lvecs, h, f, jq, param, out},

   (*righsided Eigenvectors:*)
   {rvals, rvecs} = sol[[1]]; (*rvecs[[1]] is 1st
      eigenvector. rvecs[[1]][[j]] is j-comp of first ev*)
   rvecs = Transpose@rvecs;(*has the right form now where
      the kth column is kth eigenvector*)

   PrintTemporary["Calculating Inverse...."];
   lvecs = Inverse@rvecs; (*should already be of the form
      that lvecs[[k]] = kth L-Evec*)
   PrintTemporary["Done!"];
   (*reassemble structure*)
   {h, f, jq} = sol[[2]];
   param = sol[[3]];

   out = {{rvals, lvecs}, {h, f, jq}, param};
    Return[out]];
Export["GetLeftEV.m", FullDefinition[GetLeftEV]]
```

MakeZBasisState function

takes a binary bitstring x and photon number (dimensionality of truncated oscillator Hilbert space minus one) as input and outputs the vectorized state $|x\rangle\langle x| \otimes |0\rangle\langle 0|$.

```
MakeZBasisState[bits_, phn_] :=
  (
   ClearAll[out];

   numq =
    StringLength@bits; (*length of string defines
       number of qubits*)
   dq = 2^numq; (*dimension of qubit vectorspace*)

   pos = FromDigits[bits, 2] + 1;  (* ^ position/index-
   value of requested state in qubit-space-vector/list
      *)
   \[Psi]qt = ConstantArray[0, dq];
   \[Psi]qt[[pos]] = 1;(*qubit-space-state*)
   \[Psi]osct = ConstantArray[0, phn + 1];(*vacuum osci
       state*)
   \[Psi]osct[[1]] = 1;

   \[Psi]tott =
    Flatten@KroneckerProduct[\[Psi]qt, \[Psi]osct]; (*
       total state*)
```

```
    \[Rho]tott =
     KroneckerProduct[\[Psi]tott, Conjugate@\[Psi]tott]
        // Flatten;(*total density matrix, vectorized*);
    out = \[Rho]tott;
    ClearAll[\[Psi]osct, \[Psi]qt, \[Psi]tott, \[Rho]
       tott];

    Return[out]
    );

Export["MakeZBasisState.m", FullDefinition[
    MakeZBasisState]]
```

generateBitString function

This function takes a base-10 number D as an input, aswell as the number of qubits nq, and converts it to a binary string x of length n encoding the register state implied by D. For example $D = 3$ and $nq = 5$ corresponds to the state 00010, where one qubit is in its ground state and all others are excited. $D = 4$ would be 00011 and so on. This function was actually written by *ChatGpt 4*.

```
generiereBitString[nq_, D_] :=
  Module[{binarOhneFuhrendeNullen},
   binarOhneFuhrendeNullen = IntegerString[D - 1, 2];
   StringJoin[
    Table["0", {nq - StringLength[
       binarOhneFuhrendeNullen]}],
    binarOhneFuhrendeNullen]];
Export["generiereBitString.m", FullDefinition[
    generiereBitString]]
```

cleanMatrix function

This function takes a matrix dependin g on t as an input, aswell as an upper limit "schranke", and then removes all the entries from the matrix with coefficients smaller than "schranke". This function was again coded using ChatGpt4.

```
bereinigeMatrix[matrix_, t_, schranke_] :=
  Module[{bereinigterEintrag, bereinigeTerm},
   (*PrintTemporary["Bereinige Matrix...."];*)
   bereinigeTerm[term_] :=
    term /. coeff_*Exp[expTerm_] :>
      If[Abs[coeff] < schranke, 0, coeff]*Exp[
         expTerm];
   bereinigterEintrag[ausdruck_] :=
    Total[Map[bereinigeTerm, List @@ ausdruck,
       {1}]];
   Map[bereinigterEintrag, matrix, {2}](*;
   PrintTemporary[Dimensions@matrix];
   PrintTemporary["Erledigt!
      ------------------------------------"]*)
   ];

Export["bereinigeMatrix.m", FullDefinition[
    bereinigeMatrix]]
```

Bibliography

[1] Alexandre Blais, Arne L. Grimsmo, S. M. Girvin, and Andreas Wallraff. Circuit quantum electrodynamics. *Rev. Mod. Phys.*, 93:025005, May 2021.

[2] Jay Gambetta, Alexandre Blais, D. I. Schuster, A. Wallraff, L. Frunzio, J. Majer, M. H. Devoret, S. M. Girvin, and R. J. Schoelkopf. Qubit-photon interactions in a cavity: Measurement-induced dephasing and number splitting. *Physical Review A*, 74(4), October 2006.

[3] Jay Gambetta, Alexandre Blais, M. Boissonneault, A. A. Houck, D. I. Schuster, and S. M. Girvin. Quantum trajectory approach to circuit qed: Quantum jumps and the zeno effect. *Phys. Rev. A*, 77:012112, Jan 2008.

[4] Kevin Lalumière, J. M. Gambetta, and Alexandre Blais. Tunable joint measurements in the dispersive regime of cavity qed. *Phys. Rev. A*, 81:040301, Apr 2010.

[5] Jens Koch, Terri M. Yu, Jay Gambetta, A. A. Houck, D. I. Schuster, J. Majer, Alexandre Blais, M. H. Devoret, S. M. Girvin, and R. J. Schoelkopf. Charge-insensitive qubit design derived from the cooper pair box. *Physical Review A*, 76, 2007.

[6] William Livingston, Machiel Blok, Emmanuel Flurin, Justin Dressel, Andrew Jordan, and Irfan Siddiqi. Experimental demonstration of continuous quantum error correction. *Nature Communications*, 13, 04 2022.

[7] Baptiste Royer, Shruti Puri, and Alexandre Blais. Qubit parity measurement by parametric driving in circuit qed. *Science Advances*, 4(11):eaau1695, 2018.

[8] Manuel H. Muñoz-Arias, Cristóbal Lledó, and Alexandre Blais. Qubit readout enabled by qubit cloaking. *Physical Review Applied*, 20(5), November 2023.

[9] Liangyu Chen, Hang-Xi Li, Yong Lu, Christopher W. Warren, Christian J. Križan, Sandoko Kosen, Marcus Rommel, Shahnawaz Ahmed, Amr Osman, Janka Biznárová, Anita Fadavi Roudsari, Benjamin Lienhard, Marco Caputo, Kestutis Grigoras, Leif Grönberg, Joonas Govenius, Anton Frisk Kockum, Per Delsing, Jonas Bylander, and Giovanna Tancredi. Transmon qubit readout fidelity at the threshold for quantum error correction without a quantum-limited amplifier. *npj Quantum Information*, 9(1), March 2023.

[10] Uwe von Lüpke, Yu Yang, Marius Bild, Laurent Michaud, Matteo Fadel, and Yiwen Chu. Parity measurement in the strong dispersive regime of circuit quantum acoustodynamics. *Nature Physics*, 18(7):794–799, May 2022.

[11] Claude Cohen-Tannoudji, Bernard Diu, Franck Laloë, and Susan Reid Hemley. *Quantum mechanics*. A Wiley-Interscience publication. Wiley [u.a.], New York, NY [u.a.], 1977. ;.

[12] Heinz-Peter Breuer, Francesco Petruccione, et al. *The theory of open quantum systems*. Oxford University Press on Demand, 2002.

[13] Roy J. Glauber. Coherent and Incoherent States of the Radiation Field. *Physical Review*, 131(6):2766–2788, September 1963.

[14] Marlan O. Scully and M. Suhail Zubairy. *Coherent and squeezed states of the radiation field*, page 46–71. Cambridge University Press, 1997.

[15] C. Cohen-Tannoudji, B. Diu, and F. Laloë. *Quantum Mechanics, Volume 1: Basic Concepts, Tools, and Applications*. Wiley, 2019.

[16] E. Wigner. On the Quantum Correction For Thermodynamic Equilibrium. *Physical Review*, 40(5):749–759, June 1932.

[17] Kôdi HUSIMI. Some formal properties of the density matrix. *Proceedings of the Physico-Mathematical Society of Japan. 3rd Series*, 22(4):264–314, 1940.

[18] Thomas E. Roth, Ruichao Ma, and Weng C. Chew. The transmon qubit for electromagnetics engineers: An introduction. *IEEE Antennas and Propagation Magazine*, 65(2), 2023.

[19] Bruce W. Shore and Peter L. Knight. The jaynes-cummings model. *Journal of Modern Optics*, 40(7):1195–1238, 1993.

[20] J. R. Schrieffer and P. A. Wolff. Relation between the Anderson and Kondo Hamiltonians. *Physical Review*, 149(2):491–492, September 1966.

[21] Frank Harkins Declan Millar, Jacob Watkins et al. *Circuit Quantum Electrodynamics*. Github, 2023. Qiskit Textbook Repository, accessed 02.April 2024.

[22] Sergey Bravyi, David P. DiVincenzo, and Daniel Loss. Schrieffer–wolff transformation for quantum many-body systems. *Annals of Physics*, 326(10):2793–2826, October 2011.

[23] Rukhsan Ul Haq and Keshav Singh. A systematic method for schrieffer-wolff transformation and its generalizations, 2020.

[24] Maxime Boissonneault, J. M. Gambetta, and Alexandre Blais. Dispersive regime of circuit qed: Photon-dependent qubit dephasing and relaxation rates. *Phys. Rev. A*, 79, Jan 2009.

[25] Carbonaro P., Compagno G., and Persico F. Canonical dressing of atoms by intense radiation fields. *Physics Letters A*, 73, 1979.

[26] Lev S. Bishop, Eran Ginossar, and S. M. Girvin. Response of the strongly driven jaynes-cummings oscillator. *Phys. Rev. Lett.*, 105, 2010.

[27] L. Tosi, I. Lobato, M. F. Goffman, C. Metzger, C. Urbina, and H. Pothier. Effects of the measurement power on states discrimination and dynamics in a circuit-qed experiment, 2023.

[28] W. E. Shanks, D. L. Underwood, and A. A. Houck. A scanning transmon qubit for strong coupling circuit quantum electrodynamics. *Nature Communications*, 4(1), 2013.

[29] Vittorio Gorini, Andrzej Kossakowski, and Ennackal Chandy George Sudarshan. Completely positive dynamical semigroups of n-level systems. *Journal of Mathematical Physics*, 17(5):821–825, 1976.

[30] Goran Lindblad. On the generators of quantum dynamical semigroups. *Communications in Mathematical Physics*, 48(2):119–130, 1976.

[31] Howard M Wiseman and Gerard J Milburn. *Quantum measurement and control*. Cambridge university press, 2009.

[32] Fabrizio Minganti, Adam Miranowicz, Ravindra W. Chhajlany, and Franco Nori. Quantum exceptional points of non-hermitian hamiltonians and liouvillians: The effects of quantum jumps. *Physical Review A*, 100(6), December 2019.

[33] Morag Am-Shallem, Amikam Levy, Ido Schaefer, and Ronnie Kosloff. Three approaches for representing lindblad dynamics by a matrix-vector notation, 2015.

[34] Philip Pearle. Simple derivation of the lindblad equation. *European Journal of Physics*, 33(4):805–822, April 2012.

[35] G. Ithier, E. Collin, P. Joyez, P. J. Meeson, D. Vion, D. Esteve, F. Chiarello, A. Shnirman, Y. Makhlin, J. Schriefl, and G. Schön. Decoherence in a superconducting quantum bit circuit. *Physical Review B*, 72, 2005.

[36] Athanasios Papoulis and S. Unnikrishna Pillai. *Probability, Random Variables, and Stochastic Processes*. McGraw Hill, 2002.

[37] Ronald E. Walpole, Raymond H. Myers, Sharon L. Myers, and Keying Ye. *Probability & statistics for engineers and scientists*. Pearson Education, 8th edition, 2007.

[38] Eric W. Weisstein. Central limit theorem. From MathWorld–A Wolfram Web Resource.

[39] Albert Einstein. *Über die von der molekularkinetischen Theorie der Wärme geforderte Bewegung von in ruhenden Flüssigkeiten suspendierten Teilchen*. 1905.

[40] Maximilian Schlosshauer. *Decoherence and the Quantum-To-Classical Transition*. Springer Berlin, Heidelberg, 2007.

[41] Alexander Shnirman. Physics of quantum information, May 2019. Lecture Script SS2019 Class on the Physics of Quantum Information at Karlsruher Institute of Technology, Karlsruhe, Germany.

[42] M. Werling and A. Shnirman. Landau-zener transitions in a dissipative two level system. 2020. Bachelor Thesis, unpublished.

[43] C. W. Gardiner and P. Zoller. *Quantum Noise*. Springer, second edition, 2000.

[44] Raymond F. Bishop and A. Vourdas. Coherent mixed states and a generalised p representation. *Journal of Physics A*, 20, 1987.

[45] D.F. Walls and G.J. Milburn. *Quantum Optics*. Springer Berlin Heidelberg, 2008.

[46] W. H. Zurek. Pointer basis of quantum apparatus: Into what mixture does the wave packet collapse? *Phys. Rev. D*, 24:1516–1525, Sep 1981.

[47] Alexandre Blais, Ren-Shou Huang, Andreas Wallraff, S. M. Girvin, and R. J. Schoelkopf. Cavity quantum electrodynamics for superconducting electrical circuits: An architecture for quantum computation. *Phys. Rev. A*, 69:062320, Jun 2004.

[48] Jun John Sakurai and Eugene D Commins. Modern quantum mechanics, revised edition, 1995.

[49] Kelvin Koor, Yixian Qiu, Leong Chuan Kwek, and Patrick Rebentrost. A short tutorial on wirtinger calculus with applications in quantum information, 2023.

[50] Frank Wikström. Integration by parts of wirtinger derivative, 2015. The derivation of the partial integration rule is based on the one outlined by Frank Wikström, username "mrf", in an answer on a related question on Math Stack exchange. Accessed 04.April.2024.

[51] Todd Rowland. Exterior derivative. Accessed on 04. April 2024.